Alfred-Wegener-Institut für Polar- und Meeresforschung
Universität Potsdam, Institut für Geowissenschaften

The modification of arctic permafrost coastlines

Dissertation
zur Erlangung des akademischen Grades
"doctor rerum naturalium"
(Dr. rer. nat.)
in der Wissenschaftsdisziplin Geowissenschaften

eingereicht an der
Mathematisch-Naturwissenschaftlichen Fakultät
der Universität Potsdam

von
Hugues Lantuit

Potsdam, den 14.01.2008

"When the past no longer illuminates the future, the spirit walks in darkness."

Alexis de Tocqueville

ABSTRACT

The arctic region is undergoing the most rapid environmental change experienced on Earth, and the rate of change is expected to increase over the coming decades. Arctic coasts are particularly vulnerable because they lie at the interface between terrestrial systems dominated by permafrost and marine systems dominated by sea ice. An increased rise in sea level and degradation of sea-ice as predicted by the Intergovernmental Panel on Climate Change in its most recent report and as observed recently in the Arctic will likely result in greater rates of coastal retreat. An increase in coastal erosion would result in dramatic increases in the volume of sediment, organic carbon and contaminants to the Arctic Ocean. These in turn have the potential to create dramatic changes in the geochemistry and biodiversity of the nearshore zone and affect the Arctic Ocean carbon cycle.

To calculate estimates of organic carbon input from coastal erosion to the Arctic Ocean, current methods rely on the length of the coastline in the form of non self-similar line datasets. This thesis however emphasizes that using shorelines drawn at different scales can induce changes in the amount of sediment released by 30% in some cases. It proposes a substitute method of computations of erosion based on areas instead of lengths (i.e. buffers instead of shoreline lengths) which can be easily implemented at the circum-Arctic scale. Using this method, variations in quantities of eroded sediment are, on average, 70% less affected by scale changes and are therefore a more reliable method of calculation.

Current estimates of coastal erosion rates in the Arctic are scarce and long-term datasets are a handful, which complicates assessment and prognosis of coastal processes, in particular the occurrence of coastal hazards. This thesis aims at filling the gap by providing the first long-term dataset (1951-2006) of coastal erosion on the Bykovsky Peninsula, North-East Siberia. This study shows that the coastline, which is made of ice-rich permafrost, retreated at a mean annual rate of 0.59 m/yr between 1951and 2006. Rates were highly variable: 97.0 % of the rates observed were less than 2 m/yr and 81.6% were less than 1m/yr. However, no significant trend in erosion could be recorded despite the study of five temporal subperiods within 1951-2006. The juxtaposition of wind records could not help to explain erosion records either and this thesis emphasizes the local controls on erosion, in particular the cryostratigraphy, the proximity of the Peninsula to the Lena River Delta freshwater plume and the local topographical constraints on swell development.

On ice-rich coastal stretches of the Artic, the interaction of coastal dynamics and permafrost leads to the occurrence of spectacular “C-shaped” depressions termed retrogressive thaw slumps which can reach lengths of up to 650 m. On Herschel Island and at King Point (Yukon Coastal Plain, northern Canada), topographical, sedimentological and biogeochemical surveys were conducted to investigate the present and past activity of these landforms. In particular, undisturbed tundra areas were compared with zones of former slump activity, now stabilized and re-vegetated. This thesis shows that stabilized areas are drier and less prone to plant growth than undisturbed areas and feature fundamentally different geotechnical properties. Radiocarbon dating and topographical surveys indicated until up to 300 BP a likely period of dramatic slump activity on Herschel Island, similar to the one currently observed, which led to the creation of these surfaces. This thesis hypothesizes the occurrence of a ~250 years cycle of slump activity on the Herschel Island shoreline based on the surveyed topography and cryostratigraphy and anticipates higher frequency of slump activity in the future.
The variety of processes described in this thesis highlights the changing nature of the intensity and frequency of physical processes acting upon the arctic coast. It also challenges current perceptions of the threats to existing industry and community infrastructure in the Arctic. The increasing presence of humans on Artic coasts coupled with the expected development of shipping will drive an increase in economical and industrial activity on these coasts which remains to be addressed scientifically.

ZUSAMMENFASSUNG

In der Arktis sind die derzeit stärksten Umweltänderungen weltweit zu beobachten, und es wird angenommen, dass sich deren Ausmaß sogar noch verstärken wird. Aufgrund ihrer Lage zwischen terrestrischen, von Permafrost geprägten Systemen und marinen, von Meereis geprägten Systemen, sind arktische Küstenregionen im Zuge dieses Wandels besonders sensibel.

Ein verstärkter Meeresspiegelanstieg und der Rückgang des Meereises, wie vom letzten Bericht des Intergovernmental Panel on Climate Change (IPCC) vorhergesagt und in letzter Zeit in der Arktis beobachtet, werden zu erhöhten Küstenrückzugsraten führen. Ein Anstieg der Küstenerosion würde zu einer drastischen Erhöhung von Sedimentfracht, organischem Kohlenstoff und von Schadstoffen im Arktischen Ozean führen. Durch diese wiederum drohen dramatische Änderungen in der Geochemie und Biodiversität der küstennahen Zone sowie Veränderungen im Kohlenstoffkreislauf des Arktischen Ozeans.

Modelle zur Berechnung des Eintrags organischen Kohlenstoffs in den Arktischen Ozean infolge von Küstenerosion basieren auf der Länge der Küstenlinie in Form von „non self-similar“ Datensätzen. Die vorliegende Arbeit zeigt jedoch, dass die Nutzung von Küstenlinien unterschiedlicher Maßstäbe Abweichungen in der berechneten Sedimentfracht von bis zu 30 % zur Folge haben kann. Es wird daher eine alternative Methode zur Berechnung von Erosionsraten vorgeschlagen, die auf Flächen, nicht auf Längenangaben basiert (z.B. Pufferzonen anstelle von Küstenlinien) und die auf einfache Art und Weise für die Zirkum-Arktis angewandt werden kann. Durch diese Methode ist die Variation der berechneten Erosionsmengen um durchschnittlich 70 % weniger von Maßstabsänderungen betroffen. Damit kann eine deutlich höhere Zuverlässigkeit in den Prognosen erreicht werden. Aktuelle Abschätzungen von Küstenerosionsraten in der Arktis sind spärlich und es gibt nur sehr wenige Langzeitdatensätze, so dass Einschätzungen und Prognosen zu Prozessen im Küstenbereich, insbesondere von dessen Gefährdung, schwierig sind. Die vorliegende Arbeit soll dazu beigetragen, diese Lücke zu schließen, indem der erste Langzeitdatensatz (1951-2006) zu Küstenerosionsraten auf der Bykovsky Halbinsel in Nordost-Sibirien bereitgestellt wird. Die Arbeit zeigt, dass die Küstenlinie auf der Bykovsky Halbinsel, die durch eisreichen Permafrost geprägt ist, im Zeitraum 1951-2006 um durchschnittlich 0,59 m pro Jahr zurückging. Die Rückzugsraten waren dabei äußerst variabel: 97 % aller ermittelten Raten

betrugen weniger als 2 m und 81,6 % weniger als 1 m pro Jahr. Ein signifikanter Trend in den Erosionsraten konnte dabei jedoch trotz Analyse von fünf verschiedenen zeitlichen Epochen nicht festgestellt werden. Auch die Gegenüberstellung von Winddatensätzen kann die Erosionsraten nicht erklären. Deshalb stellt diese Arbeit die Bedeutung lokaler Kontrollmechanismen wie Kryostratigraphie, die Nähe der Bykovsky Halbinsel zum Lena-Delta und seinen Süßwasservorkommen sowie die lokale Topographie und deren Einfluss auf Wellengang und Wellenbildung heraus.

Innerhalb eisreicher arktischer Küstenabschnitte führt die Interaktion zwischen Küstendynamik und Permafrost zur Ausprägung eindrucksvoller, „C-förmiger“ Depressionen, sogenannten regressiven auftaubedingten Rutschungen, die Längen von bis zu 650 m erreichen können. Auf Herschel Island und am King Point (Yukon Küste, Nordkanada) wurden topographische, sedimentologische und biogeochemische Aufnahmen durchgeführt, um die rezente und vergangene Dynamik dieser Landschaftsformen nachvollziehen zu können. Insbesondere wurden ungestörte Tundrenareale mit ehemals aktiven Rutschungszonen, die heute stabil und wiederbewachsen sind, verglichen. Die vorliegende Arbeit zeigt, dass diese ehemaligen, heute stabilisierten Rutschungszonen trockenere und für Pflanzenwachstum weniger geeignete Standorte darstellen als ungestörte Bereiche und überdies fundamental andere geotechnische Eigenschaften aufweisen. Radiocarbon-Datierungen und topographische Aufnahmen weisen darauf hin, dass es auf Herschel Island und am King Point bis vor 300 Jahren eine Periode ausgeprägter, auftaubedingter Rutschungsaktivitäten ähnlich denen, die derzeit auf der Insel beobachtet werden können, gegeben haben muss, die zur Ausbildung dieser Oberflächenstrukturen geführt haben. Diese Arbeit stellt auf Grundlage der untersuchten Topographie und Kryostratigraphie die Hypothese auf, dass an der Küstenlinie von Herschel Island ein etwa 250-jähriger Zyklus von Rutschungsaktivitäten existiert und antizipiert eine höhere Frequenz im Auftreten dieser Rutschungsaktivitäten für die Zukunft.

Die Vielfalt an Faktoren, die in dieser Arbeit beschrieben wurden, hebt die veränderte Intensität und Frequenz der auf arktische Küsten einwirkenden physikalischen Prozesse hervor. Dadurch werden auch aktuelle Auffassungen zur Bedrohung bestehender Industrie und Infrastruktur in der Arktis hinterfragt. Im Zusammenhang mit dem erwarteten Ausbau der Schifffahrt treibt der zunehmende anthropogene Einfluss die ökonomische und industrielle Entwicklung in arktischen Küstenregionen an, die Gegenstand einer wissenschaftlichen Betrachtung sein sollten.

ACKNOWLEDGEMENTS

I would like to express my gratitude to my supervisors, Dr. Volker Rachold, Dr. Hans-Wolfgang Hubberten and Dr. Wayne Pollard whose expertise, understanding, and knowledge of the Arctic science community added considerably to my experience. I appreciate their vast knowledge and skill in many areas, the always renewed inspiration they provided for numerous projects in diverse fields and the considerable opportunities they provided me by giving me enough freedom to conduct activities that were peripheral to my work.

A very special thank you goes out to the supporting staff of the Alfred Wegener Institute for Polar and Marine Research, without whom I would not have achieved to complete the work required to finish this thesis. Ute Bastian, Tina Knobel and Antje Eulenburg provided considerable help in the laboratory and I am grateful for their patient involvement at my side. Christine Litz, Dirk Holm, Gerald Müller, Sigrun Gräning and Kathrin Klein had to endure my regular visits to solve logistical issues and I thank them for their help and patience. My co-PhD students as well as my dear colleagues (they are too numerous to be written down here) have helped me to go through those three years, which can sometimes be challenging. Susanne Liebner and Thomas Opel generously translated and edited my abstract. Some special thanks go to Lutz Schirrmeister, Paul Overduin and Georg Schwamborn who attempted to keep an eye on me once in a while.

I must acknowledge the help of my friends abroad. Those that I collaborate with on almost an everyday basis (Nicole Couture, Margareta Johansson), those that have considerably helped to make this PhD an item of the 2007-2008 International Polar Year (Jenny Baeseman, Rhian Salmon), and of course the colleagues that help make field work enjoyable (Michael Grigoriev, the rangers from the Herschel Island Territorial Park).

My most important support though comes from my wife, who had to deal with living with a PhD student for three years and experience ludicrous theories on permafrost. Finally, I would like to thank with all my heart my parents and my family who always supported me and listened quietly to my long wordy stories.

TABLE OF CONTENTS

ABSTRACT ..... **II**

ZUSAMMENFASSUNG ..... **IV**

ACKNOWLEDGEMENTS ..... **VI**

TABLE OF CONTENTS ..... **VII**

LIST OF FIGURES ..... **IX**

LIST OF TABLES ..... **XI**

CHAPTER 1 - INTRODUCTION **1**

1.1 INTRODUCTION 1
1.2 SCIENTIFIC RATIONALE 1
1.3 OBJECTIVES 3
1.4 ORGANIZATION OF THESIS 3
1.5 CONTRIBUTIONS OF AUTHORS 4

CHAPTER 2 - BACKGROUND **6**

2.1 ARCTIC COASTAL EROSION 6
2.1.1 The Arctic coastline *6*
2.1.2 Long-term coastal evolution *8*
2.1.3 Arctic specificity *9*
2.1.4 Thermal-mechanical erosion *10*
2.1.5 Storms *12*
2.1.6 Tides *12*
2.1.7 Landforms in the Coastal Plain *13*
2.3 ARCTIC COASTAL EROSION IN A CHANGING CLIMATE 16
2.3.1 Environmental forcing *16*
2.3.2 Environmental and socio-economical implications *16*
2.2 PAST AND CURRENT ISSUES IN ARCTIC COASTAL EROSION SCIENCE 18
2.2.1 Arctic coastal erosion science history *18*
2.2.3 current issues *19*

CHAPTER 3 – MANUSCRIPT #1 - TOWARDS A CALCULATION OF ORGANIC CARBON RELEASE FROM EROSION OF ARCTIC COASTS USING NON FRACTAL GEOSPATIAL DATASETS. **23**

3.1 INTRODUCTION 23
3.2 BACKGROUND 25
3.2.1. Definition of erosion *25*
3.2.2 Calculation of shoreline erosion *27*
3.3 FRACTAL COASTLINES 28
3.3.1. Fractals *28*
3.3.2. Methods *30*
3.3.3 Results - Shoreline length *33*
3.3.4. Results - WVS length *34*
3.4 ALTERNATE METHOD OF EROSION MEASUREMENT 36
3.4.1. Planimetric erosion *36*
3.4.2. Planimetric erosion in a GIS *37*
3.4.3. Method test *38*
3.4.4. Results *39*
3.5 CONCLUSIONS 43

ACKNOWLEDGEMENTS: 44

CHAPTER 4 – MANUSCRIPT #2 - EROSION HISTORY AND DYNAMICS ON BYKOVSKY PENINSULA, RUSSIA, 1951-2006 45

4.1 INTRODUCTION 45
4.2 BACKGROUND 47
4.3 STUDY AREA 48
4.3.1 Location 48
4.3.2 Physiography 48
4.3.4 Coastal erosion 49
4.3.5 Storm climatology 50
4.4 METHODS 50
4.4.1 Geoprocessing of airborne and spaceborne imagery 50
4.4.2 Storm records 53
4.5 RESULTS 54
4.5.1 Coastal erosion 54
4.5.2 Meteorological records 62
4.5.3 Coastal erosion vs. Storm counts 63
DISCUSSION 65
4.6 CONCLUSION 66
ACKNOWLEDGEMENTS 67

CHAPTER 5 – MANUSCRIPT #3 - MODERN AND LATE HOLOCENE RETROGRESSIVE THAW SLUMP ACTIVITY ON THE YUKON COASTAL PLAIN AND HERSCHEL ISLAND, YUKON TERRITORY, CANADA. 68

5.1 INTRODUCTION 68
5.2 BACKGROUND 68
5.3 STUDY AREA 71
5.4 METHODS 72
5.4.1 Test site selection 72
5.4.2 DGPS surveys 75
5.4.3 Sedimentological, geochemical and geotechnical surveys 75
5.4.4 AMS radiocarbon dating 77
5.5 RESULTS 77
5.5.1 Geomorphology 77
5.5.2 AMS radiocarbon dating 78
5.5.3 Sedimentology, geochemistry and geotechnical characteristics 79
5.6 DISCUSSION 83
5.7 CONCLUSION 85

CHAPTER 6 – CONCLUSION 87

6.1 RESULTS 87
6.2 OUTLOOK 88

REFERENCES 91

ANNEX A – MANUSCRIPT #4 103

LIST OF FIGURES

CHAPTER 2

Figure 1 – The Arctic Ocean with the extent of permafrost and tides compiled after Walker (2005) as well as the locations investigated in this study. 7
Figure 2 - The coastal tract. Modified after Cowell et al. (2003). 8
Figure 3 - Processes and environmental forcing elements acting upon the coast in the Arctic, after IASC, 2001. 10
Figure 4 - An erosive ice-rich coast on the shore of the Bykovsky Peninsula, Laptev Sea, Russia. Photo: M. Grigoriev. 11
Figure 5 - Block failure. The height of the cliff is approximately 20 m. Photo: W. Pollard. 13
Figure 6 - Thermoerosive niche at Komakuk Beach. Thermoerosive niches extend as much as 6 m. 14
Figure 7 - Polycyclic retrogressive thaw slumps in Thetis Bay, Herschel Island. The slumps extend about 300 m inland and are approximately 100 m wide. 15

CHAPTER 3

Figure 1 - Location of study areas in the Canadian Beaufort Sea area 30
Figure 2 Location of study areas in the Laptev Sea area 31
Figure 3 - logarithmic chart divider length vs. shoreline length for all investigated sectors The regression equation is marked on the chart, as well as the extracted D factor. 35
Figure 4 - Standardized eroded areas computed using buffers on the Olivier Islands sector The slope of the four curves indicates the magnitude of the changes across scale in eroded areas. The difference in standardized eroded area between the four buffers is due to the curvature of the shoreline 39
Figure 5 - Standardized buffer erosion vs. buffer widths for all investigated sectors Planimetric erosion computed using buffers is standardized to a yearly erosion value based on a 1 m/yr erosion scenario. The resulting erosion values are then plotted against the buffer widths. 41
Figure 6 - WVS vs. digitized shoreline for the Olivier Islands sector. The WVS is fairly lacks both accuracy and precision, and although it was digitized from 1:250 000 scale maps, the low quality of the transfer from maps to digital format creates artificially long segments of coast. 42

CHAPTER 4

Figure 1 - Study area The Bykovsky Peninsula is located bear to the mouth of the Lena River and forms a natural protection for the harbour of Tiksi 46
Figure 2 - Statistical distribution of shore orientation of study sites 53
Figure 3 - Statistical distribution of erosion rates in classes of erosion intensity 55
Figure 4 - Erosion rate intensity and statistical variability dependence on shore orientation 56
Figure 5 - Coastal erosion rates on the shores of the Bykovsky Peninsula for the 1951-2006 period 57
Figure 6 - Ice complex exposed at the coast of the Bykovsky Peninsula Note the thermo-erosional notch at the land-water interface. 59
Figure 7 - Retrogressive thaw slump on the coast of the Bykovsky Peninsula. The picture is taken from the edge of the slump. Note the presence of Baydzarakhs (earth mounds left in place after melting of coalesced ice wedges) within the slump floor. A man in the background gives the scale of the headscarp. 59
Figure 8 - Coastline in alas north of Mammontovy Hayta on the eastern shore of the Peninsula The peat-rich alas low grounds are rapidly eroded by incident wave attack. 60
Figure 9 - Erosional sequence on an alas shoreline in the south-east part of the Peninsula. The current shoreline is close to the edge of the alas, which should result in a significant decrease in coastal erosion rates on this stretch of coastline. 61
Figure 10 - Temporal evolution of mean annual coastal erosion rates 62
Figure 11 - Storm count evolution for the 1958-2006 period 63

CHAPTER 5

Figure 1 - Conceptual scheme of retrogressive thaw slump Inset B focuses on the slump headwall. Inset C is a cross-section of the slump. The diagram shows the relation between retrogressive thaw slump development and massive ground ice occurrence. Depending on the bottom position of the massive ice body under the slump floor, a new slump might develop in the lower portion of the slump, building a polycyclic slump. After Lantuit and Pollard (2005). 69
Figure 2 – Idealized cross-sectional profiles of thermoterrace (slump floor) and illustration of the virtual point at which coastal erosion triggered the occurrence of the RTS Freely adapted from Aré et al. (2005) 71
Figure 3 - Study area with limits of Buckland phase of the Wisconsin glaciation....72
Figure 4 - Oblique helicopter views of the RTS with the survey squares investigated in this study....73
Figure 5 - Tertiary diagram of sediments sampled in active, stabilized and undisturbed zones of retrogressive thaw slumps, as well as suspended sediment samples collected in water flowing in gullies in the slump floor. 81
Figure 6 - Grain size distribution curves for samples aggregated by type 82
Figure 7 - Regression plot for dry-weight soil moisture content and Total Organic Carbon (TOC) content....83

CONCLUSION

Figure 1 - A schematic representation of spatial and temporal scales of coastal and marine systems. After Gordon et al. (1996)....88

LIST OF TABLES

CHAPTER 3

Table 1 - Study sites – Location and geomorphic characteristics 32
Table 2 Shoreline lengths computed with different dividers and the WVS The lower line refers to the difference in % between the lengths computed using the 10 and the 1000 m dividers.....33
Table 3 - Planimetric erosion (buffer area) for the Olivier Islands computed using different divider lengths and different buffer widths. The lower line refers to the difference in % between the areas computed using the 10 and the 1000 m dividers.....38

CHAPTER 4

Table 1 - Imagery used in the study All scenes have been resampled to a 2.5 m spatial resolution. 52
Table 2 - Imagery georeferencing and dilution of accuracy (DOA) for the 96 subsampled points used in the temporal analysis The periods for which the margin of error is greater than 25% of the measured average rate are highlighted in grey.....53
Table 3 - Erosion rates and coastal types 58

CHAPTER 5

Table 1 - Basic topographical and geometrical characteristics of the investigated RTS.....73
Table 2 - Overview of the applied methods 74
Table 3 - Survey and laboratory results from the survey square illustrated in figure 4.....76
Table 4 - Survey and laboratory results aggregated by type of surface (S= stabilized, U= undisturbed and A= active). 76
Table 5 - Estimated erosion since slump occurrence Estimation is based on slope angle from stabilized slump floors and estimated elevation of massive ice layer bottom position. Note that age is indicated in years before 2007 and not before present (i.e. 1950). 78
Table 6 - ^{14}C AMS ages of grass remains in the samples The 2σ range is calculated with the INTCAL04 program (Reimer *et al.* 2004) to yield calibrated age intervals. 79

CHAPTER 1 - INTRODUCTION

1.1 Introduction

The arctic region is undergoing the most rapid environmental change experienced on Earth, and the rate of change is expected to increase over the coming decades (Serreze et al., 2000; Anisimov et al., 2007). Arctic coasts are particularly vulnerable because they lie at the interface between terrestrial systems dominated by permafrost and marine systems dominated by sea ice. Most of the retreat observed along ice-rich permafrost coasts in the Arctic is due to a combination of hydrodynamical forcing, thermal denudation (often thermokarst), and thermal-mechanical erosion. An increased rise in sea level and degradation of sea-ice as predicted by the Intergovernmental Panel on Climate Change in its most recent report (Anisimov et al., 2007) will likely result in greater rates of coastal retreat.

An increase in coastal erosion would result in dramatic increases in the volume of sediment, organic carbon, and contaminants to the Arctic Ocean, which have the potential to create dramatic changes in the geochemistry and biodiversity of the nearshore zone and affect the Arctic Ocean carbon cycle

Changes in the intensity and frequency of physical processes acting upon the coast will also bring about major threats to existing industry and community infrastructure. Many communities have already been affected by the destruction of buildings due to the impact of storms. In some regions, coastal erosion has shifted the shoreline more than 100 metres in the last 50 years (Solomon, 2005). The costs of sustaining activity on these coasts is already very high and will likely increase. The increasing presence of humans on Artic coasts coupled with the expected development of shipping will drive an increase in economical and industrial activity on these coasts which remains to be addressed scientifically.

1.2 Scientific Rationale

Even though there has been considerable progress in coastal erosion science over the past five decades, particularly in Alaska, western Canada, and the Laptev Sea region, Arctic coastal research has generally been neglected and a number of issues remain unresolved. This thesis attempts to address some of the issues relevant to modern Arctic coastal erosion science. Data collected over the past fifteen years highlight the overwhelmingly importance but unexpected contribution of coastal erosion to the sediment and carbon budget of the Arctic

Ocean. Several authors have highlighted that coastal erosion could indeed provide as much terrigenous material to the Ocean as rivers flowing into it (Rachold et al., 2000). Yet the lack of a common framework to study erosion and comprehensive datasets on shoreline retreat at the circum-Arctic scale impedes attempts to reliably quantify the amount of sediment reaching the sea. To address this issue, the Arctic Coastal Dynamics (ACD) program was created to create a comprehensive classification of Arctic coasts incorporating both geomorphological and geochemical data (Brown and Solomon, 1999). Ultimately the goal of the program is to create the first accurate estimate of the release of sediment and organic carbon to the Arctic Ocean by coastal erosion. However, like many other programs, the ACD program is basing its calculations on geospatial datasets of the coastline which, unlike natural coastlines, are not fractal by nature. One of the objectives of this thesis is therefore to assess the uncertainties associated with the use of such datasets and to study the impact on the resulting sediment budget calculations.

Probably less than 5% of the Arctic coastline has been monitored effectively to provide long-term rates of coastal retreat. Past efforts in Canada (Solomon, 2005; Lantuit and Pollard, 2008), Alaska (Jorgenson and Brown, 2005) and Russia (Grigoriev, 1996) have aimed at providing such rates, but the overall coverage of the Arctic is scarce, both temporally and spatially. Compilations of retreat rates at better temporal resolutions are needed to provide more information on the evolution of the coast, to study its reaction to storms in order to be able to undertake prognosis efforts. Shoreline retreat has often been delivered as raw information and compiled over decades. The results generally lack temporal resolution that is needed to provide clues on the evolution of erosion processes. They also often lack coupling with other processes occurring at the coast and driving erosion (climate, permafrost conditions, etc.). One of the objectives of this thesis is to provide a detailed investigation of coastal erosion rates on the Bykovsky Peninsula in Northern Siberia and to correlate those to a set of climatological and rheological parameters. The strategic location of the Peninsula for future shipping plans along the northern Russian coast and the ice-rich nature of the permafrost in the area are strong incentives to provide an updated record of erosion.

Process studies are also a crucial element of Arctic coastal research because 1) they provide useful information on the inner working of slope and hydrodynamical processes in coastal settings 2) they provide boundary information that is needed to parameterize climate change scenarios 3) they can help with identifying threats in the vicinity of community and/or industrial infrastructure and 4) because they provide an insight into the past, current and future processes and changes in the coastal zone. Several process studies pertaining to the

Arctic coastal zone have been conducted in the past, but those are not extensive or not comprehensive enough to be extrapolated to the Arctic scale. Hydrodynamics of the nearshore zone, storm development, permafrost degradation and subsequent slope hazards are all but comprehensively known. This thesis answers some issues raised in former studies by Lantuit and Pollard (2008) concerning thermokarst activity (retrogressive thaw slumps) in the nearshore zone. In particular, it aims at solving unanswered questions related to the genesis, periods of activity and periods of stabilization of these spectacular features.

1.3 Objectives

The objective of this thesis is to highlight the relevance of studies of coastal erosion at multiple scales in the Arctic by using remotely sensed and geospatial data.
The specific objectives include:

1) To demonstrate the inaccuracies in current calculations of coastal erosion at the circum-Arctic scale using linear non-fractal coastline datasets and to emphasize the need for substitute methods to correctly calculate the far from negligible contribution of coastal erosion to the Arctic Ocean carbon budget
2) To provide a 55 year long record of coastal erosion for the Bykovsky Peninsula, located in northern Siberia and to compare this record with climatological data.
3) To investigate the late Holocene and current dynamics of retrogressive thaw slump activity on Herschel Island and its relation to past periods of coastal erosion

1.4 Organization of Thesis

This thesis is prepared as four manuscripts (one in the annex) for publication following University of Potsdam's Mathematics-Natural Science Faculty guidelines. Chapter 3 (Manuscript #1) examines the necessity to reconsider existing geospatial techniques to compute the quantities of carbon released through coastal erosion to the Arctic Ocean. Chapter 4 (Manuscript #2) is a twofold study on coastal erosion and storminess on the shores of the Bikovsky Peninsula over the 1951-2006 period. Chapter 5 (Manuscript #3) is a multi-approach investigation of the past and present retrogressive thaw slump activity on Herschel Island, Yukon Territory.
Annex A (Manuscript #4) is an attempt to relate coastal erosion rate on Arctic coasts to ground ice contents based on the ACD classification of Arctic coasts.
Each of these manuscripts is considered as a separate entity. Therefore, there is unavoidable repetition of basic information (field description and methods) in the manuscripts. Additional

literature review (Chapter 2) and a conclusion section (Chapter 6) have been included in the thesis to provide a more thorough discussion on coastal erosion issues that could not be included in the manuscripts.

Manuscript #1 has been accepted for publication in *Marine Geology* and is pending revision. Manuscript #2 will be submitted to *Journal of Geophysical Research*. Manuscript #3 will be submitted to *Permafrost and Periglacial Processes*. Manuscript #4 (annex A) has been submitted for peer-review and accepted for inclusion in the proceedings of the Ninth International Conference on Permafrost to be held in June-July 2008 in Fairbanks, Alaska.

1.5 Contributions of Authors

Manuscript #1 authors: Hugues Lantuit, Volker Rachold, Wayne Pollard, Frits Steenhuisen, Rune Ødegård and Hans-Wolfgang Hubberten

Drs. Rachold, Hubberten and Pollard provided guidance and help in contructing the framework and subsequent ideas presented in this manuscript. They also provided valuable advices and editing support throughout the redaction process. Dr. Pollard provided the necessary resources to obtain high resolution imagery for Herschel Island. Dr. Odegard proposed the idea behind this study during a workshop Mr. Lantuit attended and subsequently helped with the development, methods and critical review of the study. Mr. Steenhuisen helped with providing the World Vector Shoreline datasets and choosing the study sites. The geoprocessing (i.e. scanning, resampling, georegistration) of the imagery was performed by Mr. Lantuit. The digitizing was also performed by Mr. Lantuit except for the shore of Herschel Island which was digitized by Mr. Berg, intern at the Alfred-Wegener-Institute. The statistical analysis, the creation of the pictures, and the writing were entirely performed by Mr. Lantuit.

Manuscript #2 authors: Hugues Lantuit, David Atkinson, Mikhail Grigoriev, Volker Rachold, Guido Grosse and Hans-Wolfgang Hubberten.

Drs. Rachold and Hubberten provided guidance and help in constructing the framework and subsequent ideas presented in this manuscript. They also provided valuable advices and editing support throughout the redaction process. In collaboration with Dr. Grigoriev, they helped with feeding field observations into this study and validating observations made from satellite imagers. Dr. Grosse helped by providing critical comments, and helped with the cataloguing and georeferencing of satellite imagery. Dr. Atkinson produced the storm counts using an algorithm developed for a former study and helped reviewing the manuscript in

general and in detail for the part related to climatology. Mr. Lantuit processed, resampled, and georeferenced all satellite imagery, and developed the algorithm for Dilution of Accuracy estimation. Mr. Lantuit conducted the entire analysis of storm and erosion data and wrote the entire manuscript.

Manuscript #3 authors: Hugues Lantuit, Wayne Pollard, Nicole Couture, Lutz Schirrmeister, Hanno Meyer and Hans-Wolfgang Hubberten.

Drs. Pollard and Hubberten provided guidance and help in constructing the framework and subsequent ideas presented in this manuscript. They also provided valuable advice and editorial support throughout the redaction process. Drs. Pollard, Schirrmeister and Meyer, and Ms. Couture helped with the collection of samples, description of cryostratigraphy, selection of samples for dating and review of this manuscript. Mr. Lantuit performed KDGPS measurements in the field, as well as collection of samples, description of cryostratigraphy, sedimentological and geochemical analyses in the laboratory, georeferencing and processing of imagery, vegetation description, geotechnical analyses and subsequent analyses and interpretation.

Manuscript #4 authors: Hugues Lantuit, Pier Paul Overduin, Nicole Couture and Rune Ødegård.

Ms. Couture, Drs. Overduin and Ødegård provided help at an earlier stage of this study by facilitating the compilation of the ground ice data into the ACD classification. Mr. Lantuit edited the database, standardized the data, removed extraneous and eroneous records, and conducted the statistical analysis. Mr. Lantuit wrote the entire manuscript and was aided by critical reviews of the co-authors.

CHAPTER 2 - BACKGROUND

2.1 Arctic coastal erosion

The arctic region is undergoing the most rapid environmental change experienced on Earth, and the rate of change is expected to increase over the coming decades (Serreze et al., 2000; Anisimov et al., 2007). The coasts are particularly vulnerable to climate warming because they are affected by changes in three different systems – the terrestrial, the marine, and the atmospheric. In most parts of the Arctic, the greatest coastal threat from environmental change is an increase in the rate of erosion. This section reviews the scientific basis and theory of arctic coastal erosion, and in the process provide a short historical overview of the investigations conducted in this field during the 19th and 20th centuries. This chapter also identifies the challenges (present and future) remaining to be faced to truly understand coastal processes in the Arctic.

2.1.1 The Arctic coastline

Geographical extent

There are many definitions used to denote the arctic coastline and coastal zone. Because of the wide range of definitions used to define the physical limits of the Arctic, arctic coasts are equally difficult to define. For example, some authors describe arctic coastlines as coasts affected by sea ice phenomena (Walker, 2007). Others refer to coastlines directly neighbouring the Arctic Ocean, and others simply relate the coastline to some limit of the Arctic, whether it is based on latitude, environment, politics or geology.

This research focuses on Arctic coasts that border the Arctic Ocean and are affected by the presence of permafrost. Coastal erosion in the Arctic is very complex and can differ dramatically from its counterpart in temperate regions. One of the main differences is due to the short open-water season (3-4 months) and in the case of coasts composed of unconsolidated sediments (which is the primary focus of this study) the presence of permafrost, and thus of ground ice is a major variable. Bedrock coasts, which are subject to enhanced cryogenic weathering and freeze-thaw driven erosion, will not be considered in this thesis.

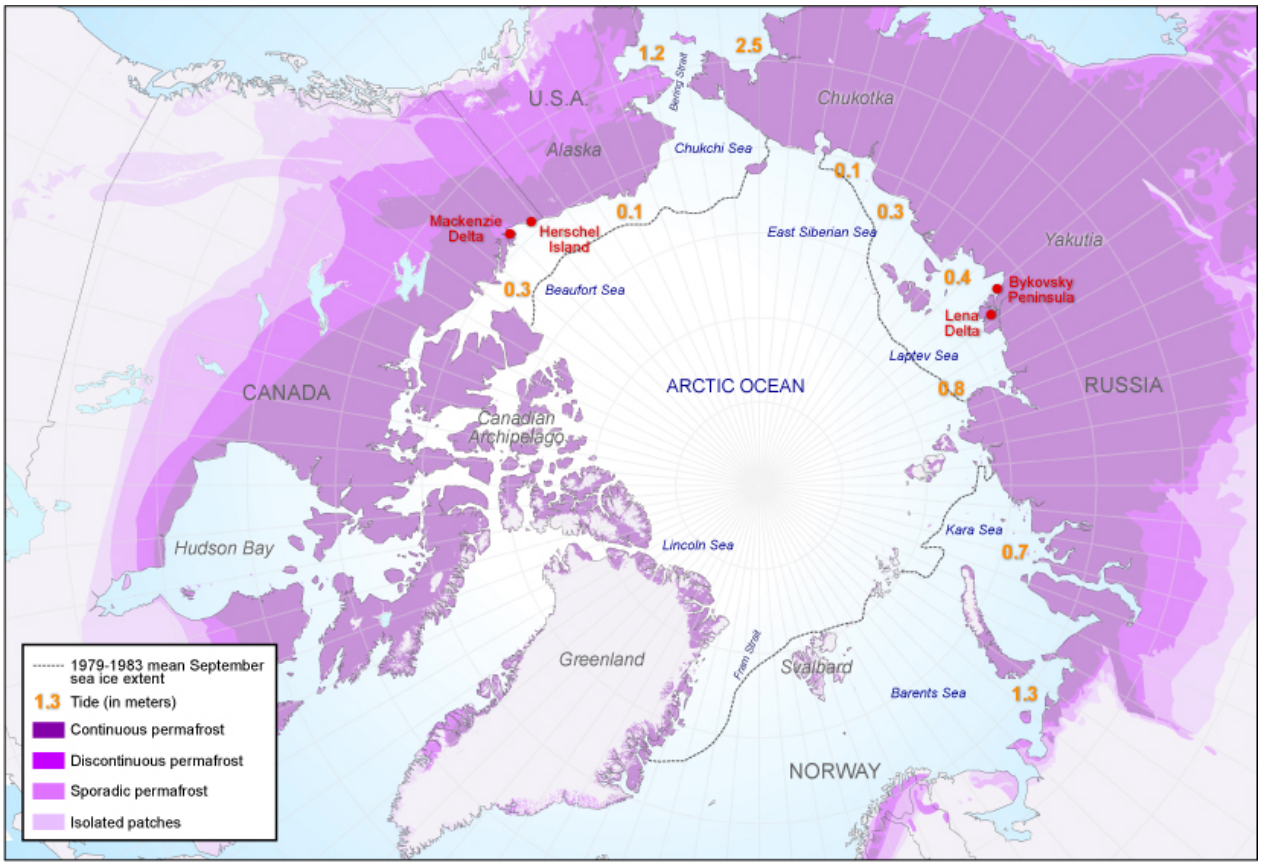

Figure 1 – The Arctic Ocean with the extent of permafrost and tides compiled after Walker (2005) as well as the locations investigated in this study.

The operational definition of Arctic coasts adopted for this study applies to the entire coastline of northern Eurasia from the North Cape in Norway to the Bering Strait in Russia(i.e. Barents Sea, Kara Sea, Laptev Sea, East Siberian Sea and Chuckchi Sea), the coasts of Alaska and Canada from the Bering Strait to the Canadian Archipelago (Beaufort Sea), the entire Canadian Archipelago and large parts of Hudson Bay and Nunavik and the northern part of Greenland (Lincoln Sea), but excludes the Bering, Baltic and Greenland Seas (figure 1).

The coastal zone

The coastal zone is even more challenging to define than the geographical extent of the arctic coastline because it is constrained by an idealized cross-shore transect of the coast with clearly defined boundaries that will differ for the various types of shoreline. Extending the definition of the coast beyond a simple boundary (line) marked by the land-ocean interface involves bringing together two environmental domainsand thus two very different scientific fields. Establishing an operational definition for the coastal zone is more about bridging different science approaches and results than establishing a single an autonomous

field of science. For this reason, a wide range of definitions and/or common frameworks aimed at defining the coastal zone have emerged over the past five decades, inspired by biologists, geomorphologists, geologists and/or oceanographers. This study will not attempt to review each one of these frameworks but will use the definition of the "coastal tract" proposed by Cowell et al. (2003) as an operational framework, as it captures reasonably enough both the subaerial and subaqueous nature of the coastal zone (figure 2).

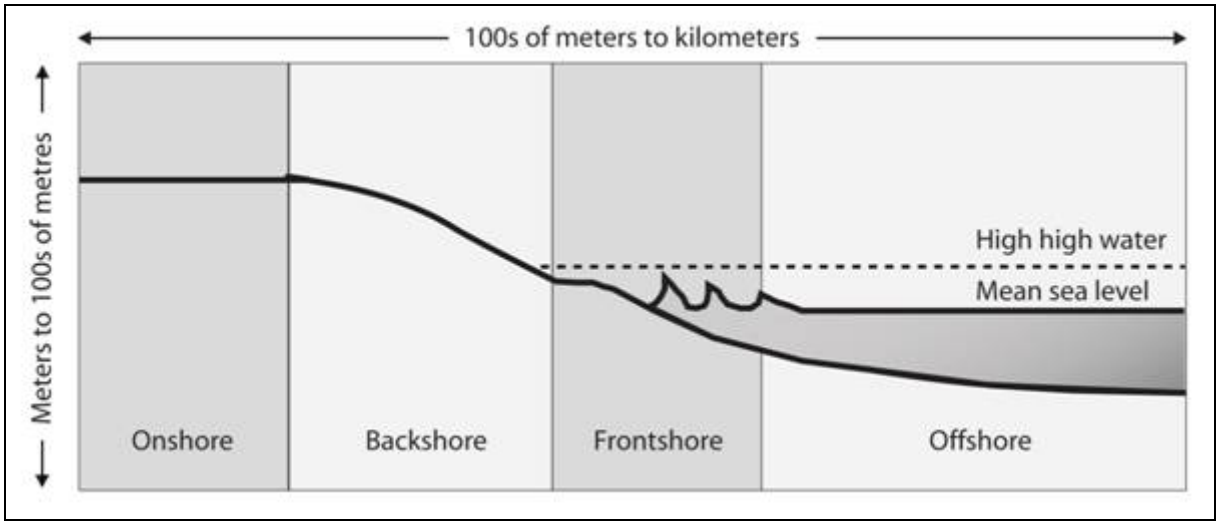

Figure 2 - The coastal tract. Modified after Cowell et al. (2003).

It should be noted that no attempt to establish a similar framework specifically for arctic coasts has been established to the knowledge of the author. Ruz et al. (1992) proposed a description of the shoreface and backshore area of the coastal tract which focused on the dynamic processes modifying the profile of the coast, specifically thermokarst. Other studies in Russia have indirectly proposed conceptual schemes of the coast (Aré, 1988), but most were biased regionally and/or focusing on specific processes. A simple conceptual description of the Arctic coastal tract incorporating uniquely arctic (polar) processes (permafrost, fast ice, sea ice, etc.) has yet to be proposed.

2.1.2 Long-term coastal evolution

Marine coasts are complex systems. As the land-ocean interface they integrate a wide range of both offshore (deep water wave formation) and nearshore (wave refraction, wave translation and longshore drift) processes. Long-term coastal erosion is often explained by a landward and upward shift of the subaqueous profile (shoreface) as a result of relative sea level rise (Bruun, 1962). In a traditional erosive scenario, the upper shoreface undergoes erosive retreat into the backshore area, while the offshore zone and the adjacent seafloor is

aggrading with the newly eroded material from the shoreface (transgressive sequence). In the transgressive scenario, the aggradation of the seafloor seaward of the erosive shoreface zone results in the widening of the nearshore platform (surf zone). In the Arctic, particularly northern Russia which hosts some of the widest and flattest coastal shelves on Earth, this phenomenon is particularly acute and leads to the widespread development of dissipative profiles along coasts located at the landward edge of large continental shelves. This is the case for the shelves of the Laptev and East Siberian Seas; the 100 m isobath often lies as much as 800 km from the coast. The 10 m isobath often referred to as the lower end of the shoreface can lie as far as dozens of km away from the coastline. This research does not address the dynamics of erosion during the late Pleistocene and throughout the Holocene, but the reader should be aware that the shore profile has been considerably influenced by the flat morphology of Arctic shelves during the Holocene.

2.1.3 Arctic specificity

Wind and tide induced wave action along the shoreline is the most important direct cause of coastal erosion in temperate regions. Waves attack the base of the shore face and remove material (in offshore and longshore directions) thus perpetually exposing new sections of the cliff to erosion. If there is insufficient sediment transported into the system (sources can include onshore and longshore transport or rivers) to replace the material carried away from a shoreline, the shore will retreat or change shape in a dynamic equilibrium with natural processes such as wave action.Erosion along unconsolidated Arctic coasts is different from similar shorelines in temperate regions due mainly to the limiting affect of the short open-water season (3-4 months) and to the presence of permafrost and ground ice (Solomon, 2005). Ice push and sea ice scour are also locally significant. Figure 3 illustrates the complexity of processes and forcing elements acting upon the Arctic coast.

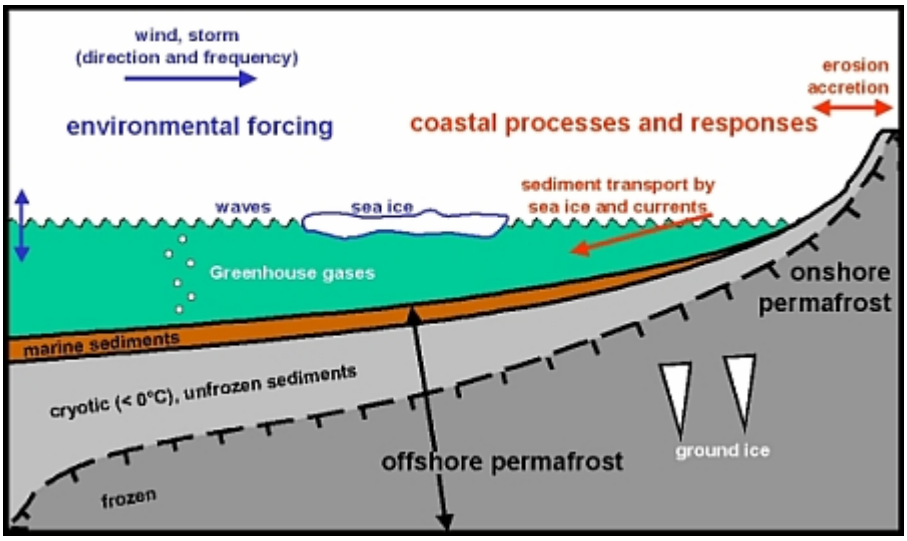

Figure 3 - Processes and environmental forcing elements acting upon the coast in the Arctic, after IASC, 2001.

The open-water season in the Arctic generally extends from June to October. Storms, which are the largest driver of erosion, occur throughout the year but their impact is limited due to the limited presence of sea ice cover during the fall, summer and spring (Atkinson, 2005). Even during the summer period, chunks of sea ice in various quantities impede and moderate the development of waves in the shore zone.

2.1.4 Thermal-mechanical erosion

Ground ice is a unique feature of polar coastal systems. It is present in the subaerial part of the shore profile, but also underneath the water column, as submarine ground ice (Mackay, 1972; Rachold et al., 2007). Its presence affects both the response of the shore to thermal-hydrodynamical forcing and the sediment budget of the coast (Are, 1988; Dallimore et al., 1996). The presence of ground ice leads to a process termed “thermal erosion” (Are, 1988) which encompasses the combined action of waves (mechanical erosion) and thawing of the permafrost (thermal abrasion). Thermal erosion has also been called “thermoerosion”, “thermal erosion” and “thermal-mechanical erosion” by several other authors. We will use the latter term, also used by Kobayashi et al. (1999), as it best portrays the combination of two distinct processes at the land-water-interface. Are (1988) suggested that erosion of frozen cliffs is a combination of thermal abrasion/denudation and mechanical erosion. Thermal abrasion plays a factor in the direct melting of permafrost in coastal bluffs, when those bluffs are in contact with sea water above 0°C. All sediments incorporated in the ground ice are released. Thermal denudation is the reduction of the strength in subaerial materials due to thawing of permafrost. Mechanical erosion is linked to the physical action of incident waves

on coastal bluffs. Thermal abrasion, combined with mechanical erosion induces an important undercutting of the coastal bluffs, which leads to the failure of the cliffs. When permafrost is characterised by large quantities of excess ice (that is, when moisture content exceeds saturation), the strength of the material is linked mainly to the cohesion (cement) of the ice matrix. Melting of the ground ice through heat conduction from seawater and/or turbulent Reynolds-type currents, the sediments lose their strength and subside, and are easily washed away by wave erosion (figure 4).

Figure 4 - An erosive ice-rich coast on the shore of the Bykovsky Peninsula, Laptev Sea, Russia. Photo: M. Grigoriev.

Kobayashi *et al.* (1999) have modelled the evolution of a two-dimensional frozen cliff and highlighted the ice content-dependence of erosion and the rapid loss of strength following first the increase in permafrost temperature and second the transfer of latent heat due to ice melting. Héquette and Barnes (1990) also demonstrated the dependence of the thermal-mechanical process to ice contents in the exposed frozen cliff, using statistical methods.

Mackay (1986), Dyke (1991), Dallimore *et al.* (1996) have suggested that the degradation (i.e. melting) of subsea permafrost by lowering the submerged profile (and therefore modifying the shoreface equilibrium may accelerate coastal retreat. According to Dallimore *et al.* (1996), "volume reduction caused by thawing of both eroded and submerged sediments can result in a substantial decrease in sediment supply to the nearshore zone and deepening of the nearshore bathymetry". Héquette and Barnes (1990) suggested sea-ice processes are an additional factor for the lowering of nearshore profiles. Ice processes including ice gouging, ice pile-up, and ice enhanced current scour (Forbes and Taylor, 1994;

Ogorodov, 2003) are eroding the shoreface and nearshore area and are "significant contributors to rapid coastal erosion and to maintaining an equilibrium shoreface profile" (Héquette and Barnes, 1990). Reimnitz and Barnes (1987), Reimnitz et al. (1990), Héquette et al. (2001) and Rekant et al. (2005) have also addressed the significance of these processes in the Beaufort and Kara Seas.

Thaw settlement and ice scour contribute to the lowering of the profile of the nearshore zone, but do not explain entirely the excessive rates of erosion observed in the Arctic. The rest is probably due to the combined action of thermal denudation and thermal abrasion. The presence of ground ice in subaerial coastal sediments indeed facilitates erosion through the occurrence of large thermokarst features in the coastal zone (Lantuit and Pollard, 2005; Lantuit and Pollard, 2008; Wolfe et al., 2001) which will be looked at in detail in section 2.1.7.

2.1.5 Storms

The greatest amount of coastal erosion occurs during these storm induced wave activity and surge events. According to Solomon *et al.* (1994) and Solomon and Covill (1995), storm surge events in the southern Beaufort Sea account for most of the observed erosion. Coastal cliffs are exposed to a wider wave-attack zone during storm surges which can reach a height of 2.4 m in the Canadian Beaufort Sea (Harper, 1990; Dallimore *et al.*, 1996). A significant part of the wave energy and subsequent transport of sediment occurs during these low frequency high magnitude events. Harper and Penland (1982) estimate that over 20% of the wave energy is expended over only 2% of the open-water season. An ice-free fetch up to several hundreds of kilometres during the open-water season allows the development of large waves which induce both mechanical and thermal processes at the land/sea interface. Melting of ground ice results in the addition of fine-grained sediment to the swash zone which is then transported along- or off-shore. Wave height, wave power, and ice contents are the critical variables influencing rates of coastal erosion during storm surges (Héquette and Barnes 1990; Solomon et al., 1994).

2.1.6 Tides

The Arctic Ocean is characterized mainly by low astronomical tide ranges (lower than 2 m) (figure 1). At a few locations in the Arctic (southeast Baffin Island, Canada and Mezen Gulf Russia), tides greater than 10 m can be observed, but the vast majority of the coastlines of the Arctic are characterized by very low tides (Walker, 2005). This is particularly true for

the two study sites included in this investigation, namely the Yukon Coastal Plain and the Bykovsky Peninsula. Despite these low tides, storm surges can affect vast areas inland when the coast is made of low coastal plain surfaces (Whalen et al., 2006), but those must be primarily attributed to the wind-induced swell.

2.1.7 Landforms in the Coastal Plain

In the subaerial part of the coastal tract, permafrost degradation (i.e. "thermal denudation" in Aré's (1988) typology) occurs in different ways, depending upon the morphologic parameters of the cliff and on the amount of ground ice.

Figure 5 - Block failure. The height of the cliff is approximately 20 m. Photo: W. Pollard.

Block failures

Where large tundra polygons separated by ice wedges which lower end is above mean sea level occur in the coastal zone, the cliff is subject to block failures (figure 5). Block failures involve the collapse of large blocks (from tens to thousands of cubic metres) characterized by angular edges which detach from the cliff under the influence of gravity. Block failures occur after: (1) the undercutting of the frozen cliff by thermal-mechanical-erosion and the formation of a thermo-erosional niche (figure 6) and (2) the failure of blocks

along ice wedge polygons, when the thermo-erosional niche extends to the point where overburden pressure exceeds the shear stress of the material. It seems likely that thermal contraction cracking associated with ice wedge formation plays a potential important role in this process (Hoque and Pollard, 2008).

Figure 6 - Thermoerosive niche at Komakuk Beach. Thermoerosive niches extend as much as 6 m.

Retrogressive thaw slumps

When ground ice is present as massive tabular ice bodies, retrogressive thaw slumps develop by backwasting of exposed ice-rich sediments. Retrogressive thaw slumps are large landslide-like features that extend inland between 5 and 500 m and range between 5 and 1000 m wide. Retrogressive thaw slumps generally consist of three main components (Lantuit and Pollard, 2008): (1) A vertical or sub-vertical headwall, comprised mostly of the active layer and ice-poor organic or non-organic materials, (2) a headscarp whose angle varies between 20 to 50°C and which retreats by the ablation of ice-rich materials due to sensible heat fluxes and solar radiation (Lewkowicz, 1987) and, (3) the slump floor, which consists of pooled water, fluid mudflow and plastic flow deposits that expand in a lobate pattern at the toe of the slump. (figure 7). If the exposed massive ice melts at rates that exceed the rates of thermal-mechanical erosion at the base of the cliff, then a retrogressive thaw slump is initiated

(Lewkowicz, 1987; Robinson, 2000). On Herschel Island, the headwalls of the retrogressive thaw slumps expose up to 13 m of ice (De Krom, 1990; Wolfe *et al.*, 2001). However, the thickness of the ground ice is probably greater since the lower portion of the ice is concealed by meltout debris that accumulates at the base of the retreating headwall.

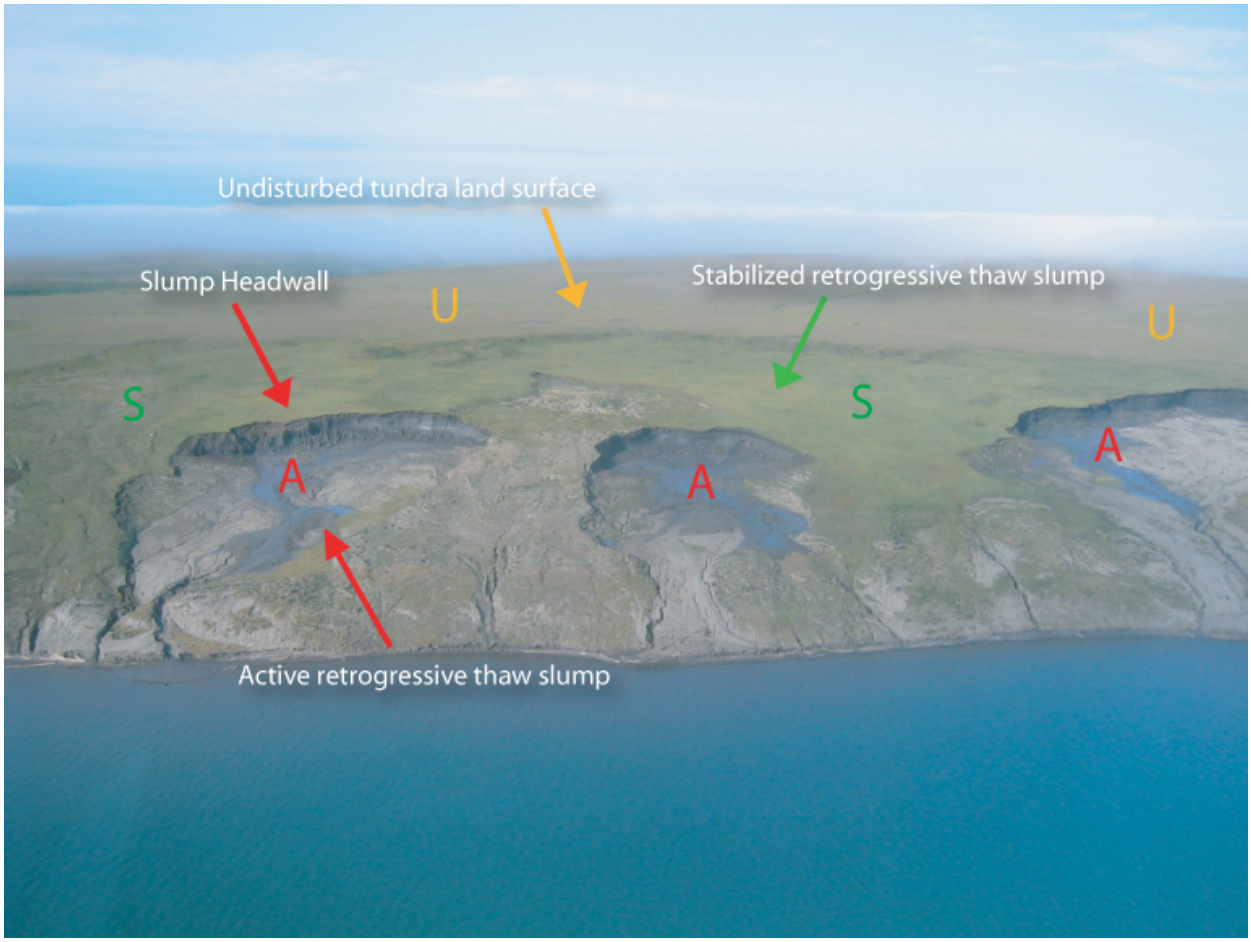

Figure 7 - Polycyclic retrogressive thaw slumps in Thetis Bay, Herschel Island. The slumps extend about 300 m inland and are approximately 100 m wide.

In coastal exposures, the rate of retrogressive thaw slump retreat is closely linked to the intensity of wave action, as the removal of retrogressive thaw slump debris by incident wave action or littoral drift aids in, (1) maintaining a steep headwall gradient and, (2) preventing the build-up of debris on the headwall and/or on the retrogressive thaw slump floor. Retrogressive thaw slumps do not require a removal of the debris to continue backwasting, since their expansion is driven mainly by massive ground ice melting or sublimation in the headwall related to solar radiation and positive air temperatures. However, the removal of debris by wave action and littoral drift helps sustain the thaw process and enhances retrogressive thaw slump activity. This type of positive feedback is most important during the initiation of coastal retrogressive thaw slumps.

2.3 Arctic coastal erosion in a changing climate

2.3.1 Environmental forcing

Most of the coastal retreat observed in the Arctic is due to a combination of hydrodynamical forcing, thermal denudation (often thermokarst), and thermal-mechanical erosion, as explained in section 2.1.4. Increased rates of sea level rise and sea-ice degradation as predicted by the Intergovernamental Panel on Climate Change in its most recent report (IPCC, see Anisimov et al., 2007) would likely result in greater rates of coastal retreat.

The extent and duration of sea ice cover directly influences the impact of storm induced wave activity by controlling both the strength and the number of stormsthat may affect a section of shoreline in any one year. Greater fetch lengths allow the development of larger waves, and a longer open water season increases the probability to get strong winds converted into strong waves. Summer sea ice extent has steadily declined in recent years, and in 2007, the sea ice cover was the lowest it has been since satellite measurements began in 1978. This trend is expected to continue (Holland et al., 2006, Stroeve et al., 2007), and can significantly increase the open water period when wave erosion occurs (Maxwell, 1997). In the Canadian Beaufort Sea, for example, open water currently lasts from June to early October (about 120 days), but the duration of open water is expected to increase by 60 days to 150 days (McGillivray et al., 1993). In the Laptev Sea and in the Beaufort Sea, the largest number of storms occur in June and October, precisely on sea ice onset and offset, which will likely prompt dramatic changes on the coast.

Sea level rise is also predicted to increase more in the Arctic due to thermal expansion of ocean waters (steric effects), changes in sea-level pressure and changes in the curvature of mean wind fields (Proshutinsky et al., 2001, Anisimov et al., 2007). Depending on the isostatic history and of the tectonic characteristics of the area, sea level rise could lead to increased flooding during storms, flooding further inland than before and also to stronger erosion rates following readjustment of the coastal tract profile.

2.3.2 Environmental and socio-economical implications

Organic carbon and contaminants

An increase in coastal erosion would result in increasing volumes of terrigenous material released from the coast. Such change could result in dramatic increases in the volume

of sediment, and hence, of organic carbon to the Arctic Ocean, which according to some authors (Rachold et al., 2000) is close to and sometimes exceeds the quantities contributed by rivers flowing to the Arctic Ocean. A change in the quantities of organic carbon released in the coastal zone could dramatically modify the Arctic carbon cycle as the dissolved organic carbon (DOC) in these sediments would probably mot be buried and could persist in the upper ocean to be transported in the surface current systems (Opsahl et al., 1999). This would result in complex and potentially important changes in DOC pathways through the Arctic and DOC storage (Stein and Macdonald, 2000, p.21, Rachold et al., 2003). Sediments, DOC, and contaminants mobilised by erosion have the potential to create dramatic changes in the geochemistry and biodiversity of the nearshore zone (Couture and Spiridonov, 2006).

Physical processes

Changes in the intensity and frequency of physical processes acting upon the coast can also induce major threats to existing infrastructure. Ultimately those threats can convert to pressures on the socio-economical structure of a region or a community. Many arctic communities are faced with increasing erosion threats. Many examples from the destructive impacts of the sea on Inuvialuit or Inupiat settlements have been showcased in national and international broadcasts. In Tuktoyaktuk, in western Canada, erosion has shifted the shoreline more than 100 metres in the last 50 years and is causing the abandonment of a school, houses and other building (Johnson et al., 2003). Costs or relocation for Tuktoyaktuk or for Shishmaref, a community on a small island off the Alaskan coast also affected by dramatic erosion processes, may reach $180 million (Couture and Spiridonov, 2006). Industry is also affected by changes in erosive potential. Ogorodov (2005) mentions the many oil and gas infrastructure located immediately at the coast experiencing major erosion processes. Climate change in likely to redefine the way the industry was protecting its pipelines in the coastal zone, the way it was building artificial islands on the shelf (Gillie, 1988), or the ways it was planning on oil and gas terminals on the coasts of the Arctic.

Socio-economical implications

The reduction of summer sea ice cover extent would mean that stretches of coast virtually untouched by wave erosion during most of the late Holocene could now be exposed to ocean waves and high rates of erosion. A large part of these coasts, and several settlements built on them, are made of unconsolidated fine sediment prone to ground ice presence and with low resistance to hydrodynamical forcing. Sea ice disappearance could therefore have

dramatic effects on communities unprepared for threats of this kind.

Current demographic projections for the Arctic tending to predict an ever-growing northern population, political will to assess possession of northern territories in the light of mineralogical and geological exploration, and economical perspectives following the opening of the Northwest Passage and the northern sea route show that the presence of man in the north is likely not to disappear. Most coastal settlements facing erosion threats may not be abandoned to the sea that easily as they often represent a combined economical and geopolitical interest for external economical and political stakeholders. The coast crystallizes the antagonism between increasing environmental changes driven by climate change and socio-economical forces. Several communities, such as the ones located along the Northwest Passage might benefit from the exposure of their coasts to the open ocean, yet this presupposes careful engineering considerations anticipating the reaction of the coast to this new physiographic setting and increasing costs of construction. In this context, coastal erosion studies such as the one pursued in this work aim at providing a basic understanding of processes occurring at present on the coast. They form the basis for the development of sustainable coastal management practices on the Arctic coast.

2.2 Past and current issues in Arctic coastal erosion science

2.2.1 Arctic coastal erosion science history

Despite early investigations of the coasts by explorers of the polar regions, Arctic coastal research has generally been neglected and is until now only practiced by a handful number of scientists.

Arctic coastal erosion science has probably started as soon as the coasts were inhabited, although it was probably not termed science yet. For instance, in a study investigating the perception of the coast among Inuit people from eastern Nunavik, Heyes and Jacobs (2008) found that the number of words used to describe the tide marks and the tide far exceeds the number of words used to describe our “coastal tract”. For instance, Inuit elders from Kangiqsualujjuaq use up to 8 different words to describe the low tide (Heyes and Jacobs, 2008, table 1). The first traces from Arctic coastal science, in the western perception of it, are found as patches of coastal science in the large environmentalist works of the early Arctic explorers. Franklin (1828) first reported in the western literature on the shores of the Polar Seas, but didn’t focus on the very physical nature of coastal erosion. Baer (1843) was the first to report on the large ice-rich exposures that, at the time, enclosed the mammoth first

discovered by Adams in 1799 (Adams, 1807) on the Bykovsky Peninsula, northern Siberia. Bunge (1895), Toll´ (1897) all presented accounts of coastal erosion occurring in Arctic Seas, but the first milestone in Arctic coastal erosion studies was the classic monograph on permafrost and coastal morphology by Leffingwell (1919) which provided detailed accounts of northern Alaska's coasts. During the rest of the twentieth century, Arctic coastal evolution started to receive a more important interest among the scientific community but split regionally to follow its national-based science organisations. Over the 1930-1990, a small but very active community started to highlight the link between thermal processes and coastal erosion, notably in the USSR, essentially, through works of F. Aré (Aré, 1964) N. Grigoriev (Grigoriev, 1962), P. K. Khmiznikov (Khmiznikov, 1934),Y.V. Klyuyev (Klyuyev, 1966, 1970) and V. P.Zenkovich (1985), but particularly through the release in English language of the reference monograph of F. Aré (Aré, 1988). In North-America, both the engineering and research communities developed parallel bodies of literature with the works of J. R. Mackay (Mackay, 1960, 1963, 1986), E. Reimnitz (Reimnitz et al., 1988) and H. J. Walker (Walker, 1982), among others. This period saw the discovery of subsea permafrost, of the link between hydrodynamical forcing and thermal action of seawater, of the role of sea ice in gouging and settling the shoreface, of the description and interpretation of thermal denudation landforms and of the identification of storms as the preponderant agent of coastline modification.

The following decade, under pressure to redefine science objectives after the end of the collapse of the USSR and the oil and gas boom, saw the community identifying some new issues to be addressed, including the relation between climatological records and erosion data, increasing demand for community-based risk-assessments, creation of monitoring programs at observatories spread throughout the Artic and assessment of sediment, nutrient and contaminant release from coastal erosion at the Arctic scale. Several of these efforts are ongoing and form the basis of the Arctic Coastal Dynamics program (ACD) (Brown and Solomon, 1999). These new orientations are the basis upon which Arctic coastal erosion science will build during the 21st century.

2.2.3 current issues

Arctic coastal erosion science is facing several issues that the research community should address over the next twenty years.

Establishment of rates of erosion and accumulation

The compilation of rates of erosion and accumulation is probably the most common

research exercise performed on coasts. It generally involves the use of airphotos and/or satellite imagery which have been acquired over long timespans. Solomon (2005), Lantuit and Pollard (2008) and many before them (Mcdonald and Lewis, 1973; Harper, 1990) have performed this kind of calculations. An inherent limit of the use of imagery is the time since it has been acquired and records generally do not extend earlier than the 1930s. Through the recent release of declassified American spy imagery, it is now conceivable to acquire low-cost high resolution imagery dating back to the 1960s, as this PhD thesis shows, and to use them to compute rates of erosion. Paradoxically, modern imagery is often more expensive to acquire because of the high costs associated with high resolution satellite imagery. The multiplication of these sensors in the near future should make it easier to sustain frequent acquisitions of imagery over key sites.

Acquiring rates of shoreline erosion and/or accumulation is therefore necessary yet not sufficient. Future studies should use these rates to investigate further and monitor corollary processes. Climatological data, Shoreface profile, hydrodynamics should be recorded parallely to shoreline retreat to gain enough information to feed into prognosis efforts. Finally the rates calculated using these methods have not been used enough in combination with sea level rise data to model coastal erosion throughout the Holocene and provide useful information to the community of paleooceanographers. A large number of questions pertaining to the sedimentological nature and the amount of sediment on the shelves of the Artic Seas could benefit from such studies. Chapter 4 in this thesis aims at combining shoreline retreat, climatological data and an outlook into the late quaternary history of the Laptev Sea shelf to suit those objectives.

Development of monitoring sites

Because monitoring efforts incorporating the above-mentioned criteria (climatology, hydrodynamics, bathymetry, etc.) are impossible to perform systematically at the Arctic scale, the future of Arctic coastal science will rely on a set of observatories where highly detailed temporal and spatial records of criteria relevant to coastal erosion should be performed. This includes the evolution of permafrost temperature, nearshore bathymetry, onshore and offshore winds measurements, sedimentology, geochemistry, etc. A challenging view would argue that the manpower to maintain those sites would probably be a deterrent to such enterprise; however, following on the International Polar Year (2007-2008), international efforts aiming at integrating networks of observatories in the Arctic devoted to all branches of science (i.e. Sustained Arctic Observatory Network, SAON) should provide the framework to combine

and rationalize the science made at Arctic observatories, and, hence, to achieve these goals.

Research on critical processes

Research on critical processes has been many fold on the Arctic coast, probably because of the large variety and uniqueness of Arctic coastal landforms, both above and below sea level (see section 2.1.7). Authors have however traditionally split in two groups, virtually separated by the shoreline: those investigating geomorphological landforms above sea level and those interested in the part below water. A further gain in knowledge on coastal processes in the Arctic will only be possible if future research integrates both aspects in a common framework.

To do so, research should focus both on identifying boundary conditions for the thermal and mechanical parts of coastal erosion. This should be done by instrumenting coastal transects within the monitoring network mentioned above and also by fostering the use of new tools, including physical modelling of both hydrodynamical conditions and permafrost behaviour. This task, which was traditionally handled by the engineering community has been largely neglected and should be a main feature of future coastal research in the Arctic. Chapter 5 of this thesis is an attempt to investigate the coastal zone of the Yukon coastal plain by providing geotechnical, sedimentological, geochemical, ecological and geomorphological indicators of present and past retrogressive thaw slump activity in order to better characterize the drivers of thermokarst triggering and activity.

Prognoses

Prognoses and modelling efforts in the Arctic have been scarce but have provided useful tools to predict the reaction of the coast to changing conditions. Kobayashi et al. (1999), Ostroumov (2005), Leont'yev (2003) and Francis-Chythlook (2004) have attempted to provide models of coastal evolution incorporating the specificities of the Arctic environmental regime. However, these models have generally been regionally biased or have focused on shoreline modelling and haven't taken into account the entire shoreface. The lack of long-term data at multiple sites is a major deterrent to provide boundary conditions to the modellers. Paradoxically, Rising concerns on the fate of the Arctic coastal environment have prompted the need for such models, and one of the major challenges of the twentieth century will be to expand local modelling efforts to the entire Arctic coastline. Global efforts exist in the framework of ACD and have proposed the compilation of a global classification of Arctic coasts to compute amounts of sediment, and organic carbon to reach the coastal zone

following erosion (Rachold et al., 2002). Chapter 3 (and annexes A and B) in this thesis present an attempt to refine the results of such computation by providing geospatial tools that reduce uncertainty due to the use of monoscale geospatial datasets.

CHAPTER 3 – MANUSCRIPT #1 - TOWARDS A CALCULATION OF ORGANIC CARBON RELEASE FROM EROSION OF ARCTIC COASTS USING NON FRACTAL GEOSPATIAL DATASETS.

3.1 Introduction

Arctic coasts are sensitive to even small changes in their environment and are therefore highly vulnerable to the potential impacts of climate change. Thawing permafrost, sea level rise, changing sea ice conditions and increased wave activity interact synergistically and may result in accelerated rates of coastal erosion and thermokarst activity (The process by which characteristic landforms result from the thawing of ice-rich permafrost) in areas of ice-rich permafrost. In these regions, considerable quantities of nutrients are released in the nearshore zone by coastal erosion. According to Rachold et al. (2000), sediment input to the Arctic shelf resulting from erosion of ice-rich, permafrost-dominated coastlines may be equal to or greater than input from river discharge. Higher coastal retreat rates will yield greater quantities of organic matter contained in sediments to the nearshore zone. Much of the dissolved organic carbon (DOC) from these sediments would not be buried and could persist in the upper ocean to be transported in the surface current systems (Opsahl et al., 1999). This would result in complex and potentially dramatic changes in DOC pathways through the Arctic and DOC storage (Stein and Macdonald, 2000, p.21). Determining present-day sediment sources and transport rates along high latitude coasts and inner shelves is therefore critical for predictions of future evolution of these coasts in response to climatic and sea level changes.

Current estimates of total organic carbon (TOC) input through coastal erosion are based upon a combination of field investigations and the study of airborne and spaceborne image time series. Sedimentological and geochemical investigations of coastal exposures are used to provide TOC values, ice contents and mechanical properties of sediments. Field surveys and /or remote sensing data provide coastal retreat rate estimates for the various types of shoreline. These characteristics are subsequently extrapolated to longer and other coastline segments with similar geomorphologic characteristics. The extent to which these estimates are performed and the uneven distribution of case studies in the Arctic greatly limits the confidence of these predictions. (Grigoriev et al. 1993).

The Arctic Coastal Dynamics Project (ACD) was established by the International

Arctic Science Committee (IASC) to address these issues and to provide the first reliable estimate of organic carbon input from coastal erosion to the Arctic Ocean. It provides a geospatial framework and refined sedimentological and geochemical estimates in coastal sectors throughout the circum-Arctic (Lantuit et al., in press; IASC, 2001; Brown and Solomon, 2000; Rachold et al., 2002). The estimates of organic carbon input are based on a single globally-consistent shoreline dataset, the World Vector Shoreline (WVS) and a geomorphological coastal segmentation implemented by regional experts (IASC, 2001; Brown and Solomon, 2000; Rachold et al., 2002).

Pan-arctic scale or global scale estimates of shoreline change are needed to complement global scale climate modelling and other earth system analyses. The latter approaches have limitations inherently linked to the scaling up process based on the extrapolation of point and small area data to larger areas based on landscape relationships between surficial geology, geomorphology, topography and coastal morphology.

However, before a reliable value can be derived from this classification, data quality assessments have to be performed on the resulting datasets. These assessments focus on the quality of the data provided by the regional experts (TOC content, ground ice content, coastal retreat rates, etc.) and the data quality losses associated with the use of geospatial tools to compute TOC release at the circum-Arctic scale.

Since the unifying control on the resolution of this calculation is a function of available datasets, the focus of this paper is to assess the uncertainties associated with geospatial manipulations providing TOC release estimates within the ACD geospatial framework. In particular it emphasizes the problems related to a non self-similar (self-similarity refers to the fact that they exhibit similar features, and hence different lengths at different scales) line dataset (the WVS) for sediment input estimates and the methods needed to minimize errors in the conversion of physical erosion processes into numerical values in a consistent manner at a circum-arctic scale.

The objectives of this paper are therefore:

1) to calculate the fractal dimension of selected Arctic coastlines (that is, the degree of complication of a statistically self-similar shoreline expressed as a dimension D) differing in type and location and show that shoreline lengths vary greatly across scales
2) to investigate the scale dependant variability of coastal length estimates compared to the WVS at the same selected sites
3) to propose a more robust method than length from digitized coastal lines to

calculate sediment volumes, and hence organic carbon, released from coastal erosion.

This paper will show that current measurements are not sufficiently accurate to provide reliable numbers of TOC release from coastal erosion and that computation methods should be revisited within the limits of existing tools and datasets.

3.2 Background

3.2.1. Definition of erosion

Coastal erosion is the removal of land/sediment from shore-backshore area to the ocean due to wave action, sea level rise and/or anthropogenic intervention. It affects the entire shore profile, including the lower and upper shoreface and the backshore (for definition of these terms see Cowell et al. (2003), and results from cumulative effects of several processes occurring at different spatial and temporal scales. There is a strong relationship between temporal and spatial scales with respect to the nature of processes occurring in the coastal zone. Short-term shoreline variability is associated mostly with seasonal to annual stochastic fluctuations in environmental conditions, while long-term shoreline changes are driven mostly by structural trends in sea level rise and sediment supply (Stive et al., 2002). This near-linear relationship between space and time is reflected in the pattern of change in the shore profile. Short-term coastal changes are generally detected in the upper shoreface and correlate well with changes in shoreline position (shoreline being defined as the high water or low water mark). Low-order trends in coastal change (102 to 103 years) on the other hand are reflected in the evolution of the lower shoreface (Cowell et al., 2003). The latter is related to the well142 known findings of Bruun (1962, 1988) on the relationship between long-term (structural) coastal erosion and sea-level rise.

The focus of the ACD project is the quantification of the current and future annual nutrient fluxes in the Arctic coastal zone. There is an apparent paradox in dealing with current (yearly) fluxes and predictions over hundreds of years since the processes driving the changes in shoreline position are of different nature and will not be detected using the same methods. Current fluxes are established using rates of erosion compiled over long (10 to 102 years) time series (Lantuit and Pollard, 2008; Solomon, 2005). These time series are used to attenuate the effect of interannual and sub-decadal shore variability and to reduce uncertainties associated with space- and air-borne imagery geoprocessing on the computation of coastal erosion rates (Anders, 1991; Crowell, 1993; Thieler, 1994; Dolan et al., 1980;

Dolan et al., 1992). Fluxes compiled over such time intervals therefore capture decadal to centennial variability in coastal changes. These time scales, referred to as intercentennial by Stive et al. (2002) are the ones of interest to ACD.

Intercentennial variability (10 to 102 years) in rates of coastal change is better explained by relative sea-level changes, regional climate variations, and extreme events frequency (Stive et al., 2002). Its effects will be visible on both the upper and lower shoreface as well as on the backshore. Sediment volume losses in the shore zone will therefore be associated with displacement in all sections of the shore profile. Knowing that the 10 m isobath, commonly accepted as the bottom limit of the lower shoreface, can sometimes lie as far as 50 km offshore in the Arctic, one can easily imagine the challenges associated with incorporating the entire shore profile in sediment and carbon flux calculations throughout the Arctic. The hypothetical inclusion of the upper and lower shorefaces in flux calculations is impractical for two reasons. First, because the quality of the bathymetric data between 0 and 10 m is generally poor and not consistent throughout the Arctic and second, it would have to be coupled to numerical models incorporating both on-offshore and longshore sediment dynamics operating at the circum-Arctic scale, which is unrealistic.

A general hypothesis in this paper is therefore that coastal erosion is restricted to its subaerial component (backshore and subaerial part of the upper shoreface) and a second hypothesis is that the detection and quantification of coastal erosion can be achieved using the position of the shoreline only. Ali (2003) points out that linear representations of the coastline "encapsulate implicitly the cumulative effects of the underlying coastal processes responsible for shoreline change" (Ali, 2003, p. 56). It is particularly true when movements of the shoreline are averaged over hundreds of years. They can then be considered to represent long term (intercentennial to centennial) trends in coastal erosion and can therefore be used as such (Stive et al, 2002).

Constraining erosion to the transfer of the subaerial part of the profile into the nearshore zone and the immediate dispersal of sediments eliminates the need to consider all on-offshore and longshore sediment movement occurring below sea level. On intercentennial scales, however these movements can be considered to be transient phenomena, in particular in regards to the carbon cycle (Stein and Macdonald, 2003; Denman, 1993). The volume of sediment released by subaerial erosion can therefore be linked to the erosion of the shore profile when averaged over long time spans. Consequently, the assessment of volumetric erosion can be extracted from the movements of the shoreline position.

3.2.2 Calculation of shoreline erosion

Monitoring changes in shoreline position and subsequently computing volumes of released sediment and TOC can be obtained by several methods including the combined use of digital terrain models and sea level models to mark the intersection or by digitizing the shoreline from aerial photos or from high resolution satellite (Li et al., 2001). Volumetric measurements have been assessed directly using softcopy photogrammetry (Lantuit and Pollard, 2005) or indirectly using photogrammetry-derived planimetric erosion rates (Lantuit and Pollard, 2008, Solomon, 2005, etc.). Such approaches are inappropriate at the global scale because of the associated costs and limited data availability. The use of a single line dataset and a consistent methodology to provide estimates of volumetric erosion at the Arctic scale is necessary. This type of calculation is a first approximation and is not intended to be used for site-specific analyses.

2.3. Erosion calculation within the ACD framework

The ACD framework provides a unified methodology for the computation of carbon release from coastal erosion at the pan or circum-Arctic scale. To do so, ACD developed a consistent coastline segmentation and classification based on a single line geospatial dataset, the WVS (Lantuit et al, in press, IASC, 2001, Brown and Solomon, 2000, Rachold et al., 2002). The ACD classification was conceived as a broad framework designed to encompass existing classification schemes while capturing fundamental information for the assessment of climate change impacts and coastal processes. The classification was implemented by regional experts using various digital and paper products as well as personal knowledge and unpublished field data. This information was gathered into a circum-Arctic coastal database. This is a new and objective classification system that is primarily geomorphological in nature. It is described in more detail in Lantuit et al. (2008) and Rachold et al. (2002).

The classification scheme was used to create geomorphically homogeneous segments along the Arctic coast. The length of these segments (extracted from the WVS) varies between 1 and 50 km. Each of the segments is distinguished by common geomorphological, sedimentological and geochemical characteristics. This approach implies that geomorphic characteristics spanning tens of kilometers were integrated into single coastal units. Discussions on the accuracy of the upscaling steps and associated processes are discussed in detail in Lantuit et al. (in press). Our objective here is not to discuss the quality of the classification and segmentation process, but the issues associated with the use of a single line dataset in volumetric coastal erosion calculations. The segmentation used in the ACD

geospatial framework is based entirely on the WVS (Soluri and Woodson, 1990). The WVS is a digital data file extracted from each country's national map series at the 1:250 000 scale to represent shorelines globally. It is used in the ACD framework as the basis for the segmentation of the Arctic coasts and as a mean (approximate) position to compute first approximations of retreat and sediment (including carbon) volumes released to the nearshore zone by coastal erosion. It is also used to inventory ground ice content and its role in coastal retreat. Segments are stored in the ACD system as polygons in order to facilitate future updates to the WVS or the generation of a new shoreline dataset. The subaerial erosion and carbon flux are calculated using the following equation:

$$C_{tot} = \sum_{j=1}^{n} \left[C_j \cdot \rho_{s_j} \cdot \left(1 - \theta_{i_j}\right) \cdot \left(h_j \cdot l_j \cdot R_j\right) \right] \quad (1)$$

where C_{tot} is the total amount of organic carbon released to the nearshore zone, n is the total number of segments, C the total organic carbon content (by weight) of the cliff in %, ρ the dry bulk density of the enclosing sediment, θ the volumetric ice content in the cliff in %, h the height of the cliff, l the length of the segment and R the annual coastal retreat rate. This equation combines inputs from the classification itself (organic carbon content, dry bulk density of the material, ground ice content, backshore elevation and coastal retreat rates), and a geospatial characteristic extracted from the WVS (coastline length).

The major advantage of this type of empirical solution is that it is usable on vast areas and only requires the one geospatial input. Its main limitation, however, is that the accuracy of the coastline length is correlated with the intrinsic quality of the shoreline dataset and the scale of analysis to which it is applied. For our purposes, specifically the ACD computation of coastal change and volume fluxes, there is no indication that the WVS scale of 1:250 000 better than any other scale. The limitations of this dataset with respect to ACD analysis is a real concern and raises the question "are there other more suitable methods to compute coastal change and volume fluxes?"

3.3 Fractal coastlines

3.3.1. Fractals

Shoreline representations are *de facto* different for different scales and therefore estimations of shoreline length will vary with different scales of representation. Addressed first by Richardson (1961) in his analysis of coastlines in Australia, this property of spatial

data was further conceptualized by Mandelbrot (1967). The same coastline extracted from maps at different scales will have different lengths. More specifically and not surprising is the fact that data extracted from larger scale maps produces longer estimates of shoreline length. Mandelbrot (1967) expressed the relationship between scale and linear measure as the *fractal dimension* of the coastline, which is generally expressed through the *D* factor in Equation #2,

$$L(G) = MG^{1-D} \tag{2}$$

where L is the length of the coastline measured with a unit of length G, M a positive constant, and D the fractal dimension of the shoreline.

Mandelbrot further ascertained that coastlines would reproduce their planimetric pattern over a gradient of scales, resulting in what he terms their "self-similarity". Although the "self similarity" concept was later disputed by several authors in its relevance to real-world geomorphological processes (Andrle, 1996, Goodchild, 1980), the concept of fractal dimension is valid in its description of increasing coastline lengths with increasing scale.

Using the length of a shoreline dataset to compute volumetric coastal erosion as in Equation #1 is therefore problematic since the resulting values can vary greatly depending on the scale of the shoreline used. The errors in the calculation of volumetric coastal erosion associated with shorelines created at different scales are identified in several international projects attempting to quantify nutrient release to the nearshore zone (Bartley et al., 2001; Smith, 2005), but have not been systematically assessed. There is therefore a real need to investigate the uncertainties associated with the use of different shorelines.

The WVS is widely recognized as the most globally-consistent shoreline dataset, and is therefore an ideal proxy for calculations at the global scale because inconsistencies are reduced (i.e. it is a consistent dataset, that is, compiled from maps at the 1:250 000 scale from different sources, but by a single agency and using a consistent geoprocessing protocol). However, the WVS is a digital vector shoreline and is composed of arcs independent of scale. A WVS arc length will, for that reason, be distinguished by a constant length over scale gradients. The coastline length provided by the WVS will be constant across scales but there is no indication that this length will provide accurate volumetric coastal erosion estimates.

The WVS, as pointed out by Bartley et al. (2001), is relevant only within a certain range of scales, which are not necessarily compatible with volume computations. In that sense, using the WVS for this calculation is highly arbitrary. Obtaining information about the variations of Arctic coastline lengths across scales is therefore necessary and can only help us to gain an insight about the quality of the WVS and its relevance to calculations of total organic carbon (TOC) release.

Finding the length of Arctic coasts across scales and comparing it to the WVS is necessary but not sufficient. Additionally, Arctic coastlines differ in type and characteristics. There are sandy and rocky shorelines, consolidated or unconsolidated shore material, accumulative and erosive coastlines. Lacey patterns produced by thaw lake development are unique to arctic coasts and are particularly problematic. Arctic coastal types will feature patterns and sinuosities that differ considerably from elsewhere on Earth. Consequently, these shoreline types will be characterized by varying fractal dimensions. A sand spit shoreline delineation will vary less across scales than will a rocky shoreline. The challenge in computing volumetric coastal erosion at the pan-Arctic scale is therefore one of overcoming the 305 difficulties associated with differing coastal types. Coastal types have to be considered independently in this process. One of the objectives of this paper is to assess whether the WVS length is uniformly paired with coastlines created at a specific scale across coastal types. Ultimately, providing a means to calculate reliable estimates of volumetric change at the local scale, while dealing with the global nature of the issue is the main objective of this paper. The use of a simple shoreline dataset within a GIS is necessary to handle the data and the computation at this scale.

3.3.2. Methods

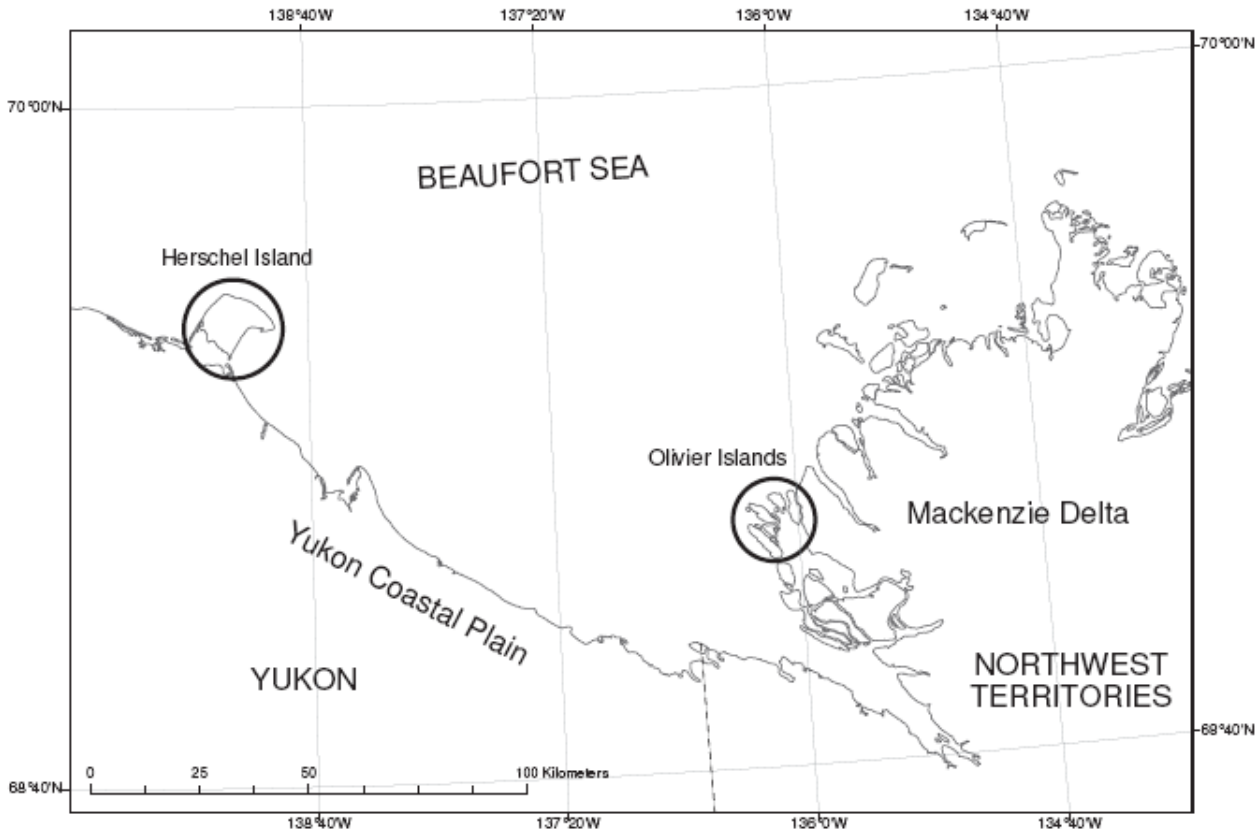

Figure 1 - Location of study areas in the Canadian Beaufort Sea area.

Eight study areas, located in the Laptev and Beaufort Seas were selected for this study. We focused on areas where long-term records of coastal erosion are available. Six of the areas were located in the Lena Delta area (Figure 1) and two on the Canadian Beaufort Sea coast (Figure 2). The Lena Delta area was investigated in detail by Rachold (2000), using archived and recent imagery to provide coastal retreat rates, and field investigations to characterize its rheological and geomorphological nature. The two sites located in the Beaufort Sea were studied using similar methods by Lantuit and Pollard (2008), Solomon (2005) and Jenner and Hill (1998). The sites were chosen to illustrate several coastline types (Table 1). Coastlines were divided into erosive, accumulative to stable, and thermokarst types. Thermokarst coasts are characterized by the presence of submerged ellipsoidal lakes which give the coast its lacey pattern. For a thorough definition of these terms, see Are (1988) and van Everdingen (1998).

In order to derive the fractal dimension of the shorelines, the coastlines were digitized using dividers varying in length (10, 20, 50, 100, 200, 500 and 1000 m). The divider method was originally used by Mandelbrot (1967) in his study of the coast of Britain. In this study, the operator followed the coastline and drew its path using constant divider spacings. Starting and ending points were fixed for all dividers

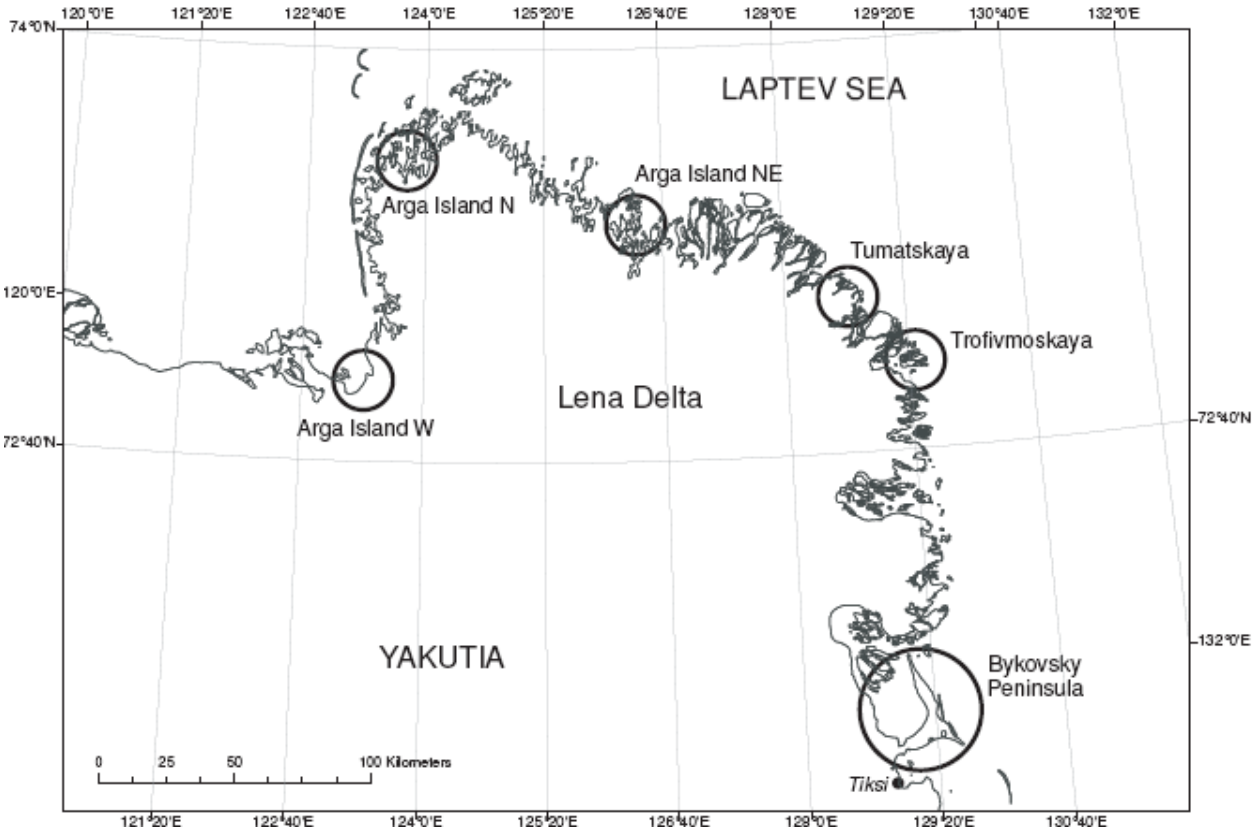

Figure 2 Location of study areas in the Laptev Sea area

The Laptev and Beaufort coastlines were digitized from Corona and Ikonos images. Corona images have been used to address coastal issues in Arctic settings (Grosse et al., 2005)

and have the added advantage of providing a low-cost high-resolution imagery of the coast, as well as having been captured in the 1960's, that is, the time at which most maps the WVS is based on were created. Corona original films were scanned on a photogrammetric-level scanner and resampled to a 2.5 m spatial resolution. An Ikonos image from 2000 resampled to 2.5 m spatial resolution for consistency purpose, was used to digitize the northern coastline of Herschel Island.

Table 1 - Study sites – Location and geomorphic characteristics

Site number	Site name	Coordinates	Coastal type	Description	References
Site 1	Bykovsky Peninsula	71°49'N, 129°21'E	Erosive coast	Ice-rich unconsolidated sediments undergoing strong erosion (2 to 3 m/yr)	Rachold (2000)
Site 2	western Arga Island	72°54'N, 123°19'E	Erosive coast	Sandy cliffs (2 to 5 m high) undergoind strong erosion	Rachold (2000)
Site 3	north-eastern Arga Island	73°25'N, 126°21'E	Thermokarst coast	Low sandy cliffs undergoing moderate erosion 2m/yr	Rachold (2000)
Site 4	northern Arga Island	73°37'N, 123°45'E	Thermokarst coast	Low sandy cliffs undergoing moderate erosion 2m/yr	Rachold (2000)
Site 5	Tumatskaya channel	73°10'N, 128°50'E	Accumulative to stable coast	Frontal delta lobe	Rachold (2000)
Site 6	Trofimovskaya channel	72°57'N, 129°26'E	Accumulative to stable coast	Frontal delta lobe	Rachold (2000)
Site 7	Herschel Island	69°37'N, 221°01'E	Erosive coast	High ice-rich cliffs made of unconsolidated sediments undergoing moderate to strong erosion (~ 0.8 m/yr	Lantuit and Pollard (2008)
Site 8	Olivier Islands	69°10'N, 223°47'E	Accumulative to stable coast	Accumulative delta lobe	Solomon (2005); Jenner and Hill (1998)

3.3.3 Results - Shoreline length

Our results, presented in Table 2 and Figure 3, show that the variation in length of Arctic coasts across scale is significantly high. For example, the length of the Trofimovskaya section of coast can differ by as much as 32.3 % between the coastline digitized using the 10m and the 1000 m divider (and probably greater if dividers outside of the 10-1000 m range are used). For the eight sectors used in this study, three featured variations greater than 20% and five greater than 10%. A direct consequence of these differences would be the large discrepancies in estimated volume fluxes for sediment and organic carbon if these data for coastline lengths are entered directly into equation (1).The D factors computed for the eight sectors can be grouped into categories (i.e. coastline type).

Table 2 Shoreline lengths computed with different dividers and the WVS
The lower line refers to the difference in % between the lengths computed using the 10 and the 1000 m dividers.

	Coastline length (m)							
divider length (m)	**Bykovsky**	**ArgaW**	**ArgaNE**	**ArgaN**	**Trofimovskaya**	**Tumatskaya**	**Olivier Islands**	**Herschel**
10	7159	7638	5894	7074	18791	7799	10474	15537
20	6966	7477	5741	6424	18603	7401	9465	15340
50	6880	7417	5640	5902	18093	7118	8695	15240
100	6853	7402	5570	5734	17483	6975	8498	15191
200	6838	7388	5461	5545	16859	6722	8312	15173
500	6822	7361	5253	5380	14188	6478	8188	15110
1000	6786	7217	5177	5309	12718	6326	8030	15010
WVS	7280	7626	6035	5713	16406	6853	10714	16061
Max value	7159	7638	5894	7074	18791	7799	10474	15537
Min value	6786	7217	5177	5309	12718	6326	8030	15010
diff. min-max (%)	5.2	5.5	12.2	24.9	32.3	18.9	23.3	3.4

Erosive coasts are characterized by the smallest D factors, while stable to accumulative coasts are characterized by much greater D factors. The difference between the length of the coastline computed with the 10 and the 1000 m dividers did not exceed 5.5 % for erosive sectors (western Arga Island), but was often over 20% for aggrading coasts. In other words, the erosive coasts considered in this study are considerably less sinuous than the stable to aggrading coasts. Thermokarst coasts exhibited an intermediate behaviour.

Despite the potentially large discrepancies and associated D-factors, net error may not be as high given that erosive coasts, which release the greatest quantities of sediment are associated with the smallest D-factors. However, changes in the erosive/aggradational nature of the coast are common in these regions (Aré, 1988) and the uncertainties associated with erosive and thermokarst coasts alone are large enough to justify correction. In other words, using the length of linear datasets as it is done in relation #1 is not good enough to model erosion at the pan-Arctic

scale.

3.3.4. Results - WVS length

The length of the WVS, which is the proxy for the length of the eroded shoreline in the ACD framework, is a constant. Nonetheless, there is no indication that its length is the "true" length of the coastline. Its length was found to be always greater than the length of the coastline digitized using 200, 500 and 1000 m dividers. For four of the eight study areas, the length of the WVS was found to be greater than any of the lengths found using the dividers. On the whole, the WVS did not correlate to any specific divider and did not reflect adequately the path of the digitized coastline at very large scales (10 and 20 m dividers).

The most effective method to relate the WVS to the "true" shoreline is to introduce a correction factor, that when applied to a specific type of coastline would transform its WVS length into a "true" length. The correction factor would be computed from a few type areas (i.e. coastline types) and then extrapolated to the whole Arctic coast by applying the same correction factor to similar coastline types. It would be a rapid and light-computing method based upon existing data. However, the generation of a correction factor for coastline self-similarity is subject to two problems. The first is the classification of coastline types and in particular how many coastline types are required to provide an objective and representative overview of the Arctic. For example, rocky shorelines, present in Svalbard, the Taymir Peninsula and the Canadian Archipelago will probably be characterized by different fractal dimensions, and hence require different correction factors. The list of coastlines types needed to fully represent the range of coastal patterns is potentially quite extensive. The second and most important problem is that the correction factor would have to be based on consistent empirical relationships. In other words, a shoreline digitized at a specific scale (i.e. with a specific divider) would have to be chosen over others as the "true" shoreline and the correction factor would then simply consist in the ratio of the WVS length to the "true" shoreline length. This means assuming that there is a "true" shoreline (i.e. a "true" scale).

As discussed previously, erosion acts over a wide range of temporal and spatial scales and therefore can not be limited to a single spatial scale. Additionally, a major challenge is to relate the length of a divider (scale of segmentation) to the scale of processes acting upon the coast. If coastal erosion could be restricted or defined in terms of one specific or dominant process, then identifying the divider that is best fitted to this process would in itself be a challenge.

Figure 3 - logarithmic chart divider length vs. shoreline length for all investigated sectors
The regression equation is marked on the chart, as well as the extracted D factor.

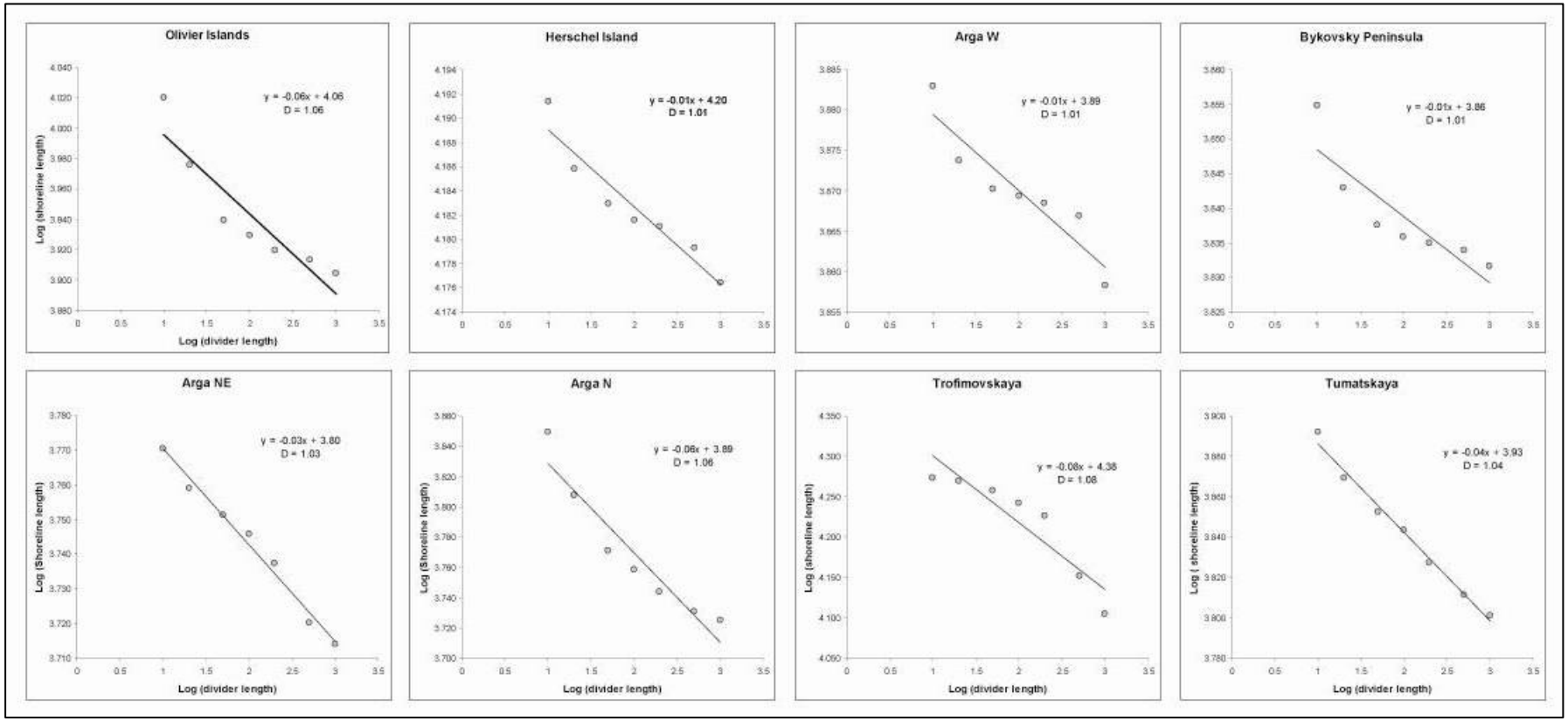

Introducing a correction factor is potentially a misleading undertaking as it attempts to correct one shoreline against another shoreline, which is fractal by nature. Using lengths in general and WVS lengths in particular to compute erosion volumes is therefore not sufficiently accurate

As Hugo Steinhaus stated (Steinhaus, 1954):

''a statement nearly adequate to describe reality would be to call most arcs encountered in nature not rectifiable. This statement is contrary to the belief that non rectifiable arcs are an invention of mathematicians and that natural arcs are rectifiable: it is the opposite that is true.''

3.4 Alternate method of erosion measurement

3.4.1. Planimetric erosion

The literature on the fractal dimension of coastlines provides some clues on how to overcome the changing lengths of coastlines. The issue of fractals had originally been addressed using a line of varying length; areas enclosed by these lines, however have been shown to be influenced very little by the fractal dimension of this same line. As emphasized by Hakanson (1978, p.144):

"When the scale is increased, small bays and capes will disappear on the map. This will primarily affect the l-value (the length) and not the A-value (the area), since A is generally determined by means of planimetric techniques, which implies that positive errors (capes) would be cancelled out by negative errors (bays)."

The area, as acknowledged by Hakanson (1978, p.144) is also sensitive to scale: "[...] however, the value of *A* may depend on the scale, but to a much lesser scale than the value of *l*".

Modelling erosion using area (i.e. planimetric erosion) rather than length may therefore overcome many uncertainties by eliminating the considerable variations observed with coastline lengths. Using this approach the volume of organic carbon released to the nearshore zone would then be calculated using equation 3,

$$C_{tot} = \sum_{j=1}^{n} \left[C_j \cdot \rho_{s_j} \cdot \left(1 - \theta_{ij}\right) \cdot \left(h_j \cdot A_j\right) \right] \tag{3}$$

where A_j is the eroded area per segment.

Modelling planimetric erosion is a well-documented topic in the literature. "Line modelling" or "shoreline modelling" methods have been developed for a wide range of applications and places, including Arctic shorelines (Li, 2001; Leont'yev, 2003). These methods have usually been developed to focus on a specific stretch of coast and require exhaustive climatological and hydrodynamical input data. The extent to which erosion modelling shall be performed within the ACD framework is unfortunately much greater than these studies, and the volume of information required to run these models is unavailable in a consistent pan-Arctic manner. Shoreline modelling shall therefore be based on a simple method taking advantage of the classification of Arctic coasts to provide an erosion estimate. Srivastava et al. (2005) demonstrated the effectiveness of simple Euclidean buffers to model erosion in coastal settings.

3.4.2. Planimetric erosion in a GIS

The calculation of eroded area (A_j) can be performed using buffer areas extracted from the WVS and the data from the classification of Arctic coasts. Using a simple GIS routine, buffers can be built from the WVS using an Euclidean distance based on the coastal erosion rate of the segment. By repeating the operation on every segment of the Arctic coast, a representation of the total area eroded per year is computed.

Hakanson's (1978) areas are less sensitive to changes in scale than lengths; however, this is true as long as these areas are larger than the lower limit to the area of geographically meaningful features. In their study on the complexity of California coasts, Bartley et al. (2001) showed that the WVS was hardly usable as a positional feature below 1 km and completely irrelevant below 100 m. Similarly, areas must be large enough to represent the erosion we are attempting to model.

In other words, we must increase the timeframe over which we look at coastal erosion to work with greater areas, hence minimizing potential errors. Indeed, using a shorter time span (i.e. a smaller area) results in numbers that can still be greatly affected by the quality or the scale at which the coastline was elaborated. For instance, on the Laptev Sea coast, the current rate of coastal erosion of the Bykovky Peninsula is 2.7 m/yr (Rachold, 2000). By using a 50-year time interval, we would obtain eroded areas small enough to be influenced by the resolution of the coastline. Since the WVS is considered irrelevant as positional feature below 100m and is made of segments up to 50 m short which are far too basic geometrically to adequately model the curvature of the shoreline, any attempt to model the eroded area with narrow buffers (i.e. short timescales) will result in false estimations. In other words, the Euclidean distance used to create the buffers would be too small in comparison with the length of the segments used to digitize the WVS. The resulting extracted areas would be driven more by the geometric construction of the

shoreline rather than by its "true" pattern. It is therefore necessary to use far greater intervals.

Additionally, using a greater time interval reduces the uncertainty associated with the changing pattern of the shoreline. Coastal erosion on longer time scales (that is, further penetration inland) on all coastal types is a relatively steady process under climatic equilibrium conditions (Stive et al,, 2002). We can assume that erosion over 1000 years under climatic equilibrium conditions and stable coastal lithology over a segment length will result in the reproduction of a similar shoreline pattern further inland. This latter aspect eliminates the need for taking into account the variability of nearshore zone bathymetry, wave dynamics, etc. since those can be considered to impact uniformly the whole length of a coastal section over such a time period. The representation of erosion can therefore be done using a simple geostatistical method resulting in an uniform erosion normal to the shore over a very long time period. Li et al. (2001) demonstrated the value of such approach on the Lake Erie shore by extrapolating a constant rate-of-change value over a stretch of shoreline.

3.4.3. Method test

To test the validity of the buffer method and its sensitivity to scale changes, we created several buffers from the coastline sectors described in section 3.2. We considered the coastlines

Table 3 - Planimetric erosion (buffer area) for the Olivier Islands computed using different divider lengths and different buffer widths.
The lower line refers to the difference in % between the areas computed using the 10 and the 1000 m dividers.

	Buffer area (m²)			
Divider length (m)	**100 m buffer**	**200 m buffer**	**500 m buffer**	**1000 m buffer**
10m	877070	1670322	3801613	6282674
20m	860678	1652967	3785107	6271829
50m	837081	1627909	3767706	6263816
100m	829379	1617333	3747406	6246662
200m	812414	1589529	3708564	6214291
500m	799796	1563749	3640545	6186560
1000m	781498	1522069	3498362	5932063
WVS	1049667	2053932	4696300	7014807
Max value	877070	1670322	3801613	6282674
Min value	781498	1522069	3498362	5932063
diff. min-max (%)	10.9	8.9	8.0	5.6

digitized using the 10, 20, 50, 100, 200, 500 and 1000 m dividers as well as the WVS separately. For each of these coastlines, buffers based on 100, 200, 500 and 1000 m Euclidean radii were created. The buffers were created for the onshore side of the coastline only. They were delimited at each end of the sectors using a common boundary based on a straight line perpendicular to the coastline

direction.

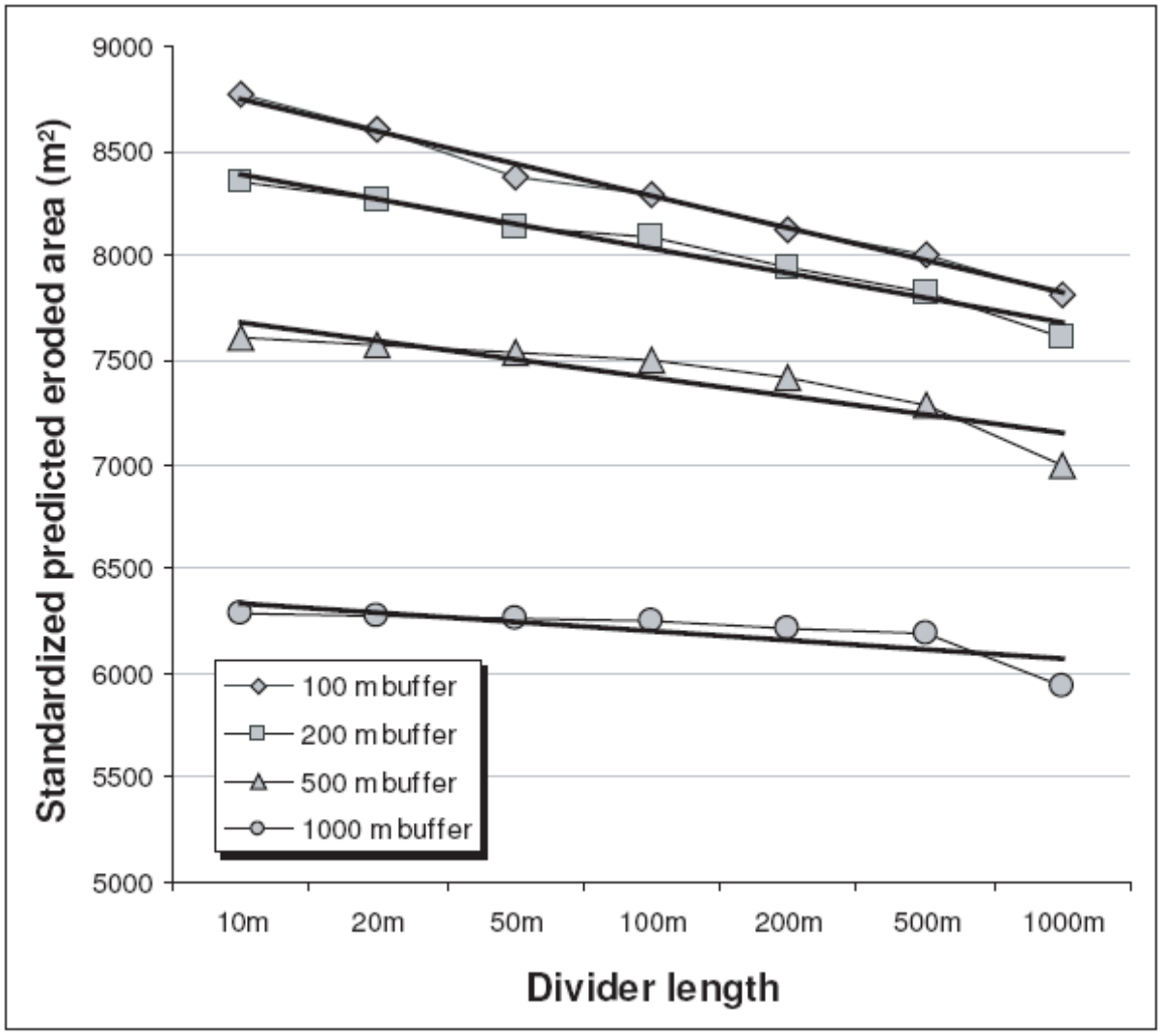

Figure 4 - Standardized eroded areas computed using buffers on the Olivier Islands sector
The slope of the four curves indicates the magnitude of the changes across scale in eroded areas. The difference in standardized eroded area between the four buffers is due to the curvature of the shoreline

The buffer areas were then calculated using a simple GIS routine in ArcGIS. The raw results for the Olivier Island sector are shown in table 3. The buffers were then standardized to represent yearly erosion under a 1m/yr erosion scenario, by dividing the area by the buffer radius. The results are shown in detail for the Olivier Islands sector in figure 4. Finally, the standardized areas were compared to the ones obtained using the WVS for all sectors (figure 5).

3.4.4. Results

Figure 5 shows that the range of erosion values across scale is considerably smaller using areas rather than lines. For the Olivier Islands area, for instance (table 3), the largest difference in areas between the values obtained from the 10m and the 1000 m divider shorelines is 10.9 % (using the 100 m buffer). Comparatively, the same section of coast showed differences in

coastline lengths between the same two shorelines of 23.3 % (table 2). All eight sections featured this same strong discrepancy (figure 5). Areas are, as expected, less sensitive to scale variations than lines. They do therefore provide a valuable substitute to computations based on shoreline lengths.

As Hakanson (1978) acknowledged, areas are nonetheless sensitive to scale and in our study, changes in eroded area across scale are observable at all eight coastal sections (figure 5). While the difference between buffers digitized from the 10m divider and the 1000 m divider shorelines is lower than the one extracted from shorelines (27.0 % at the most using a 100 m buffer for the Trofimovskaya section versus 32.3 % using shoreline length), it nevertheless remains important for some sections. However, the magnitude of these changes differs depending on the radius of the buffer used. The greater the radius (i.e. the longer the timescale chosen to model erosion), the smaller the error range. For the same Trofimovskaya section, modelling erosion using a 1000 m buffer leads to a reduced error range (13.3 % vs. 27.0 %). For seven of the eight sectors the error range is well below 6 % using a 1000 m buffer.

The error range obtained with greater radiuses is smaller, and is therefore an incentive to use these radiuses in the calculation of A_j. Yet, while the error ranges are indeed smaller, the values of standardized eroded area differ depending on the buffer used. For several sectors, it is possible to show that although the error range is reduced, the standardized values of erosion themselves decrease or increase with increasing buffer radiuses. On the Olivier Islands section, for instance, computed standardized eroded areas oscillate around 8250 m² using the 100 m buffer, and around 6250 m² using the 1000 m buffer. In this case, eroded areas are clearly smaller using a greater radius. In contrast, on the Bykovsky Peninsula and Arga Island North East sections, eroded areas are greater using the 1000 m buffer.

This counter intuitive behaviour is related principally to the curvature of the coastline. A perfectly straight shoreline, under the assumption of uniform erosion would be eroded in a consistent manner, whatever the radius of the buffer. Curved shorelines tending towards closure (i.e. a cape or a promontory, e.g. figure 6), under the assumption of uniform erosive processes acting upon the shoreline, undergo less and less erosion (i.e. eroded area) with time (figure 4). The more curved the shoreline the stronger the decrease in “erosion capacity”. On the other hand, curved shorelines tending towards opening (i.e. a bay, an inlet) yield greater eroded areas with time, under the same assumption. The decrease or increase in eroded area with the increasing buffer radius is not an effect of scale or a lack of accuracy of the buffer method, but an effect of the shoreline curvature. On the other hand, the error range mentioned earlier is directly related to the fractal dimension of the coastline and not to curvature effects. A small radius is therefore more sensitive to scale effects; it will contribute above all to a loss in the precision of the prediction of .

Figure 5 - Standardized buffer erosion vs. buffer widths for all investigated sectors
Planimetric erosion computed using buffers is standardized to a yearly erosion value based on a 1 m/yr erosion scenario. The resulting erosion values are then plotted against the buffer widths.

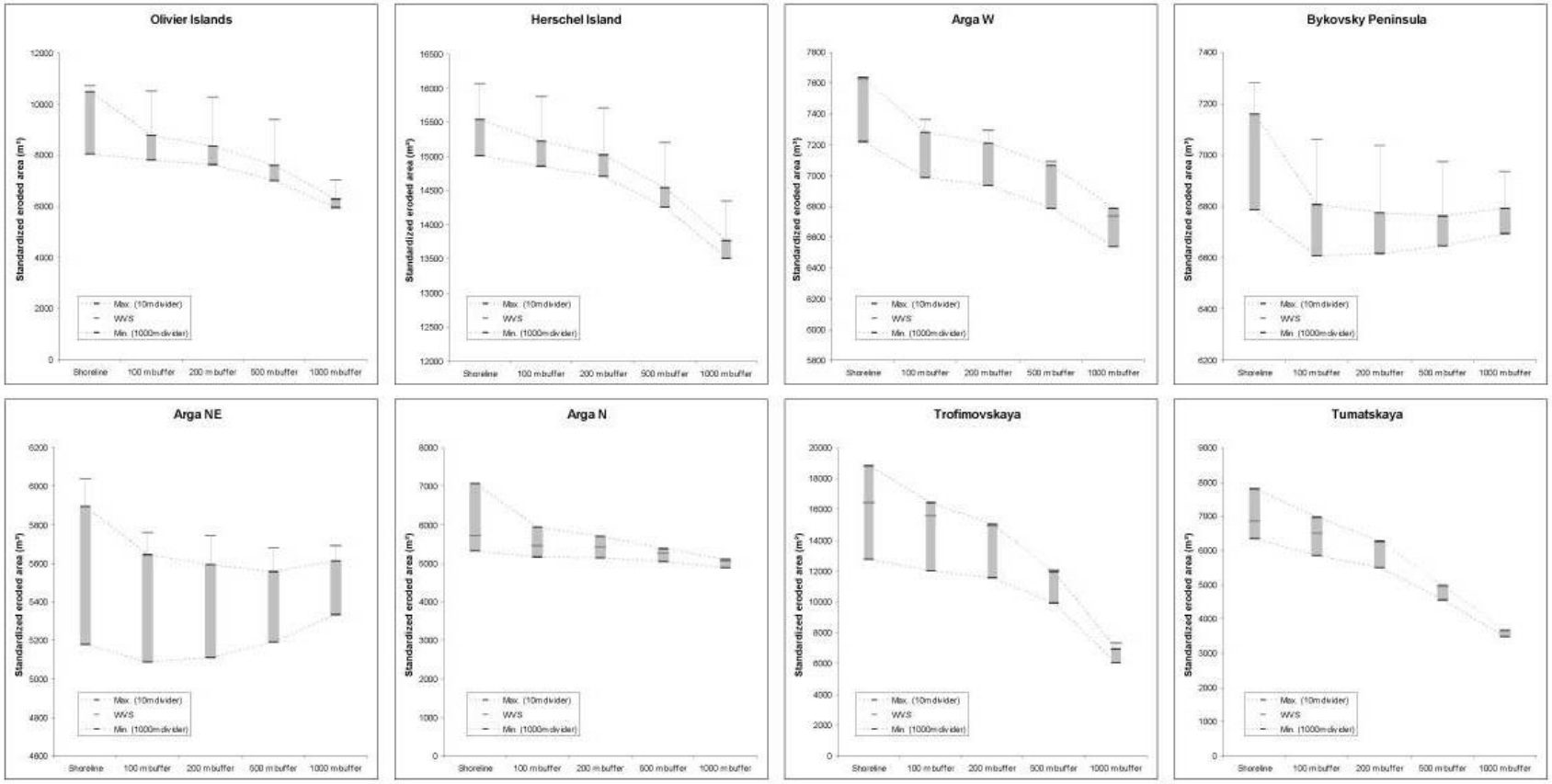

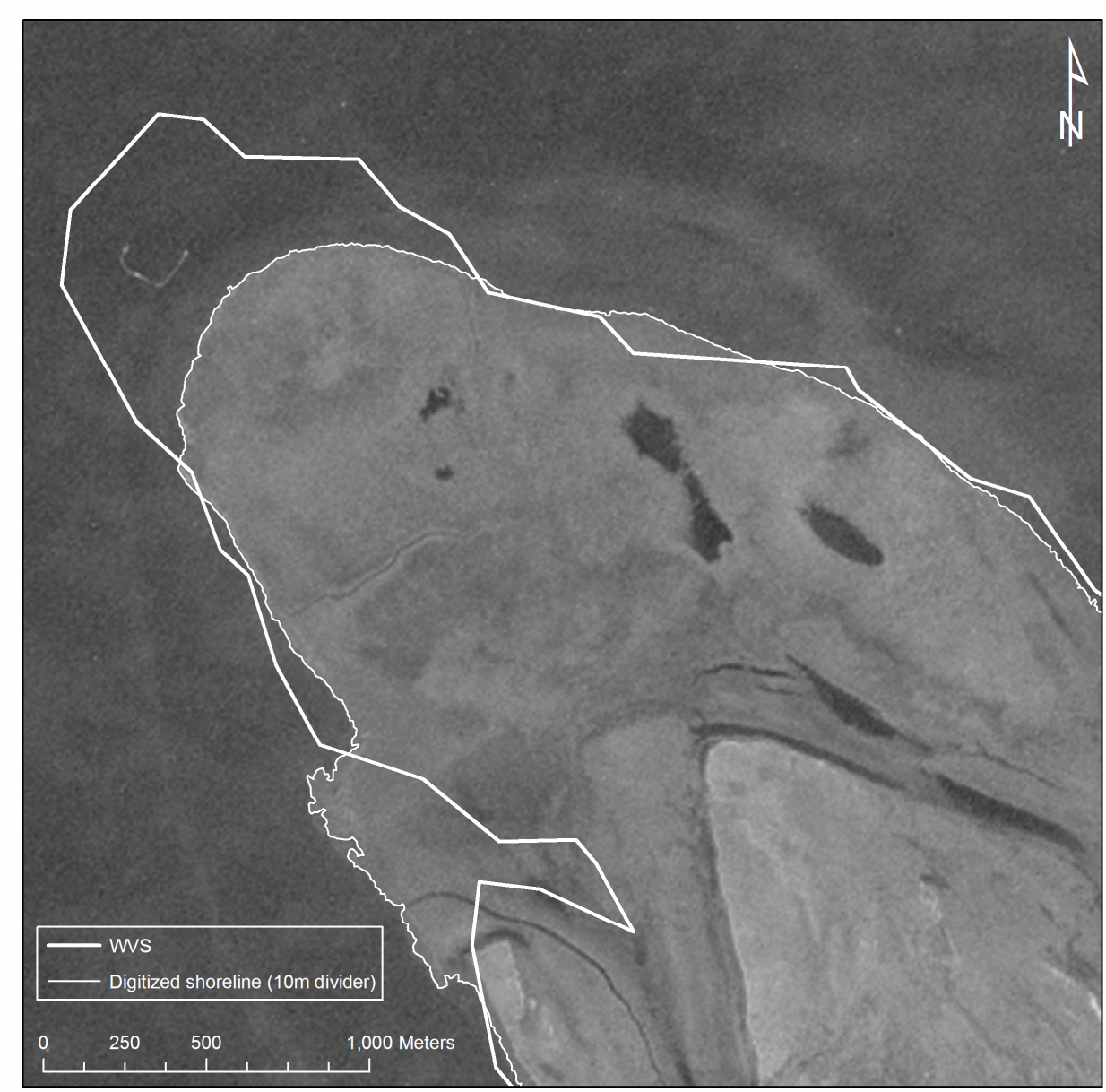

Figure 6 - WVS vs. digitized shoreline for the Olivier Islands sector.
The WVS is fairly lacks both accuracy and precision, and although it was digitized from 1:250 000 scale maps, the low quality of the transfer from maps to digital format creates artificially long segments of coast.

eroded areas, but not necessarily to a loss in accuracy.

Buffers, by modelling erosion as Euclidean distance, imply that erosion is uniform along segments in the ACD classification, and provide a greater independence from scale effects. They are therefore better adapted to the computation of erosion over very large areas such as the ones the ACD project is focusing on.

If buffers drawn from coastlines digitized manually from high resolution imagery accurately fulfil the purpose of modelling uniform erosion along coastline segments, buffers drawn from the WVS are suspect. Buffers computed from the WVS do not always fall within the range of values calculated using buffers from digitized shorelines. In particular, buffers from the

WVS do not adequately represent eroded areas on erosive coastlines, and consistently overestimate eroded areas. The artificial sinuosity of the WVS, due to the rough division of the coastline in segments always greater than 50 m (figure 6), is the main cause for the lack of accuracy of the buffers computed using the WVS. It induces false spatial variations of the shoreline position and increases the size of the buffers, hence creating false erosion values. Of the sectors investigated, this overestimation never exceeded 5%. It is reasonable to assume that this percentage is an upper value, since the sections investigated in this paper included several sections of coastlines of very low fractal dimensions. This overestimation was not strictly limited to erosive shores and is hard to relate either to fractal dimensions or shoreline

curvature. It is largely induced by the original processing of the WVS data. A direct consequence of the random nature of this processing artefact is that an arbitrary provisional loss of accuracy of 5% can be assumed from measurements extracted from the WVS. This lack of accuracy is believed to be a maximum value since most buffers extracted from the WVS actually fell within the range of buffers computed using digitized shorelines. Additionally, it is to compare with the large error ranges obtained with computations with shoreline lengths.

3.5 Conclusions

Using coastline lengths combined with cliff heights and costal erosion rates to calculate volumes eroded from the coasts seems like an adequate and simple method to cope with the constraints associated with Arctic-wide scales. However, this paper shows the potential errors in both accuracy and precision are too large to make it a reliable method. The outcome in terms of sediments and hence, organic carbon released from the coasts would suffer from considerable uncertainty. There is, however a rationale for providing estimates of sediment and organic carbon release from coastal erosion from Arctic coasts at the circum-Arctic level. Unfortunately, as emphasized in the introduction section, most precise methods of coastal erosion measurements lack the potential to cover extensive areas. The use of simple and globally consistent datasets such as the WVS is therefore justified but alternative methods of calculation avoiding the effects of scale on line datasets must be sought. While methods aiming at correcting or compensating for the effects of scale on the length of the WVS could provide a solution to this issue, eroded areas (i.e. buffers) offer a more precise way to address this issue.

Recent initiatives aimed at building a better shoreline of the world (National Geospatial-Intelligence Agency Office of Global Navigation, Maritime Division, Global Shoreline Dataset) from remotely sensed imagery constitutes a promising tool for the refinement of erosion measurements, in particular for the improvement of the accuracy of the WVS. However, errors due to misinterpretation of shoreline lengths are by nature possible with any line dataset and

methods based on areas provide a valuable substitute to those. The upcoming release of the Arctic Coastal Dynamics classification of Arctic coasts and the subsequent re-evaluation of the carbon budget of the Arctic Ocean will be performed using the method developed in this paper.

Acknowledgements:

This study is part of the project Arctic Coastal Dynamics, initiated by the International Arctic Science Committee. Md. Azharul Hoque provided helpful discussion on the nature of coastal erosion and its relation to both temporal and spatial scales. This paper could not have been possible without the help of Jan-Erik Kruse and Mathias Berg who helped in digitizing datasets. Nicole Couture provided considerable help to improve the quality of this manuscript. This research is also a contribution to themes 1.2 and 1.3 ArcticNet, one of the Canadian Networks of Excellence.

CHAPTER 4 – MANUSCRIPT #2 - EROSION HISTORY AND DYNAMICS ON BYKOVSKY PENINSULA, RUSSIA, 1951-2006

4.1 Introduction

Bykovsky Peninsula is located northeast of the harbour-town of Tiksi, in the northernmost part of Siberia (figure 1), and forms a natural protection for the harbour. Tiksi was founded in the 1930's and rapidly grew as a hub for shipping on the Northern Sea Route which links the Bering Strait to Northern Europe though Russian Arctic waters. The collapse of the Soviet Union led to the virtual abandonment of the industrial harbour, but projections of reduced sea-ice cover during the summer months have provided an incentive to upgrade plans to operate the Northern Sea Route industrially. Tiksi, which is sheltered from storms by the Bykovsky Peninsula, is of crucial importance as part of these plans (Matushenko, 2000). The peninsula is characterized by the presence of ice-rich sediment (ice complex) and exhibits large rates of erosion induced by periodic storms and thermal-mechanical erosion of ice-rich sediments. These rates are estimated at 2-6 m/yr, with highs of 20 m/yr (Are, 1988, p.117, Rachold et al., 2000). These rate estimates are crude, however, and have not considered the spatial and temporal variability of coastal erosion on the peninsula. The potential increased exploitation of the Northern Sea route, encouraged by the continued retreat of the polar ice pack, and the subsequent expected increasing activity in Tiksi Bay (Matushenko, 2000), provide an incentive to undertake in this region a more spatially detailed examination of erosion rates and to consider in greater depth possible driving mechanisms. The modification of the Bykovsky Peninsula shoreline could directly impact the harbour infrastructure. In light of this, this paper has two objectives:

- build a spatially comprehensive and up to date compilation of coastal retreat rates from the Bykovsky Peninsula based on aerial photography (1951, 1981, 1986) and satellite imagery (1964, 1969, 1975, 2006), and
- analyze these data with respect to new information about coastal environmental forcing, including seasonal wind/storm activity and thermal energy magnitudes.

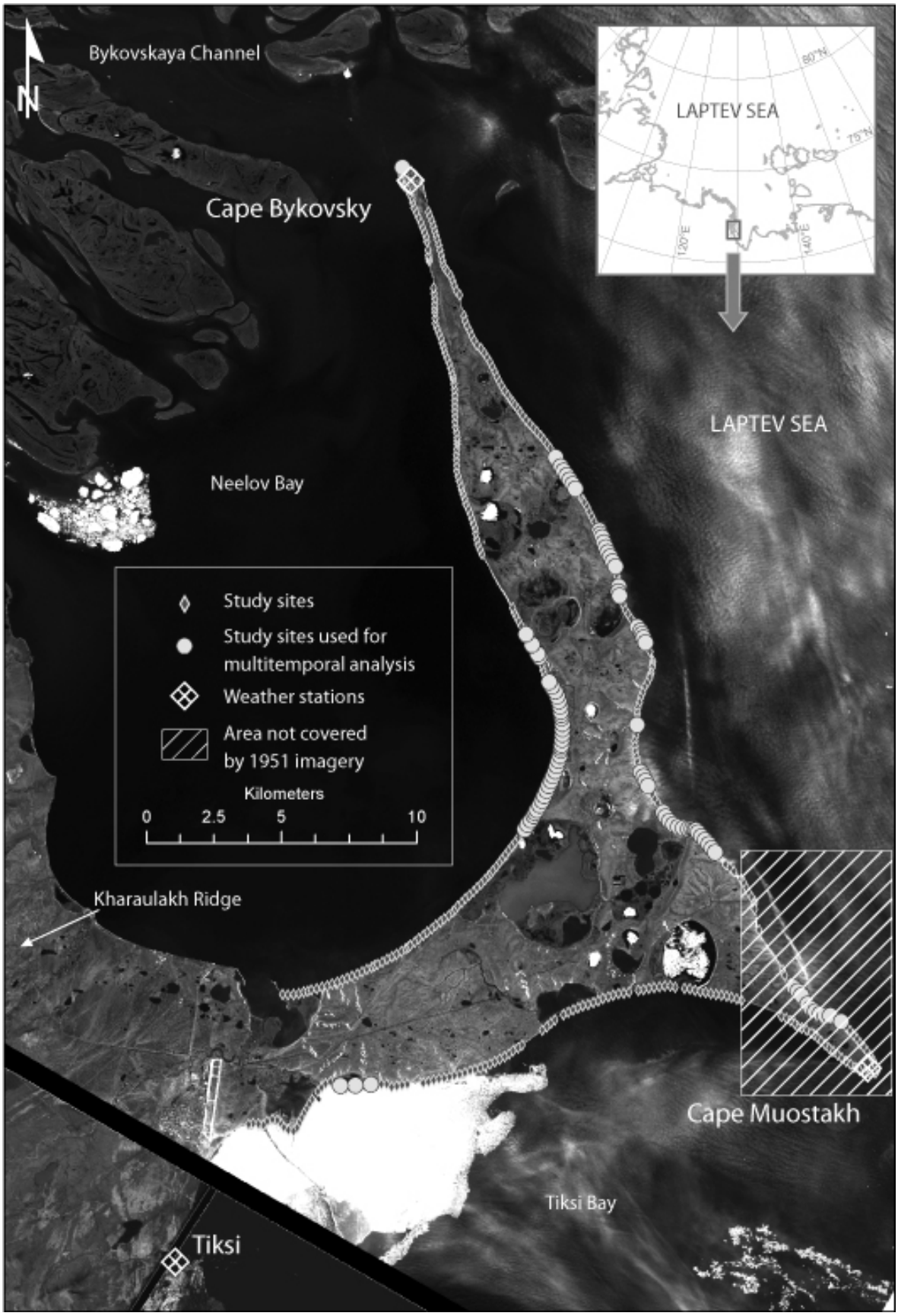

Figure 1 - Study area
The Bykovsky Peninsula is located bear to the mouth of the Lena River and forms a natural protection for the harbour of Tiksi

The resulting dataset and analysis results in combination with forecast/hindcast scenarios of environmental forcing can be used to predict future rates of erosion using shoreline modelling techniques such as the end-point rate (EPR) method (Dolan et al., 1991), contribute to regional sediment budgets, and assess the temporal variability over the second half of the twentieth century, and ultimately aid planning and infrastructure development.

4.2 Background

Coastal erosion in the Arctic differs from its counterpart in temperate regions due to the short open-water season (3-4 months) and to the presence of ice in the marine and terrestrial environments (that is, permafrost, and ground ice).

The open-water season in the southern Laptev Sea extends on average from June to mid-October. Storms, which are the largest driver of erosion, occur throughout the year but their impact is limited due to the presence of sea ice cover during the fall, summer and spring (Atkinson, 2005). Even during the summer period, chunks of sea ice in various quantities can impede the development of waves in the shore zone.

Coastal retreat rates are also highly variable both spatially and temporally (Lantuit and Pollard, 2008; Rachold et al., 2000; Solomon, 2005). Spatial variability is mainly due to variations in the lithology, cryology, and geomorphology of coastal cliffs. Temporal variability is related to the variation of the climatic forcing which affects the degree of storminess, thermal conditions, and sea-ice conditions in the coastal zone (Solomon et al., 1994).

Ground ice is a unique feature of polar coastal systems. It is present in the subaerial part of the shore profile, but also underneath the water column, as submarine ground ice (Mackay, 1972; Rachold et al., 2007). Its presence affects both the response of the shore to thermal-hydrodynamical forcing and the sediment budget of the coast (Are, 1988; Dallimore et al., 1996). The presence of ground ice leads to a process termed “thermal abrasion” (Are, 1988) which encompasses the combined kinetic action of waves and thawing of the permafrost. Upon melting it enhances coastal zone susceptibility to erosion, (Héquette and Barnes, 1990; Kobayashi et al., 1999), especially when present as massive ice in coastal cliffs, or through the occurrence of large thermokarst features in the coastal zone (Lantuit and Pollard, 2005; Lantuit and Pollard, 2008; Wolfe et al., 2001)

The very high rates of erosion observed on many Arctic coasts, exceeding that observed on many temperate coasts exposed to year-round wave activity (Rachold et al., 2000), suggests contribution from mechanisms in addition to thaw and kinetic erosion.

Dallimore et al. (1996) suggested that thaw settlement of ice-rich sediments in the nearshore zone could induce a change in the shoreface profile and so support larger and more powerful waves. However, not all Arctic coastlines are characterized by subsea ice-rich permafrost and other explanations must be sought. Héquette and Barnes (1990) studied statistically the relationship between erosion rates and hydrodynamic and geomorphic factors and concluded on the necessary involvement of an additional force to drive the strong retreat rates. They attributed those to the occurrence of ice scours and sediment entrainment by sea ice in the offshore zone. As shown by Forbes and Taylor (1994), these can alter significantly the coastal sediment budget.

4.3 Study area

4.3.1 Location

Bykovskaya Peninsula extends in a NNW-SSE orientation at the tip of one of the outflow channels of the Lena River Delta (Bykovskaya channel), at the foot of the Kharaulakh Ridge. It lies within the zone of continuous permafrost which reaches down to 500-600m below the surface (Grigoriev et al., 1996). The peninsula is located in the Polar Tundra zone of the Köppen-Geiger classification (Peel et al., 2007) and, although located on a coast, experiences large annual temperature range that suggest an almost continental climate (-12°C mean annual temperature).

4.3.2 Physiography

Bykovsky Peninsula is underlain by extensive ice-complexes and reaches up to 45 m a.s.l. The ice complex is "an ice-rich unconsolidated permafrost deposit with a large content of ice wedges" (Are, 1988, p.11). The ice wedges are up to 5m in width and up to 40-50 m in depth; they coalesce to form the ice complex and segregated ice is present in the sediment between the wedges. The ice complex deposits and the upper Holocene cover are made of poorly sorted sandy silt to silty sand and are remarkably homogeneous from a sedimentological standpoint. (Siegert et al., 2000). Holocene deposits are found as a cover layer on top of the Ice Complex and in basins and valleys formed by thermokarst. They consist of reworked sediments of the Ice Complex, often with enrichment of organic matter in peat horizons.

The two dominant backshore coastal landforms are cliffs and low-lying topographical depressions. Cliff morphology ranges from relatively stable, vegetated slopes to nearly

vertical cliffs, reaching 45 m in some places and often containing exposures of ice complex sediments. Subaerial cliff erosion (thermal denudation) is dominated by the occurrence of large retrogressive thaw slumps, often extending along as much as a kilometre of shoreline and up to several hundred metres inland.

The low-lying depressions are thermokarst basins formed by thawing the ice-rich permafrost that have caused subsequent surface subsidence. About 46% of Bykovsky Peninsula is covered by such basins (Grosse et al., 2005). They contain reworked and unconsolidated ice complex sediments accumulated under lacustrine conditions during the Holocene. In some basins, middle Holocene lake drainage by tapping from coastal erosion has resulted in the formation of thick peat horizons and the establishment of various periglacial features, including refreezing of the lacustrine sediments, the growth of up to 2 m wide ice wedges, and pingos in the former lake bottoms (Grosse et al., 2007).

The ice complex once covered vast areas on the Laptev Sea shelf (Romanovskii et al., 2000) which were, according to theory, progressively flooded following sea-level rise. Sea level reached its current elevation at around 5000 BP (Bauch et al., 2001) giving the Bykovsky Peninsula its current shape.

The position of the peninsula in the axis of the Bykovskaya channel, which is one of the largest of the Lena River outflow channels by discharge (Pavlova and Dorozhkina, 2002), induces the presence of freshwater along proximal coasts throughout the melt season.

4.3.4 Coastal erosion

The erosion of Bykovsky Peninsula coasts has been the subject of detailed investigations since Adams launched scientific investigations in the region and discovered the first entire mammoth on the Peninsula in 1799 (Adams, 1807). Subsequent investigators provided considerable information on the geomorphology of its coasts, including coastal erosion rates (Khmiznikov, 1934; Klyuyev, 1970). In the 1980s, Are (1988) compiled a detailed summary focussing on processes acting upon Arctic coasts with large excerpts dedicated to Bykovsky Peninsula. Grigoriev (1996) and Rachold et al. (2000) provided the most recent update of coastal erosion rates for the period 1951-1999 based on airphoto imagery and ground-based measurements but focused on short stretches of coast along the peninsula. They published two retreat rates (2.0 and 2.7 m/yr for two sections on the northeast coast of the peninsula. Are (1988) highlighted the high spatial and temporal variability of coastal erosion on the peninsula, a phenomenon observed elsewhere in the Arctic (Lantuit and Pollard, 2008; Solomon, 2005). In particular he noted the apparently random occurrence of

periods of intense erosion followed by periods of stabilization of the coast. He related those to several factors, including the occurrence of subaerial thermal denudation features, differences in coastal lithology and/or morphology, and a possible cyclical evolution of the shoreface profile.

The tidal regime in Bykovsky Peninsula is micro-tidal and tidally-based sea level oscillations have little influence on the height of storm surges. The intensity of erosion is therefore thought to be largely correlated only to the strength of storm-wind driven waves and water-level surges.

Establishing clear direction in this debate, however, is hampered by lack of a continuous record of erosion for Bykovsky Peninsula. This limits the explanatory power of results derived from statistical relations of erosion to meteorological factors.

4.3.5 Storm climatology

Storm activity in the vicinity of the Lena River Delta and the broader region of the Laptev Sea consists mostly of transient systems migrating into the region from two main directions: over the continent from the southwest, and along the northern coast from the west (Survey of Climatology book on Russia). Little local storm formation is observed. Storm activity, defined in this case as storm counts, varies over the course of a year with a peak in activity coming in late-summer/early-fall, coincident with maximum ice-free period (Atkinson, 2005). This is in contrast with north Russian coastal zones to the east and west, which are both more strongly dominated by the proximity of Atlantic/Pacific sector storm activity and which shows up as a frequency peak occurring later in the year in October/November. Storms in this area tend to be of 43 hours in duration and bring wind speeds of 10.3 m/s. The prevailing storm-wind direction is NNE. There has been no particular trend in coastal storm activity in this region observed since 1950, although there was a marked jump from one activity level to another that occurred in the mid-1970s. This was consistent with other north Russian coastal regions as well as indicators of atmospheric circulation changes that occurred at this time (Savelieva et al., 2000).

4.4 Methods

4.4.1 Geoprocessing of airborne and spaceborne imagery

Geoprocessing of airphotos and satellite imagery was conducted to obtain a ±2.5 m horizontal accuracy for images of Bykovsky Peninsula coastline from 1951, 1964, 1969,

1975, 1981, 1986 and 2006. We used imagery from a variety of sensors (Airphotos, Corona, Resurs-R KFA 1000 and SPOT 5) to both extend the time range of the study and to obtain better temporal resolution (table1). The airphotos as well as the Resurs-R KFA 1000 image were obtained from the Russian national archives, while the declassified Corona imagery and the SPOT 5 imagery were purchased through commercial portals. All images were resampled to a standard 2.5 m nadir resolution. The Resurs KFA-1000 1986 image was originally acquired at lower resolution and its original resolution should be considered closer to 7 m. However, due to its limited availability only in paper format, its quality was even lower in comparison to the other products and the interpretation of coastal retreat limited.

The lack of a reliable net of ground control points in the area as well as the difficulties in getting authorisation to use high precision differential global positioning system induced some constraints for the georeferencing process. Unlike similar studies (Lantuit and Pollard, 2008), which were able to utilize absolute georeferencing based on a fixed number of surveyed ground control points, the present study used co-referencing to position the imagery. In other words, the images were not georeferenced to ground control points. Instead, the 1975 image was referenced to WGS84 Universal Transverse Mercator 52 North projection using basic Russian topographic maps, and the rest of the images were georeferenced according to this “base” image. A set of stable landforms were determined on all seven sets of imagery to collect the tie points. The number of tie points always exceeded 30 and corresponded to intersections of polygon edges, anthropological features, or small ponds. Tie points were picked preferentially in low-lying areas to avoid relief distortion, as orthorectification of imagery was not possible due to the lack of information on the camera used for the airphotos and the impossibility to obtain stereo-capable products for all the years studied.

The images were registered using off-the-shelf remote sensing software. The Root Mean Square (RMS) errors associated with the registration are listed in table 1. RMS error never exceeded 13 m and that particular high RMS error was associated only with the Resurs KFA-1000 image, which is understandable considering the low quality of this image. RMS error for locations derived from the other images ranged up to 11 m. The coastline of the peninsula was manually digitized after the 2006 SPOT-5 image. The presence of snow and heavy sediment loads in the coastal zone prompted the choice of manual digitizing over methods based on spectral information, which would have frequently misinterpreted the contour of the coastline. The digitized shoreline was then divided in 565 segments of equal

Table 1 - Imagery used in the study
All scenes have been resampled to a 2.5 m spatial resolution.

Date	Type	Name	RMS (m)
1951	Aerial photography	II-51-11118	7.81
	Aerial photography	II-51-11162	7.97
	Aerial photography	II-51-11167	9.99
	Aerial photography	II-51-11217	9.51
	Aerial photography	II-51-11219	4.58
	Aerial photography	II-51-11221	3.64
	Aerial photography	II-51-11276	4.90
1964	Corona	D003003m1107-1aft	10.11
	Corona	D003002m1107-1aft	8.13
1969	Corona	036019dsfwd1007-1	9.63
	Corona	036020dsfwd1007-1	11.71
1975	Corona	1975-II	0.00
1981	Aerial photography	3-914-81-94	5.74
	Aerial photography	3-914-81-96	3.76
	Aerial photography	3-914-81-98	4.64
	Aerial photography	3-914-81-105	5.24
	Aerial photography	3-914-81-125	8.84
	Aerial photography	3-914-81-128	7.32
1986	Resurs KFK 1000	Resurs KFK 1000	12.02
2006	SPOT scene (panchromatic)	SPOT scene	8.64

lengths. Erosion for the 1951-2006 period (or 1964-2006, where 1951 images were not available) was then calculated for each individual point. Sites for which estimation of erosion was too difficult were removed from the analysis. The resulting dataset includes 494 sites. Erosion values computed from the movement of the cliff foot (or the shoreline, when cliff foot was not clearly delineable) were converted to yearly rates of erosion.

The points were then selected to conduct analyses on the multi-period evolution of coastal erosion rates. Points characterized by erosion rates smaller than 1 m/yr were removed from the subsequent analysis. The erosion retreat over four- to five-year periods at these sites was small enough as to be potentially indistinguishable from the error induced by geospatial processing (i.e. Maximum dilution of accuracy of 3.13 m for the 1964-1969 period, see table 2).

The 494 sites are distributed such that they face virtually all directions of wave attack. The subsampled sites, however, were much less representative and mostly located on coastline sections facing north-eastern, western and southern azimuths (figure 2).

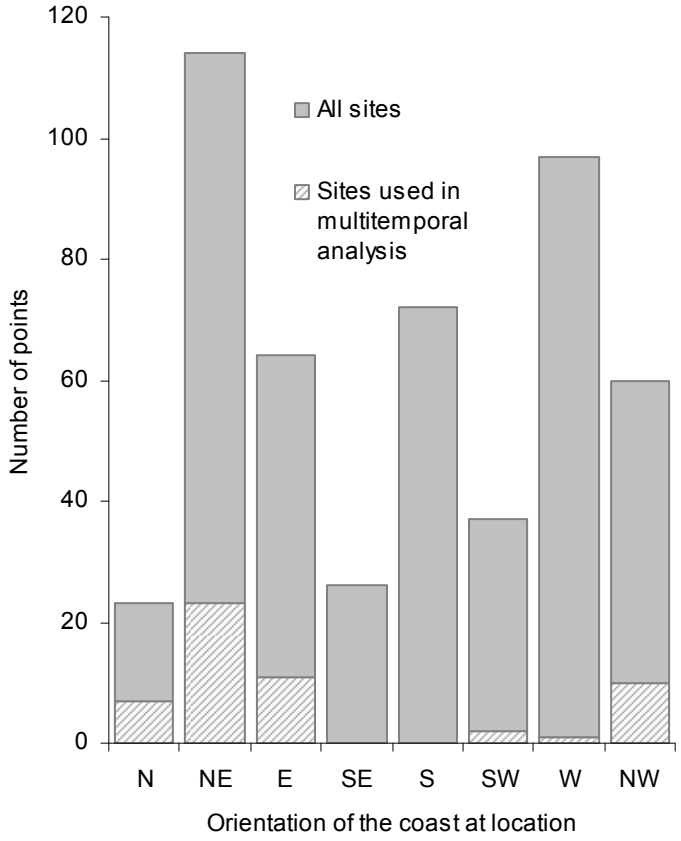

Figure 2 - Statistical distribution of shore orientation of study sites

Table 2 - Imagery georeferencing and dilution of accuracy (DOA) for the 96 subsampled points used in the temporal analysis
The periods for which the margin of error is greater than 25% of the measured average rate are highlighted in grey.

Date	Maximum DOA (m)	Average retreat (m)
1951-1964	1.11	20.22
1964-1969	3.13	5.89
1969-1975	2.00	9.73
1975-1981	1.53	12.36
1981-1986	3.03	7.83
1986-2006	0.75	21.83
1981-2006	0.50	38.85

4.4.2 Storm records

A database of storm events was constructed using the method specified in Atkinson (2005). The database was derived using observational data gathered from two local weather stations: Tiksi (in operation 1933 – current) and Cape Bykovsky (in operation 1958 – 1989) (location on figure 1). The data sets exhibited variable observing regimes, including periods of hourly observation and other periods of six hourly observation (that is, one observation taken every six hours). To create a uniform basis from which to build a storm event database

both data series were subsampled to six hourly following Atkinson (2005) and the storm extraction algorithm was run on the subsampled data sets.

The method identifies a "storm" as a wind event that exceeds 10m/s speed for at least 6 hours. Wind direction is not a constraining parameter; instead prevalent wind direction is an output parameter that can be used for subsequent analysis. The speed threshold was set following other arctic coastal studies that identified this speed as one able to generate waves that can cause impact at the coast (Eid and Cardone, 1992; Hudak and Young, 2002; Solomon et al., 1994). For a detailed description of the method, see Atkinson (2005). The meteorological records started in 1958 leaving seven years of erosion record without corresponding storm data. We arbitrarily constrained the open-water season to the four months and a half of the Arctic summer and Autumn (June 1st to October 15th) and extracted storm events that possessed start dates falling within that time window.

4.5 Results

4.5.1 Coastal erosion

In this study both sedimentation and erosion were evaluated. Sedimentation in the coastal zone was mostly linked to littoral drift-driven depositional landforms such as sand/gravel spits and lagoons. The size and shape of some of these lagoons changed dramatically over the 50-year study period, in some cases reflecting possible changes in drift patterns, and in other cases, in drift supply. However, positive shoreline position changes (that is, aggradation) were encountered at only 25 study sites; apart from these sites little beach development was observed. The changes associated with these sedimentary features were highly transitory (i.e. sand spits, lagoons, beach berms) and since they represent a very small proportion of the total coastal change, they will not be discussed further.

Coastal erosion rates were first compiled for the 1951-2006 period, and for the 1964-2006 period at sites where 1951 airphotos were not available (see figure 1). The mean yearly coastal retreat rate for all sites was 0.59 m/yr, or around 30 m of shoreline retreat. This is comparable to if not lower than rates observed in other Arctic regions. Lantuit and Pollard (2007) found a rate of 0.61 m/yr on similar ice-rich coasts in northern Canada. Solomon (2005) indicated rates of 0.6 m/yr for the 1972-2000 period in the Beaufort-Mackenzie region, slightly lower than the ones found by Harper (1990) for the 1972-1985 period (1-2 m/yr). Mars and Houseknecht (2007) found greater rates, ranging from 1.4 m/yr to 5.4 m/yr, along a

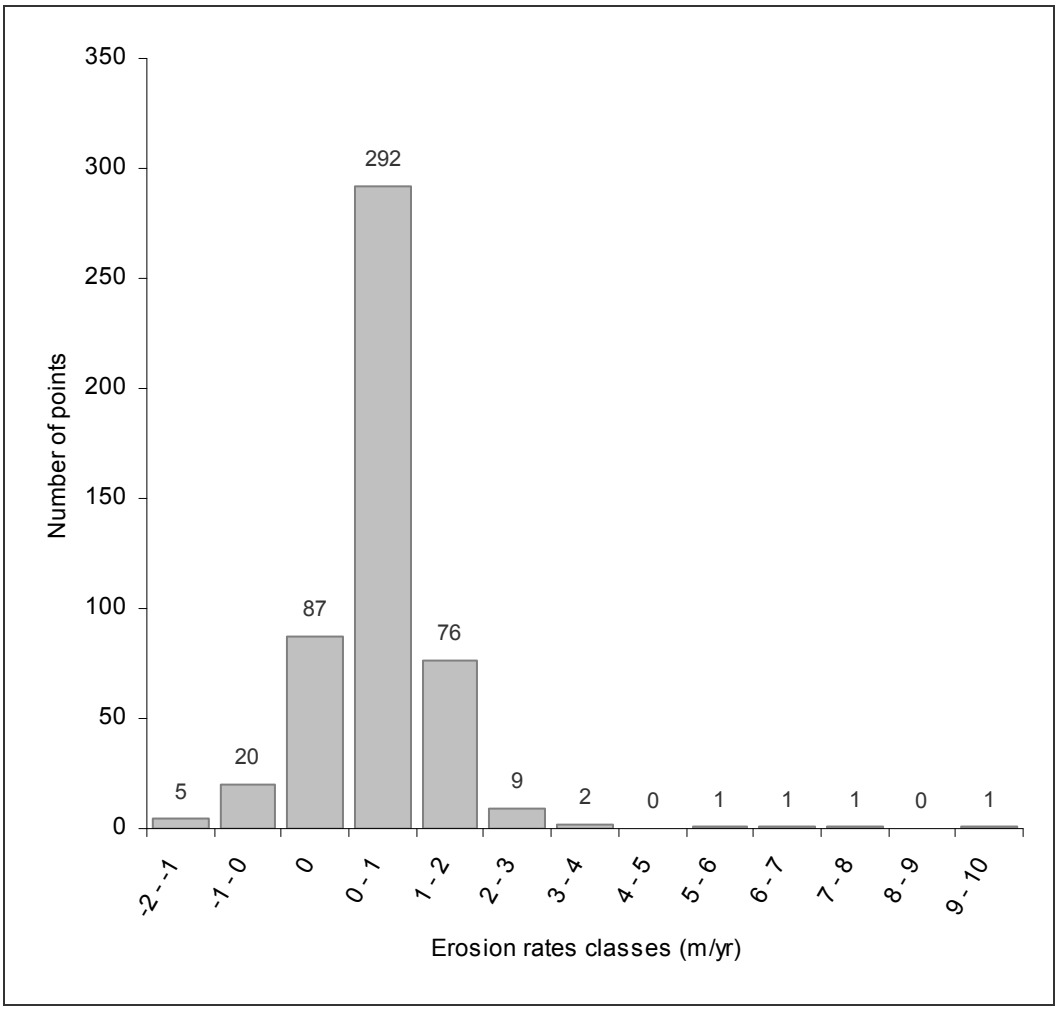

Figure 3 - Statistical distribution of erosion rates in classes of erosion intensity

coastal section of the Alaska Coastal Plain but generally rates of erosion along the Alaskan Coastal Plain are lower (Jorgenson and Brown, 2005). Total changes for the 1951-2006 period ranged from –434 m to +92 m (negative changes are erosional) and exhibited large variable (σ=45.4). Sites with the largest changes (>100m erosion) were clustered together in four small zones along the coastline; conversely, 97.0 % of the rates observed were less than 2 m/yr and 81.6% were less than 1m/yr (figure 3)

The largest erosion totals were observed on the north and northeast facing shores of the peninsula (1.05 and 0.97 m/yr respectively) and the smallest on the southeast facing shores (0.27 m/yr). All other sectors featured mean erosion rates ranging from 0.42 to 0.61 m/yr (figure 4). Erosion rates are mapped on figure 5. In addition to exhibiting the largest rates of erosion the north and northeast facing shores also exhibited the largest standard deviations (σ_N=1.77 and σ_{NE}=1.22 respectively while other sectors feature σ<0.6), and these sites also possessed the few extreme erosion values observed along the coastline. All sites featuring erosion rates greater than 2.5 m/yr are facing the north and the northeast.

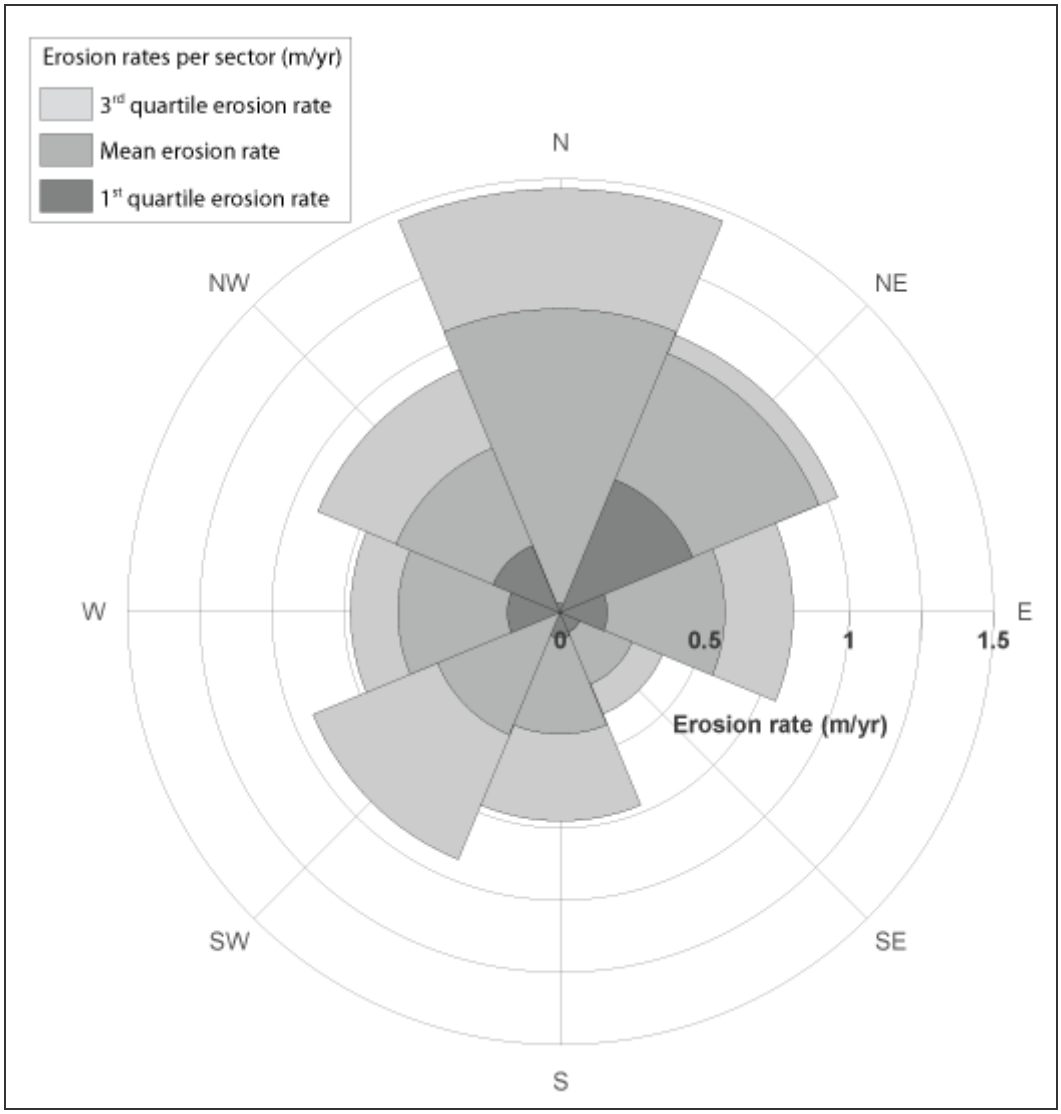

Figure 4 - Erosion rate intensity and statistical variability dependence on shore orientation

It is remarkable to observe that the east- and west-facing shores feature fairly similar mean erosion rates of erosion (0.57 m/yr vs. 0.56 m/yr), although most of the Peninsula's western part is bordering an enclosed shallow bay (< 2 m deep) that is constrained topographically on its western side by the Kharaulakh Ridge. The relatively constrained width of the bay combined with its shallow depth limits the height of waves that can potentially form on the western side of the peninsula and the presence of the ridge will limit wind speeds which will further limit wave heights. Inversely, except for the north and northeast facing shores, the sections of coastline potentially exposed to waves formed in the offshore zone are not characterised by large erosion rates.

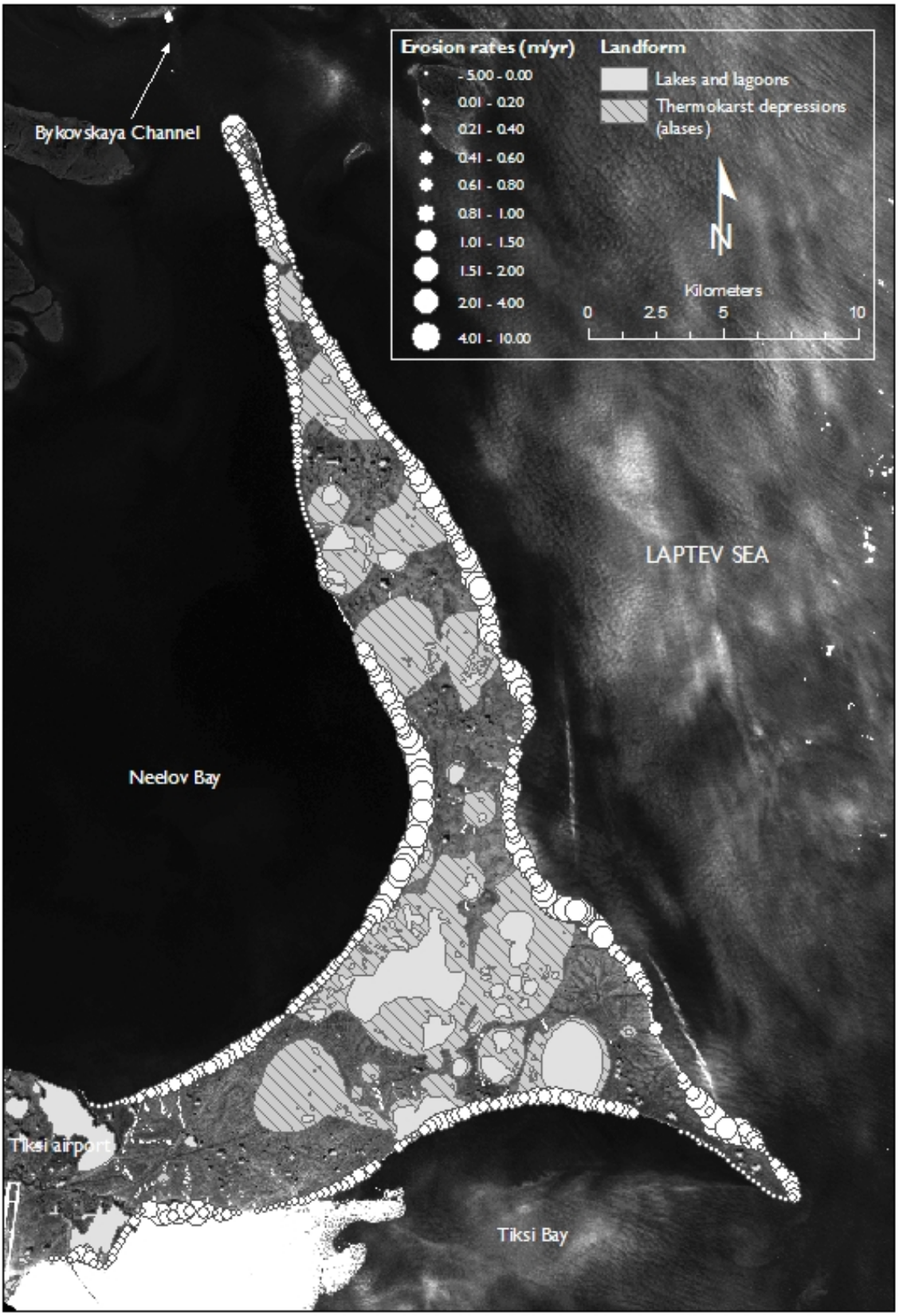

Figure 5 - Coastal erosion rates on the shores of the Bykovsky Peninsula for the 1951-2006 period

Coastal evolution on the Bykovsky Peninsula is strongly influenced by the local lithology and geomorphology. It is not unusual to observe neighbouring sites (hundreds of metres apart) along the coastline featuring very different erosion rates which can often be correlated to changes in the nature of the backshore material. Sites located in alases are in this manner affected by strong erosion rates, while sites barred by cliffs undergo smaller erosion rates. The smallest retreat rates are always associated with sand bars, followed by lagoon barriers, coastal cliffs (ice complex), retrogressive thaw slump-affected coasts and alases (Table 3).

Table 3 - Erosion rates and coastal types

Coastal type	Rate (m/yr)	standard deviation	Site count	Lower quartile (m/yr)	higher quartile (m/yr)
accretional sand bar	0.40	0.56	22	0.00	0.60
alas	1.02	1.38	115	0.35	1.10
cliff	0.47	0.46	255	0.00	0.69
lagoon barrier	0.47	0.35	41	0.16	0.80
retrogressive thaw slumps	0.91	0.75	60	0.28	1.35
Total	0.65	0.84	493	0.16	0.86

The small rates associated with sand bars are an artefact of the method used to calculate those rates and do not necessarily reflect an erosion of the backshore part of the coast, but rather the rapid movement of longshore sedimentary forms following the release of sediment by thermal denudation and/or thermal abrasion. The large differences in coastal erosion rates are common along Arctic coasts (e.g. Solomon (2005)) and can be explained by the geotechnical characteristics of the coast. Ice-rich cliffs such as the ones illustrated in figure 6 are eroded during storms through thermal abrasion. The erosion process requires great amounts of energy to melt the cohesive ice matrix. The sediment cohesion is virtually null; the material strength is derived almost exclusively from the ice matrix. When these coasts are affected by thermal denudation processes, such as the ones featured in figure 7, part of the exposure is already melted when the bottom of the cliff is affected by hydrodynamical processes, reducing the amount of kinetic energy necessary to erode coastal material. A similar process has been observed by Lantuit and Pollard (2008) on Herschel Island, whereby intense retrogressive thaw slump activity had considerably lowered the shore profile, hence increasing the impact of erosion in a general context of decreasing rates.

Figure 6 - Ice complex exposed at the coast of the Bykovsky Peninsula
Note the thermo-erosional notch at the land-water interface.

Figure 7 - Retrogressive thaw slump on the coast of the Bykovsky Peninsula.
The picture is taken from the edge of the slump. Note the presence of Baydzarakhs (earth mounds left in place after melting of coalesced ice wedges) within the slump floor. A man in the background gives the scale of the headscarp.

Figure 8 - Coastline in alas north of Mammontovy Hayta on the eastern shore of the Peninsula
The peat-rich alas low grounds are rapidly eroded by incident wave attack.

Alases (figure 8) are the end member of the thermokarst development: Following the thaw of ice-rich sediments, and often the formation of a thermokarst lake in a depression, the ground subsides, the lake expands, but is eventually filled by sediment resulting in the apparition of an alas. Alas sediments are not as high and as ice-rich as either ice complex coasts or retrogressive thaw slumps-affected coasts. This facilitates the thermal abrasion process and results in higher rates on alas coasts. The highest rates of erosion were observed in an alas located in the south-east part of the island (figure 9) resulting in rates close to 10 m/yr in one location. However, these strong erosion rates are often associated with narrow stretches of coast. Rapid erosion on alas coasts creates embayments which ultimately reduce the impact of hydrodynamic forcing, by diffracting waves on more dissipative shore profiles.

Temporal records were obtained for six periods within the project time frame, 1951 to 2006. The data suggested no significant temporal trend in erosion (figure 10) but strong interannual to interdecadal variability. Mean erosion rates for the points subsampled for temporal analysis ranged from 1.09 m/yr (1986-2006) to 2.06 m/yr (1975-1981). This is consistent with observations by Aré (1988) who reported that “thermal erosion occurs very

unevenly in time" on the Bykovsky Peninsula (Aré, 1988, p. 117). These results highlight the difficulty in establishing reliable significant time series trends in erosion in the Arctic.

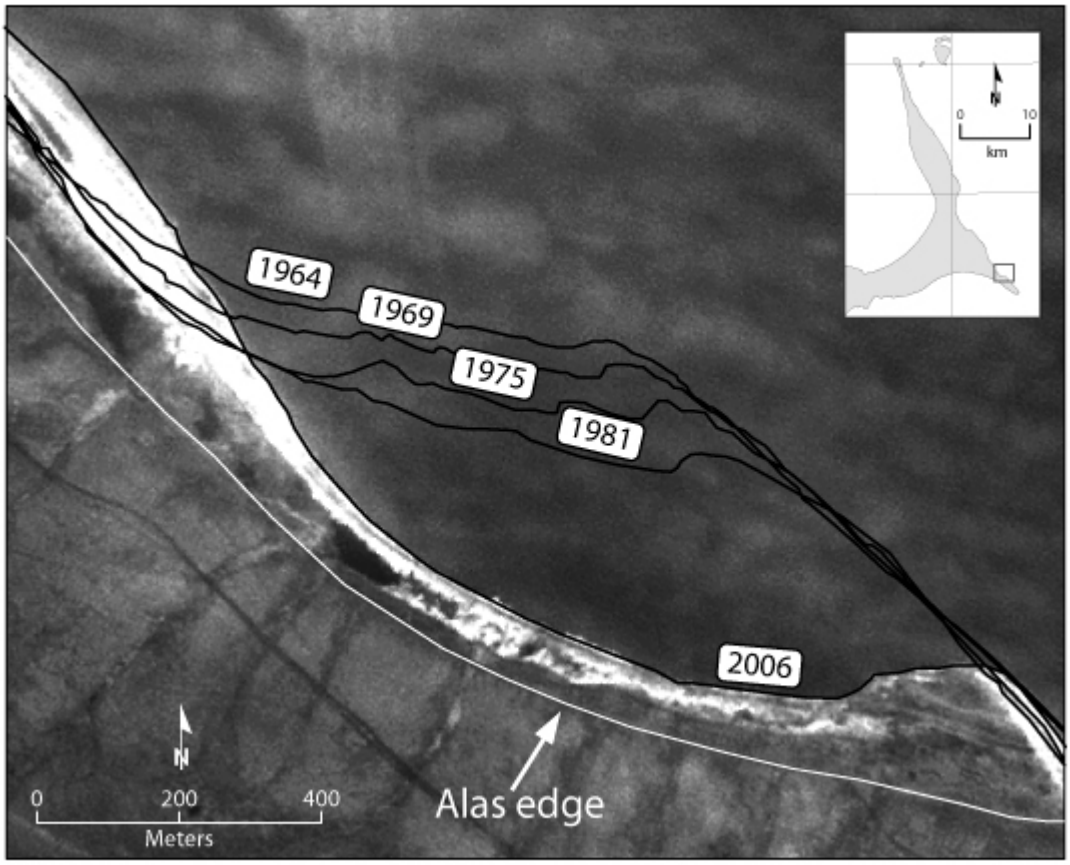

Figure 9 - Erosional sequence on an alas shoreline in the south-east part of the Peninsula.
The current shoreline is close to the edge of the alas, which should result in a significant decrease in coastal erosion rates on this stretch of coastline.

Solomon, (2005) and Lantuit and Pollard, (2007) found stable to decreasing trends in coastal erosion on the Southern Canadian Beaufort Sea Coast. Mars and Houseknecht (2007) found dramatically increasing rates of erosion for a short stretch of coast on the North Slope of Alaska. Vasiliev (2003, 2005), using one of the only annual record of erosion on Arctic coasts, highlighted the strong interannual variability in coastal erosion rates and the possible connections to the Arctic Oscillation (AO). On the Bykovsky Peninsula, rates of erosion can vary by one order of magnitude from one decade to the other, making it challenging to assert a reliable trend. Longer time series will be needed to subdue the interannual and interdecadal variability.

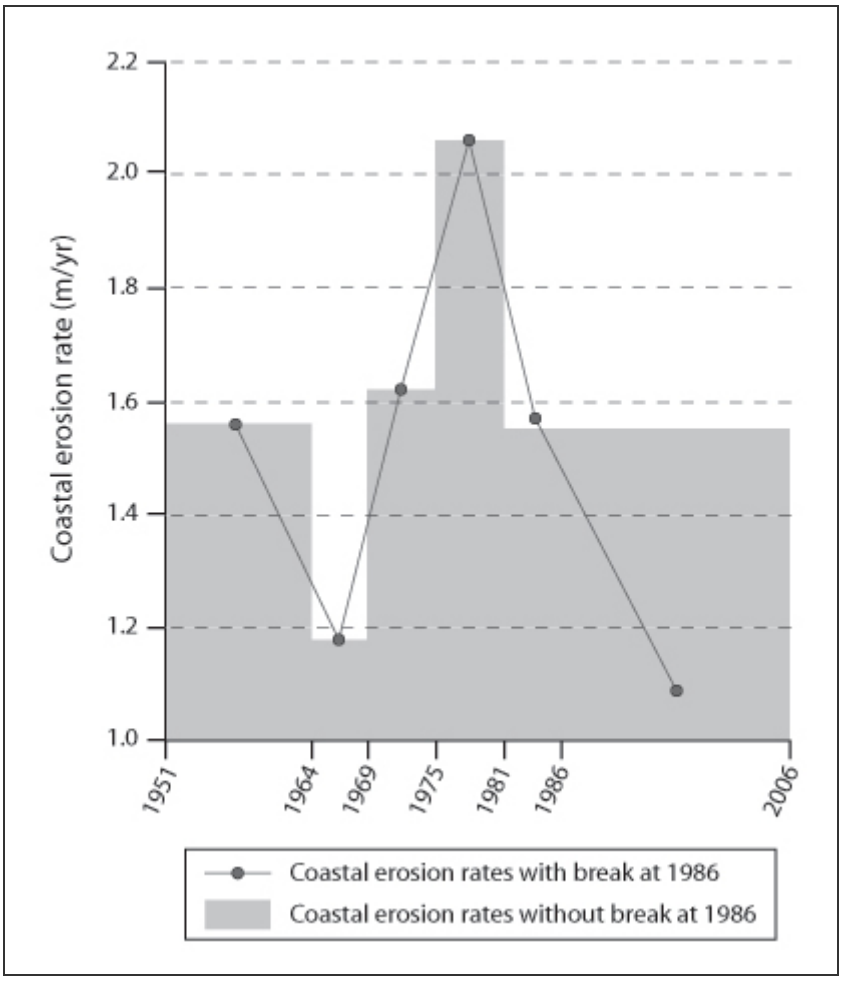

Figure 10 - Temporal evolution of mean annual coastal erosion rates

4.5.2 Meteorological records

665 storms were recorded for Tiksi between 1958 and 2006 (figure 11), that is, around 13.6 storms a year between June 1st and October 15th. The variance within the susbsampled time interval was important ($\sigma = 7.9$) and reflects the strong interannual variability in storm counts. Six years featured no storms and three years featured more than 25 storms during the four months and a half summer interval (1969, 1970 and 1994). No significant trend in storm counts was observed at the Tiksi harbour, unlike other places in the Arctic according to some other studies (Serreze et al., 1993; Savelieva et al., 2000). Instead, periods of increased activity were noted. From 1958 to 1973, wind records are characterized by a strong variability, including several years with no storms activity and others with large storm counts. This period is followed by a period of relatively low but consistent activity (1973-1986), slightly less variable than the early period. After 1986, rates rise and remain high and steady until 1994. After 1994, the level of activity drops and a period of storminess decline is

entered that persists up to 2001. The following five years (2002-2006) feature a similar behaviour to the 1986-1994 period with storm counts steadily above average.

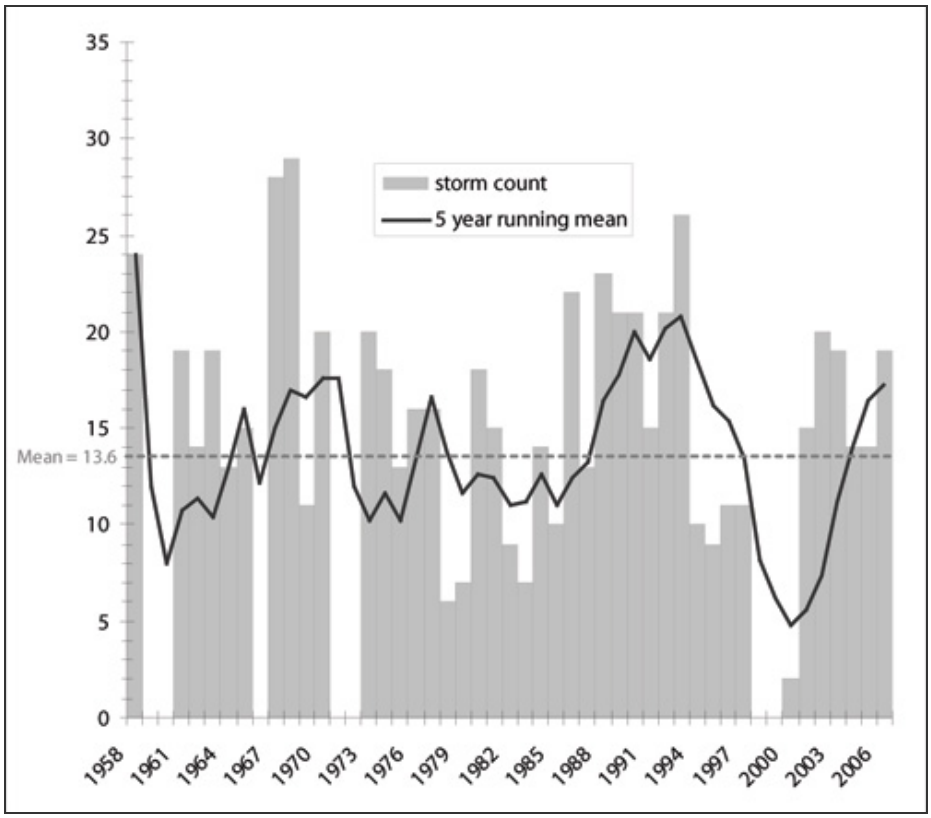

Figure 11 - Storm count evolution for the 1958-2006 period

A summary of the mean direction of storm winds for the 1958-2006 period at the Tiksi weather stations are shown in figure 12. Of the 665 storms recorded during the investigation period, 69% exhibited dominant wind direction of northwest, west, and southwest, with 54% from the west and southwest. This distribution of storm primary wind direction is fairly consistent from decade to decade. We compared the before- and after-1986 periods (Table 4) and found similar distributions. Storms winds at Tiksi originate primarily and steadily from the west and south-west, moving over the bay but opposite the direction necessary to favour wave development from the open ocean. The 25% strongest storms recorded also showed a similar directional distribution clustering around the west, southwest and northwest (83% of the strongest storms originated from these azimuths).

4.5.3 Coastal erosion vs. Storm counts

Direct relationships between storm records and erosion observations are often hard to establish, when the impacts of individual storms cannot be resolved and when various confounding influences are present (eg variable sea ice, sediments/ground ice contents). A

direct relationship between storminess and erosion for the Bykovsky Peninsula is essentially non-existent for the 1958-2006 period. Our erosion record is not detailed enough to conduct a formal statistical analysis of the relation between erosion and storminess at the Tiksi weather erosion, however even the larger temporal peaks in erosion seem not to match peaks in storminess at the coast. A "lag effect" (Solomon and Covill, 1993; Lantuit and Pollard, 2008) is often observed on ice-rich coasts and consists of the delayed movement of the shoreline following major storms due to the presence of large collapsed blocks in the coastal zone, which can take up to two or three years to be eroded. However, no lag effect could be identified on the Bykovsky Peninsula to explain the lack of coincidence between erosion records and storminess.

The spatial distribution of the main erosion zones and main storm directions are also strongly discordant. West, north-west, and south-west facing shores are not characterised by the strongest erosion rates, although storms winds in Tiksi favour these directions. The relatively small and shallow bodies of water located offshore in these directions explain these average rates of erosion. The fact that erosional features are nonetheless observed ubiquitously on the west-facing shores of the Peninsula is actually an evidence for the formation of high power waves over very small water bodies. The wave height potential on the western shore is probably low but it does compare with coasts possessing full ocean exposure.

Strong storm winds originating from the west are therefore probably needed to develop these waves, but other factors such as large spring freshwater discharges from the Lena into Neelov Bay probably helps with the early melt of the landfast ice (Eicken et al., 2005) and therefore lengthening the open-water season.

There are several likely reasons why the largest rates of erosion (north and northwest facing shores) are not observed on shores where the greatest number of storms is recorded First, as mentioned above, the relief constrains the formation of efficient storm surges and the angle of attack free of topographical obstacle to the Bykovsky Peninsula is limited to the spectrum where the strongest erosion rates have been recorded. Second, the number of study sites used to record erosion on north-facing shores is small and characterised by a great intravariability (see figure 4). Several of these sites are additionally located at the Cape Bykovsky and are morphologically likely to endure stronger erosion rates due to the protruding shape of the cape. Third, the eastern coast is affected by strong thermokarst development and by the presence of a large alas in the south-west part of the Peninsula which has been featuring the largest rates of erosion of the whole Peninsula. In this case, the large

erosion rates seem to be constrained by the morphological and cryological nature of the coast.

Discussion

The difficulties in relating meteorological records to erosion data in our study and in others in the Arctic are known but are yet difficult to overcome. Higher frequency of erosion measurements, but also temporally detailed records of ice onset/offset, wave currents, and water level are needed to overcome these challenges. The storm data presented in this study is based on the Tiksi weather station which is located on land and records the atmospheric pressure and wind data at the location of erosion (or very close to it). The wind data is used as a proxy for storminess and storm surges, but it is a shortcut that is used because wind data over offshore zones (where waves are formed) is not recorded in the area. A large part of the apparent discrepancy in time between erosion data and storminess may actually be due to the flawed representation of storms in the nearshore zone when using local weather data instead of offshore wind fields. It is incorrect to use these data in transfer models to compute storm surges, and hence erosion, since waves develop hundreds of kilometres away from the coast in the offshore zone. However, transfer models from modelled wind fields to storm surges do not take yet into account the whole palette of phenomena occurring in the Arctic coastal zone, and sea ice in particular, and are therefore not readily applicable to this specific context. A greater effort should be put into shoreline monitoring in several sites of the Arctic shoreline to resolve interannual variability in coastal erosion as well as better representation of storm surges through offshore monitoring of wind fields and development of better transfer functions between wind and storm surges.

Like several other studies related to coastal erosion in the Arctic, this study reports on the difficulties to assess reliable trends of coastal erosion. Decreasing sea ice extent, longer open-water season and potential longer fetches should lead to stronger rates of erosion (Maxwell, 1997; Anisimov et al., 2007) but little evidence is yet available to support this hypothesis in a consistent manner throughout the Arctic. One important reason is the lack of data to assess such trends. Statistical significance is hard to accomplish with the strong interannual to interdecadal variability in both erosion and storminess. This again prompts the need for datasets with better temporal resolution and with longer time coverage. There are almost no places where coastal erosion has been recorded yearly in the Arctic. Former Soviet stations in the Barents, Kara and Laptev Seas had records matching those standards until the late1980's, but the surveys were often discontinued before starting again in the early 2000's. The current trends are currently being subdued by the strong interannual variability in both

erosion and storminess and several more decades of yearly erosion and storm records will be needed to improve the quality of our charts, in the case of the Bykovsky Peninsula.

The absence of trend for the 1951-2006 period is however not an indication that erosion will remain steady over the next decades and/or centuries on the Bykovsky Peninsula. Atkinson (2005) showed that the greatest amount of storms, independently from the presence of sea ice, were occurring in June and in October in the Laptev Sea area. Under changing sea ice conditions and lengthening of the open-water season, the number of storms affecting the coasts (as recorded in Tiksi) could potentially double in a few decades. An ice-free Arctic ocean in the summer in 2040 or even in 2025 as reported by Holland et al. (2006) would however not only lengthen the open-water season but also potentially modify the dynamics of storms in this region of the Arctic, with subsequently impacts on the magnitude of the surges and waves observed during storms. Until better characterisation of the relation between storminess and erosion is available, the magnitude of the increase in coastal erosion will be difficult to assess, but the recent drop in summer sea ice extent (Stroeve et al., 2007) provides an incentive to re-visit shore protection measures in the Arctic region.

The current pace of erosion on the shores of the Bykovsky Peninsula is an indicator that the ice-rich sediments deposited on the shelf of the Laptev Sea until the last glacial maximum could not have been eroded entirely but must have been submerged during Holocene transgression as reported by Romanovskii et al. (2000): By extrapolating the Bruun rule on beach erosion (Bruun, 1962) onto the entire Laptev Sea shelf (that is, by assuming a steady slope) and feeding the current rate of erosion of the ice-rich sections of the Bykovsky Peninsula (not alases or aggradational sections) into the Bruun equation, one obtains a coastal retreat considerably lower than the one observed during the Holocene transgression, which tends to confirm that vast areas of the Laptev Sea Shelf could not be eroded entirely and could still entail ice-rich permafrost sediments.

4.6 Conclusion

This paper builds on a long tradition of Russian scientific investigations in the Tiksi area to provide an updated version of coastal erosion rates on the Bykovsky Peninsula. The rates observed along the more than 150 kilometers of coast investigated are unsurprisingly highly spatially variable and highlight the strong role of the cryostratigraphic nature of sediments in the erosional process. Of the various stretches of coast, alases are prone to the strongest erosion, followed by retrogressive thaw slump-affected coasts and finally by ice-complex coasts, which is not unlike other stretches of coasts in the Canadian and Alaskan

Arctic.

The variability in erosion rates is also temporal and is surprisingly poorly linked to storminess at the Tiksi Station. We hypothetize that offshore winds could more successfully be employed to model storm surges and waves, and hence erosion, along the Bykovsky Peninsula shoreline and that the strong storm winds from the west, northwest and southwest are constrained topographically by the mountain ridges and by the shallow bay to hamper the development of waves.

The lack of a significant trend in coastal erosion over the past sixty years does not mean that the current modifications of the Arctic cryosphere will not affect the rhythm of erosion. In addition to enhanced thermokarst in the shore zone, the extension of the open-water season to the whole months of June and October, which are the stormiest in the area, could strongly modify the impact of surges. Readjustements of the shoreface profile could not be taking place at the same pace as before and changing conditions at the land-water interface can be expected.

Acknowledgements

The authors wish to thank the Tiksi Hydrobase for logistical support during several expeditions to the Laptev Sea. The SPOT images (Copyright Centre National d'Etudes Spatiales) were acquired through the SPOT Image distribution / OASIS programme, funded by the European Commission, Directorate General Research. The authors wish to thank Lutz Schirrmeister for his invaluable help preparing this manuscript and during fieldwork.

CHAPTER 5 – MANUSCRIPT #3 - MODERN AND LATE HOLOCENE RETROGRESSIVE THAW SLUMP ACTIVITY ON THE YUKON COASTAL PLAIN AND HERSCHEL ISLAND, YUKON TERRITORY, CANADA.

5.1 Introduction

Retrogressive thaw slumps (RTS) are very distinctive "C-shaped" depressions formed in ice-rich permafrost regions which help form spectacular landscapes in the Western Canadian Artic and elsewhere. They are horizontal backwearing thermokarst features that are generally initiated by wave erosion and retreat by melting of a newly exposed headwall which can expose up to 20 m of ice-rich permafrost (Lewkowicz, 1987b, Burn and Lewkowicz, 1990). Their length (up to 650 m), width (sometimes greater than a kilometre) and frequency are particularly outstanding in the Western Canadian Arctic, but they have also been observed elsewhere in the Arctic (Lewkowicz, 1987a, Pollard, 1991, Leibman, 1995, Robinson, 2000). On Herschel Island and on the Yukon Coastal Plain, RTS are ubiquitous and are surrounded by large stabilized zones which correspond to former phases of RTS activity (Mackay, 1966; Wolfe et al., 2001; Lantuit and Pollard, 2008). The sedimentological, geochemical and ecological characteristics of these zones as well as the time at which they developed have barely been investigated, except for the studies of Burn and Friele (1989) and Bartleman et al. (2001) in more southerly conditions. The conditions of initiation of these landforms in the past could provide useful clues on the reasons for the current increase in occurrence in slumps on the Yukon Coastal Plain and on Herschel Island and on their sensitivity to climatic change.

The aims of this paper are therefore to (a) provide a detailed study of the environmental features of the stable zone surrounding active RTS and (b) to relate those to present and past RTS activity in the area.

5.2 Background

RTS, when they occur in massive tabular ice bodies, have three main elements (figure 1): (1) a vertical or sub-vertical headwall, comprised mostly of the active layer and ice-poor organic or non-organic materials, (2) a headscarp whose angle varies between 20 and 50° and which retreats by the ablation of ice-rich materials due to sensible heat fluxes and solar radiation, and (3) the slump floor, which consists of a fluid mudflow and flow deposits that expand in a lobe pattern at the toe of the slump (de Krom, 1990; Lewkowicz, 1987b).

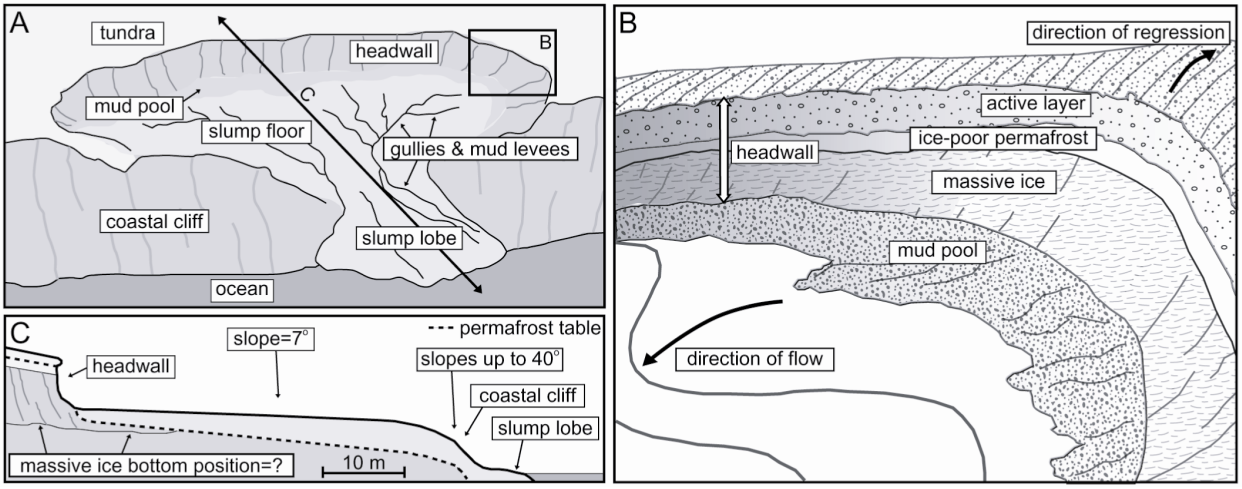

Figure 1 - Conceptual scheme of retrogressive thaw slump
Inset B focuses on the slump headwall. Inset C is a cross-section of the slump. The diagram shows the relation between retrogressive thaw slump development and massive ground ice occurrence. Depending on the bottom position of the massive ice body under the slump floor, a new slump might develop in the lower portion of the slump, building a polycyclic slump. After Lantuit and Pollard (2005).

RTS are often initiated by wave erosion at the base of ice-rich coastal bluffs which uncovers massive ice and leads to ice ablation (de Krom, 1990) or by active layer detachments (de Krom, 1990; Lewkowicz, 1990). If the massive ice melts at a rate that exceeds the rate of erosion along the coast, then a retrogressive thaw slump forms (Lewkowicz, 1987b). On Herschel Island, average headwall retreat rates of 9.6 m/yr outpace average coastal retreat rates of 0.6 m/yr (Lantuit et al., 2005).In the headwalls of the RTS 15 – 20 m of ice are often exposed, depending on the thickness of the debris that accumulates at the base of the headwall (de Krom, 1990; Wolfe *et al.*, 2001). In some areas, RTS are the most prominent landform in the coastal zone. On Banks Island, Lewkowicz (1987a) estimated that 15% of the land within 1 km of the coast of the Sand Hills Moraine region, South-West of Banks Island, has been affected by RTS activity. On Herschel Island alone (108 km²), Lantuit and Pollard (2008) counted up to 164 slumps in the coastal zone. Wolfe et al. (2001) counted 73 slumps between Shingle Point and Kay Point on the Yukon Coastal Plain, including the King Point area.

Most of the RTS they counted are polycyclic, that is they develop in zones formerly affected by episodes of RTS activity. In some areas, up to 90 % of active RTS occur in former slump floors (Lantuit and Pollard, 2008). Polycyclicity is linked to pulses of slump activity that can be driven by many factors, including coastal erosion, changes in the geotechnical properties of the sediments and surficial erosion.

According to Lacelle et al. (2004), there may have been at least three periods of RTS activity during the Holocene: the first during the end of the early Holocene warm interval (9000-8000 BP), the second during the mid- Holocene (4000-2000 BP) and the third during

the Little Ice Age. This is consistent with observations of thermokarst lake expansion in Southern Yukon by Burn and Smith (1990), who described thermokarst lake initiation that "may have originated at the height of the Neoglacial" (Burn and Smith, 1990, p.172).

Existing late Holocene paleoenvironmental records for the Yukon coastal plain area do not resolve climate fluctuations at high enough resolution to relate thermokarst activity to climatic variations, but the concomitance of warm temperatures and longer summer season have often been used to explain rising RTS activity in other places, including Northern Yukon (Cwynar, 1982). Hegginbottom (1984) and Lewkowicz (1987) have emphasized that inputs from both radiation and sensible heat fluxes can explain a large part of the headwall recession rates of RTS. Warmer and longer summers are therefore likely to induce larger headwall retreat rates (Lewkowicz, 1991). A dramatic increase in headwall retreat rates has not been reported yet in the area, but Wolfe et al. (2001) and Lantuit and Pollard (2008) documented an increase in frequency of RTS occurrence on both the Yukon Coast and Herschel Island, which seems to show that the second half of the twentieth century has principally driven the initiation or rather re-initiation of RTS. As mentioned above, initiation of RTS is due to sudden exposure of massive ground ice to subaerial conditions and subsequent melting. In most cases this is related to coastal or river erosion and the occurrence of new RTS can logically be explained by dramatic erosion of coastal cliffs by major storms. If warmer temperatures help to sustain high ablation rates during the thaw season, bluff erosion has a fundamental role in the initiation of RTS.

Aré et al. (2005) have attempted to relate the cross-shore profile of thermoterraces (i.e. slump floors) in the Laptev Sea to the timing of initiation of the slump. Using topographical transects, they relate the virtual intersection of a line extending from the slope of stabilized thermoterraces with the horizontal bottom limit of massive ice to the place "where the upper cliff was created in the past by storm" (Aré et al., 2005, p.124) (figure 2).This scheme provides a useful conceptual framework because it links RTS initiation to coastal erosion and because it allows us to integrate thermoterraces into a chronological sequence. This paper will apply this concept to the stabilized slump floors of the Herschel Island and King Point's coastal zone and relate it to other environmental parameters to better characterize the reasons that lead to slump triggering.

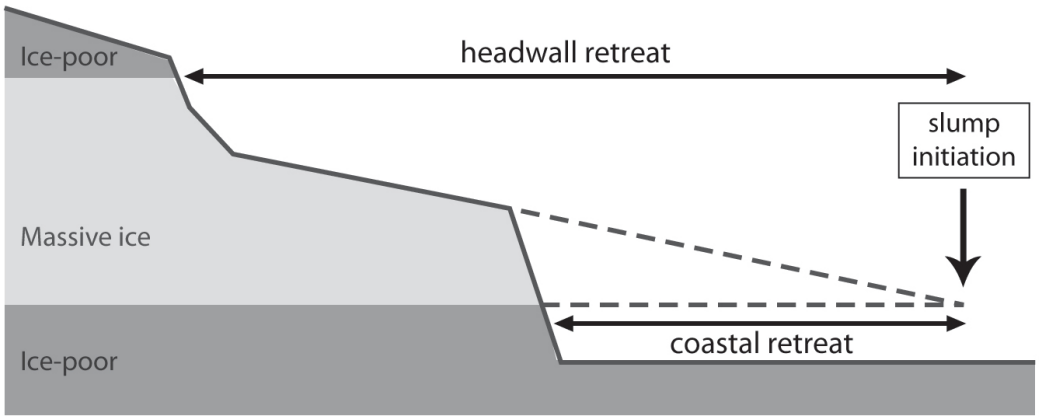

Figure 2 – Idealized cross-sectional profiles of thermoterrace (slump floor) and illustration of the virtual point at which coastal erosion triggered the occurrence of the RTS
Freely adapted from Aré et al. (2005)

5.3 Study area

This study focuses on two sites on the Yukon Coastal Plain, namely Herschel Island (69°34'N; 138°55'W) and King Point (69°05'N; 137°54'W). Herschel Island is the most Northern point of the Yukon Territory and King Point is located along the Beaufort Sea coast approximately 50 km East of Herschel Island (figure 3). Both are characterised by the presence of ice-rich permafrost sediments (Mackay, 1966; Pollard, 1990).

Herschel Island is part of an ice-pushed structure formed by the westward advance of a lobe of the Laurentide ice sheet during the Buckland Stage of the Wisconsin Glaciation (40 ka BP)(Mackay, 1959; Rampton, 1982). It is composed of mainly fine-grained marine sediments dredged from the Herschel Basin and coarser grained coastal deposits. King Point is part of an ice-push moraine similarly formed during a re-advance phase (or stillstand) of the Wisconsin Glaciation termed the Sabine Phase (18-22 ka BP). It is made mostly of unconsolidated clayey marine sediments. Permafrost is relatively deep and in places along the Yukon Coastal Plain is 600+ m thick (Smith and Burgess, 2000). Ground ice is widespread and underlies most of Herschel Island and of King Point's narrow coastal zone except for beaches and spits. In places it constitutes up to 60-70% of the upper 10-15 m of permafrost (Harry et al., 1988; Pollard, 1990). Segregated (intrasedimental) ice is the most common massive ground ice type (Pollard, 1990). The observed thickness of massive ice bodies ranges between 4 and 20 m (Pollard, 1990) but is probably greater since only the upper part of the ice body is exposed by retrogressive thaw slumps.

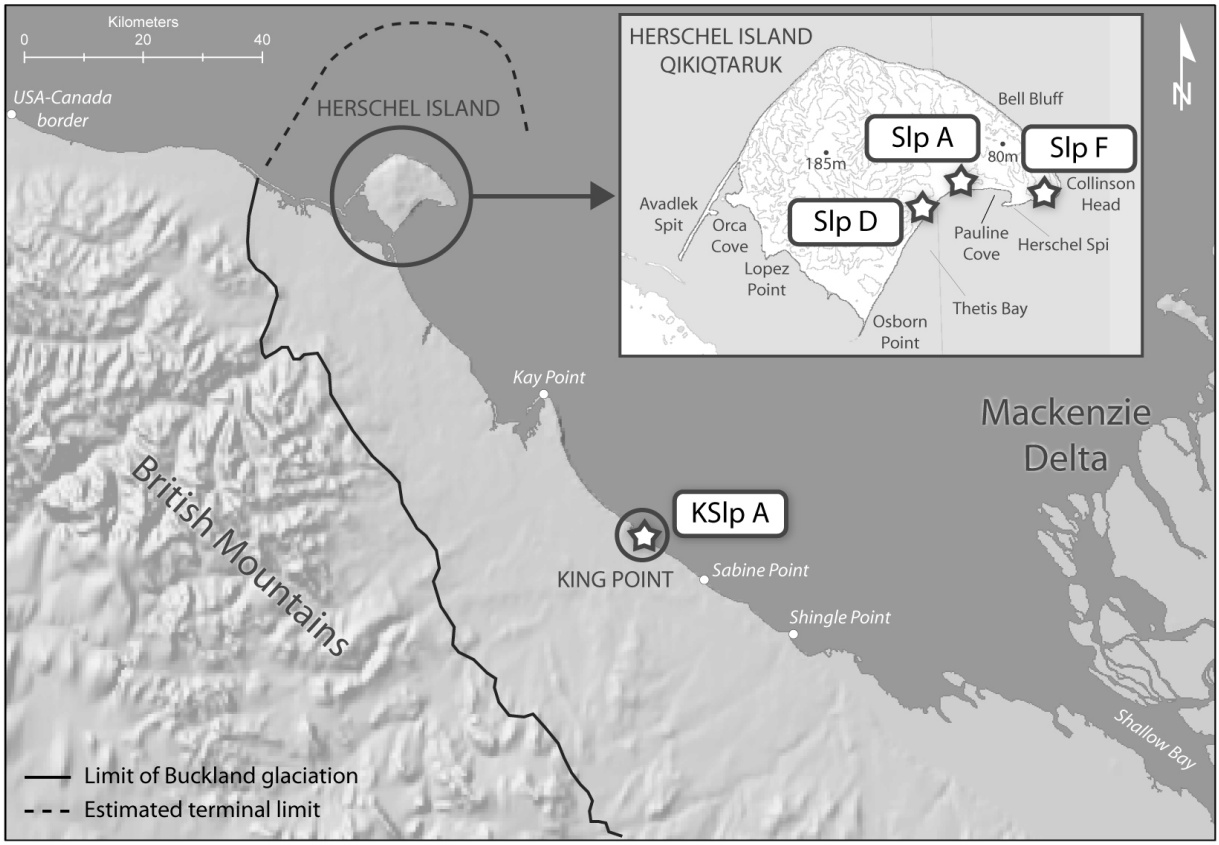

Figure 3 - Study area with limits of Buckland phase of the Wisconsin glaciation

5.4 Methods

5.4.1 Test site selection

We selected four slumps (three on Herschel Island [Slp A, Slp D and Slp F]and one at King Point [KSlp A]), all located in the coastal zone for detailed investigation. Two of these slumps (Slp D & Slp F) have been investigated in a former study to calculate the volume of sediment released by slumping during the 1952-2000 period (Lantuit and Pollard, 2005). Their headwall retreat rates have also been calculated for the 2000-2004 period (Lantuit et al., 2005). To compare both the undisturbed and disturbed (i.e. stabilized) areas, we devised a simple and systematic method that we repeated for each one. We created squares of 30 m in both the undisturbed areas and stabilized zones of the slump, where the boundary between both zones could be clearly established. The size of the squares was partially driven by the size of SPOT multispectral bands spatial resolution (i.e. 15 m) that will be used in a companion paper to map the extent of slump activity. It was meant to include at least one full pixel of a SPOT scene within our squares. Because we needed to find “homogeneous” squares

both within the stabilized and in the undisturbed zone surrounding the slumps, the four slumps had to be larger than average - that is the zones must have been able to enclose a 30m side square. The basic topographical and geometrical characteristics of the slumps are listed in table 1. Oblique helicopter views of the four slumps with the squares are provided in figure 4.

Figure 4 - Oblique helicopter views of the RTS with the survey squares investigated in this study.

Slump Slp A is located on the eastern shore of Herschel Island, in Thetis Bay. Slp A is a large slump which resulted from the coalescence of three smaller slumps at the beginning of the 2000s. Its shape and retreat upslope have been fairly typical and steady for a retrogressive thaw slump. The headwall exposure is about 15 to 20 m high and is made of ice-rich permafrost, but non massive ice.

Table 1 - Basic topographical and geometrical characteristics of the investigated RTS.

	SlpA	Slp D	Slp F	KSlp A
Length (m)	201	420	148	178
Width (m)	241	413	117	241
Max headwall retreat rate (m/yr) (2004-2006)	9.0	9.0	10.5	4.0
Max. elevation (masl.)	39	413	46	19

Slump Slp D is also located on the Eastern shore of the island, in Thetis Bay. It is the largest slump on Herschel Island and has been shown to erode 2,152,800 m³ of permafrost in 48 years (Lantuit and Pollard, 2005). Slp D was labelled "Slump A" in Lantuit and Pollard (2005). Slp D is highly polycyclic and features at least three different cycles of RTS activity in the last 60 years (i.e. since 1944).

Both Slp A and Slp D headwalls are comprised between 25 and 45 masl. and are truncated by a coastal cliff in the lower section of the RTS.

Slump Slp F (Slump B in Lantuit and Pollard [2005]) is located on Collison Head, the easternmost tip of Herschel Island and sits on slightly higher grounds than Slp A and Slp D (> 35 masl.). The cliff truncating the slump floor in the lower part of the slump is greater than 30 m high and undergoes large erosion (> 1 m/yr [Lantuit and Pollard, 2008]). Slp F is much smaller than the Slp A and Slp D and unlike those, it re-activated only after 1970.

Kslp A is located two kilometres east of King Point in an area described earlier by Mackay (1966), Rampton (1982) and Hill (1990). Mackay (1966) in particular has extensively described the nature of the ice face exposed in KSlp A which is composed of a layered ice-rich permafrost truncated at the top by a 2 m deep thaw unconformity. KSlp A's slump floor is a few metres above sea level unlike the three other slumps. It is also polycyclic and has been so since the early 1950s.

At each slump we monitored the headwall and conducted transects to obtain topographical information. We also investigated each square with a systematic set of measurements which are detailed in the following sections. In total, 12 squares were surveyed around Slp A, Slp D, Slp F and KSlp A. Because of topographical constraints and of the difficulty to identify squares as homogeneous as possible, the number of squares surveyed varied from slump to slump.

The methods used in the study are summarized in table 2. Raw results are presented in table 3.

Table 2 - Overview of the applied methods

Methods	Study subjects	Equipment
Radiocarbon age determination (AMS)	Plant remains	Finnigan MAT Delta E gas isotope ratio mass spectrometer
Grain size analysis	Permafrost sediments	Laser particle analyzer LS 200, Fa. Coulter
Biogeochemical investivations (TOC)	Permafrost sediments	Vario EL III element analyser
Shear strength survey	Permafrost sediments	Pilcon handheld vane tester
Topographic survey	Topography	Trimble 4700 KDGPS system

5.4.2 DGPS surveys

The slumps were monitored in July 2006 using a KDGPS (Kinematic Differential Global Positioning System) Trimble 4700 system in order to provide accurate positioning. With appropriate reference station positioning and work at close range between the reference station (Typically <100 km) and the rover, errors due to lack of intervisibility, satellite ephemeris, tropospheric and ionospheric interference can be greatly reduced to achieve submeter absolute accuracy (Monteiro et al., 2005). On each slump, transects were conducted both within the slump floor and on stabilized areas. The position of the slump headwalls was also monitored on all four slumps to compare with data published in Lantuit et al. (2005). The KDGPS device was also used to record with precision the location of the squares used in this study

5.4.3 Sedimentological, geochemical and geotechnical surveys

Each square was surveyed with an active layer probe and a calibrated Pilcon hand vane tester to provide estimates of the median active layer depths and shear strength for the entire square. However, for logistical reasons, shear strength testing could not be completed at KSlp A. On average, 30 measurements were performed for each square for both shear strength and active layer depth surveys. In the centre of each square a hole was dug to the top of permafrost to describe the active layer stratigraphy, and sample just below the humic horizon and at the top of permafrost. When the active layer exceeded 45 cm in the hole, a sample was collected every 20 cm vertically starting from the top. The samples were split in the field to be dried to assess dry-weight moisture content on the day of sampling. The rest of the samples were subsequently freeze-dried in the laboratory to estimate dry-weight moisture content and featured similar results. Each sample was then processed for studies of grain-size distributions in the clay-silt-sand range using a laser particle analyser (LS200, Beckman Coulter, Inc.).

Total organic carbon (TOC) was measured with a Vario EL III element analyser in samples (5 mg) that had been treated with HCl (10%) at a temperature of 80°C to remove carbonate. International standard reference materials covering the measured range as well as double measurements were used to check for external precision. The following errors were accepted: ±5% for TOC content >1 wt%; ±10% for TOC content <1 wt%..

Table 3 - Survey and laboratory results from the survey square illustrated in figure 4

Survey square	Mean shear strength (N/m²)	Mean active layer (cm)	std. deviation active layer	mean median grain size (µm)	soil moisture (%)	mean C/TOC (%)
KSlp A S 1	not measured	69	16.0	12.4	18.2	1.9
KSlp A U 1	not measured	29	7.4	15.3	23.3	4.8
Slp A S 1	348.8	37	9.9	7.5	18.8	2.2
Slp A S 2	472.3	41	7.4	12.5	14.0	1.9
Slp A U 1	218.8	26	6.1	10.4	23.0	3.7
Slp A U 2	212.3	25	8.4	6.8	26.7	5.3
Slp D S 1	283.0	29	8.4	16.1	48.5	11.3
Slp D S 2	712.2	90	0.0	18.1	17.7	1.8
Slp D U 1	265.7	27	8.2	7.6	23.9	3.8
Slp F S 1	739.1	55	9.1	22.1	16.4	1.9
Slp F S 2	1145.1	80	not measured	6.6	19.1	1.6
Slp F A	655.5	> 80	not measured	8.0	16.2	1.4

Table 4 - Survey and laboratory results aggregated by type of surface (S= stabilized, U= undisturbed and A= active).

surface type	Mean shear strength (N/m²)	Mean active layer (cm)	std. deviation active layer	mean median grain size (µm)	mean soil moisture (%)	mean C/TOC (%)
S	616.7	57.3	5.8	13.8	22.4	3.5
U	232.3	26.7	7.5	10.0	24.2	4.4
A	655.5	> 80	not measured	8.0	16.2	1.4

5.4.4 AMS radiocarbon dating

Plant macro-remains (i.e. grass remains) were handpicked from individual exposures for Accelerator Mass Spectrometry (AMS) radiocarbon dating. The sampling in the exposure was done so that samples could be interpreted as grass (tundra) remains buried by the last slumping event and now stabilized. Dating slumps and landslides alike is generally a difficult task, because the samples collected for dating can have been re-buried or remobilized (Lang et al., 1999). In polycyclic RTS, the problem is even more acute since up to six stages can coexist in the same slope (Lantuit and Pollard, 2008). To reduce errors, we collected samples below the stabilized slump floor in clear exposures or in active layer pits in order to validate sampling location with the help of the local cryostratigraphy. Errors due to mislocation of samples selected for AMS analysis are nevertheless possible, because overturning, re-burying of dead vegetation and other movements due to slope processes are possible in polycyclic RTS.

The dating was performed at the Leibniz Laboratory, University of Kiel. ^{14}C ages were calibrated into calendar years before the present (cal. yr BP) using the IntCal04 program (Reimer et al. 2004).

5.5 Results

5.5.1 Geomorphology

We conducted 13 profile surveys in or around the four slumps (see figure 4) and extracted the mean slope using a linear regression fitted through the profile. We compiled means of the slope angles by type of area (active, undisturbed or stabilized) which are listed in table 4. The slope angles of stabilized and active zones do not differ significantly (6.16° vs. 5.82°) which is logical since stabilized zones are former active slump floors. The intravariability was large and angles for these two types of area ranged from 4.45° to 8.50°, which is consistent with observations of retrogressive thaw slump slopes by McRoberts and Morgenstern (1974). The low angle assigned to undisturbed areas is probably highly biased since it was measured on one slump only (Slp A) and on one side of the slump (East). But undisturbed areas are generally identifiable in the field precisely because of the break in topography between the two zones and we can reasonably assume from our field observations that undisturbed areas in the area are generally characterized by lower slope angles.

Low slope angles do not rule out the occurrence of mass-movements such as skin

flows, active layer detachments or solifluction in the upper part of the ground (McRoberts and Morgenstern, 1974). Cross-sections of the coast clearly indicate however that the nature of the processes that created stabilized areas in the coastal zone mobilized great volumes of sediments along several hundreds of meters. This observation is only consistent with RTS occurrence in the area as highlighted by Lantuit and Pollard (2005).

Using the profiles compiled for each slump, we extended the slope line into the ocean in order to compare our data with the one of Aré *et al.* (2005) on the angle of thermoterraces in the Laptev Sea area. We selected the most representative profile for stabilized zone and extended it in the offshore direction. The elevation of the bottom limit of massive ice was often buried under mudflows and could not be estimated with accuracy. Instead, we provided a range of values based on field observations and literature sources (Bouchard, 1974; Rampton, 1982) computed estimated erosion since slump initiation is presented in table 5. The range of distances obtained with Aré *et al.* (2005)'s method is large but is to be constrained within 400 m (375 m is the maximum estimated erosion since slump initiation for Slump D). Using current rates of erosion on Herschel Island from Lantuit and Pollard (2008) and estimates of erosion from Mackay (1963) for King Point, we inferred ages of 280 to 471 years before 2007 for the three RTS on Herschel Island and an age of 67 years before 2007 (i.e. 1940) for the RTS at King Point. These dates are not the dates of initiation of the current RTS, but the dates at which the slumps stabilized. The active slumps which developed in these stabilized zones initiated much later.

Table 5 - Estimated erosion since slump occurrence
Estimation is based on slope angle from stabilized slump floors and estimated elevation of massive ice layer bottom position. Note that age is indicated in years before 2007 and not before present (i.e. 1950).

	elevation bottom massive ice		eroded distance		estimated ages (y before 2007)
RTS	lower estimation (m)	higher estimation (m)	lower estimation (m)	higher estimation (m)	
Slp A	15	25	157	229	280 ± 52
Slp D	15	25	275	375	471 ± 73
Slp F	25	35	207	285	357 ± 57
KSlp A	10	2	20	114	67 ± 47

5.5.2 AMS radiocarbon dating

The calibrated AMS ^{14}C ages are showed in table 6. Ages range from 2845 BP to post-1954 AD. Two samples (KIA 32233 und 32239) featured traces of bomb ^{14}C and were therefore assigned to the post-1954 period. The sample collected directly in the slump floor of KSlp A was one of those, which correlates well with the ages estimated using the

thermoterrace dimension method (i.e.10 ± 47 BP). Airphotos also indicate stabilization of the slump in this specific zone in the early 1940s. The age of Slump Slp A's stabilized surrounding area is also surprisingly well matched to the ages estimated with the thermoterrace dimension method (230 ± 52 BP vs. 304 ± 27 BP). Samples from Slump Slp F included a date of 623 ±34 BP and a post 1954 sample. Both samples were collected in the headwall of Slp F but at a different location. The post-1954 sample (KIA32233) was collected 2 m under the surface at the interface between the underlying ice-rich layers and the disturbed horizons that were interpreted as former slump surfaces and have probably been contaminated.(Fritz, 2008). The 623 ± 34 BP date obtained for the other sample in Slp F is larger than the dates obtained with Aré et al. (2005)'s method, but the cryostratigraphy provides indications that there could have been several successive stages of RTS activity in Slp F (Fritz, 2008). The sample itself was collected below the slump floor in what could be described as a depression probably linked to former stages of RTS activity.

The sample collected in Slp D (KIA32237) was dated at ~ 2760 BP which largely outdates the age predicted by the thermoterrace dimension method. We assume that the sample was first buried at around 2760 BP and re-mobilized in a following RTS episode. Fritz (2008) describes a slightly younger date for a sample (KIA32236 2288 ± 31) also collected in Slp D's headwall which seems to indicate that KIA 32237 did not represent the latest stage of RTS activity. The angle of the stabilized surface slope surrounding Slp D is too high to have been formed 2760 BP under current conditions of coastal erosion. Further samples will have to be collected in Slp D to assert precisely the age of the stabilized slump floor

Table 6 - ^{14}C AMS ages of grass remains in the samples
The 2σ range is calculated with the INTCAL04 program (Reimer *et al.* 2004) to yield calibrated age intervals.

Lab no.	dated material	RTS	sampling location	AMS age (^{14}Cyr BP)	Calibrated age interval (cal. yr BP)
KIA32238	Grass remains	Slp A	slump headwall W	304 ± 27	300-459
KIA32237	Grass remains	Slp D	slump headwall SW	2652 ± 31	2739-2845
KIA32234	Grass remains	Slp F	slump headwall N	623 ± 34	550-660
KIA32233	Grass remains	Slp F	slump headwall W	>1954 A.D.	NA
KIA32239	Grass remains	KSlp A	active layer pit	>1954 A.D.	NA

5.5.3 Sedimentology, geochemistry and geotechnical characteristics

The results from grain size analysis are plotted in figure 5 as a standard grain size tertiary diagram. Three samples have been collected in water flowing in gullies cutting

through the lobe and two samples directly within the slump floor. We didn't record a significant difference between grain size properties between samples from stabilized slump floors and the ones from undisturbed areas. The spread of samples from stabilized slump floors indicated a wider range of silt contents, but the clustering of both types was not precise enough to differentiate them. Water samples featured slightly higher contents in fines, but the difference with other groups of samples was not significant. The grain size distribution curve (figure 6) featured a bimodal shape typical of Herschel Island's marine clays (Fritz, 2008) which was slightly altered through the RTS process. Samples from stabilized zones featured higher silt and lower clay contents. When soil grains were moved downslope, whether by mass-transport or mass-movement, sorting didn't seem to take place but mass-transport probably carried away a part of the fines released by headwall melting.

Total Organic Carbon (TOC) contents for stabilized and undisturbed areas, on the other hand, featured significantly different values, which appear to be strongly controlled by soil moisture (figure 7). TOC and moisture values were higher on undisturbed grounds and lower in stabilized slump floors. Steeper slopes on stabilized slump floors are probably responsible for better drainage and runoff which results in lower moisture contents and les effective plant growth. Also, ice contents underneath the permafrost table are higher in undisturbed areas despite the presence of the hypsithermal (Pollard, 1990; Fritz, 2008). This in turn leads to the release of supernatant water in the early spring, a significant water supply.

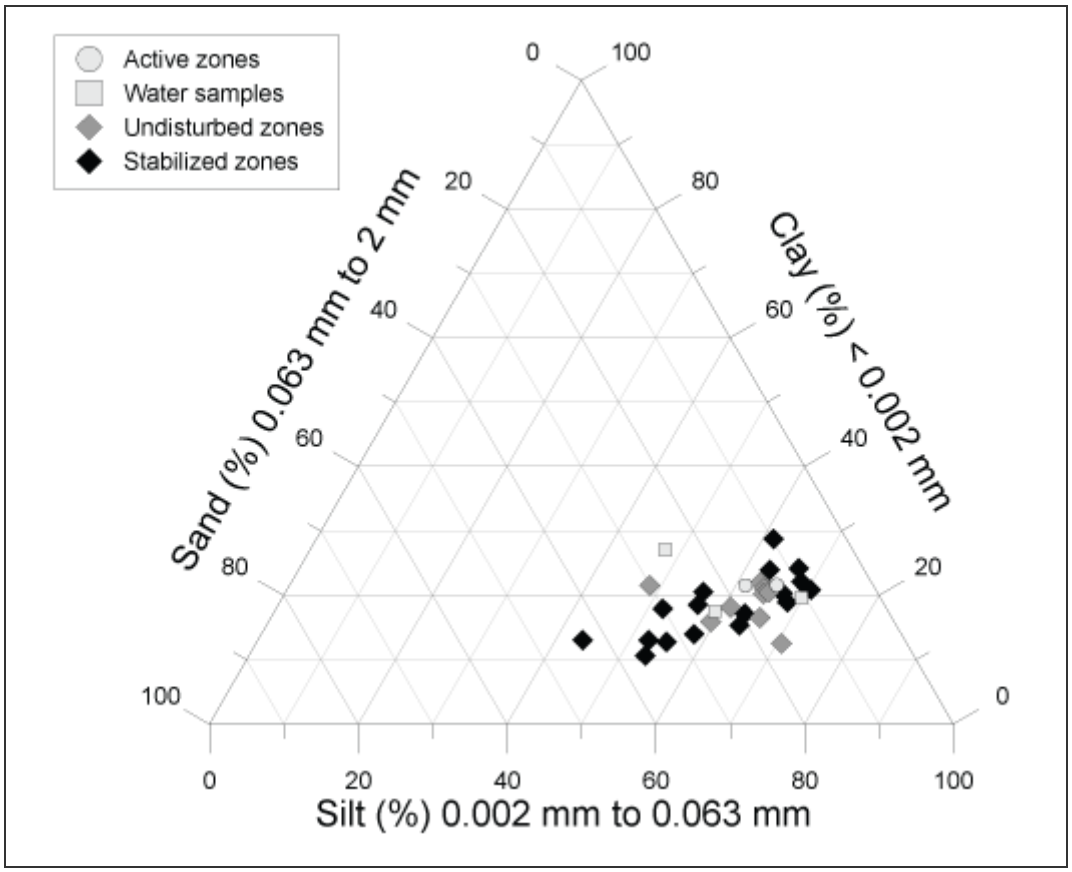

Figure 5 - Tertiary diagram of sediments sampled in active, stabilized and undisturbed zones of retrogressive thaw slumps, as well as suspended sediment samples collected in water flowing in gullies in the slump floor.

Shear strengths were measured in undisturbed, stabilized and active RTS areas and found to be significantly higher in stabilized and active slump floors (617 and 655 N/m²) than in undisturbed areas (mean shear strength: 232 N/m²). Paradoxically, stabilized slump floors are the areas where most new slumps occur, principally through the failure of coastal exposures, that is, because of a net imbalance between the forces tending to cause downslope movements and shear strengths. We explain the higher strengths in stabilized and active slump floors by the lack of advanced soil development, by the nature of the depositional process in the slump floor and by the absence of large soil deformation features (i.e. cryoturbation)

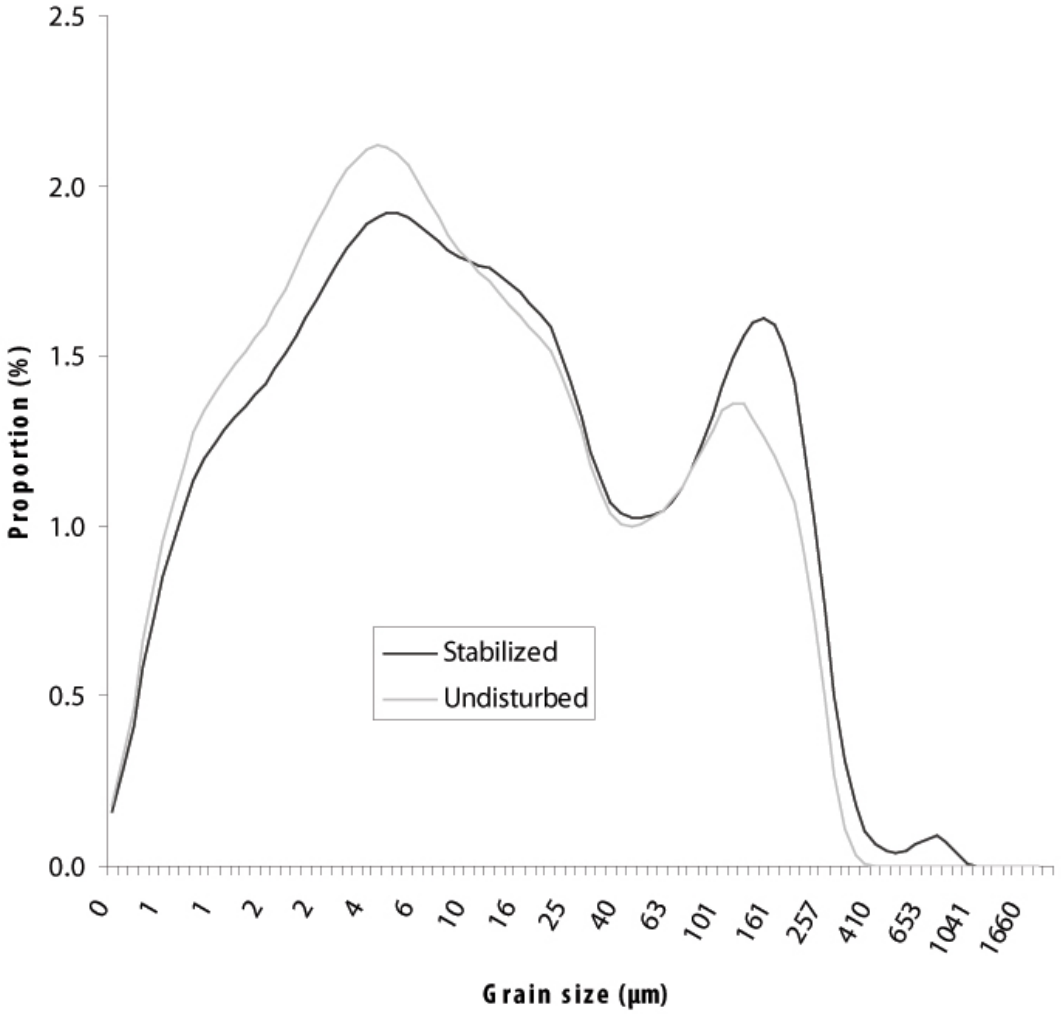

Figure 6 - Grain size distribution curves for samples aggregated by type

The sample collected in Slp D S 1 differed from the rest of the samples and featured a smaller shear strength, much higher TOC and moisture contents than the rest of the samples. The Slp D S 1 survey square was located directly below what was identified as the paleo-headwall in an inflexion of the topography that could lead to higher water contents in the soil (figure 4). The surface of Slp D S 1 could also have been affected by mass movement (skin flows, solifluction or creep) at an earlier period, rather than the RTS activity that we assigned to it. Slp D S 1 is located in a slope that extends southwards into a gully that could have been activated at the time indicated by the KIA32237 sample (~ 2760 BP).

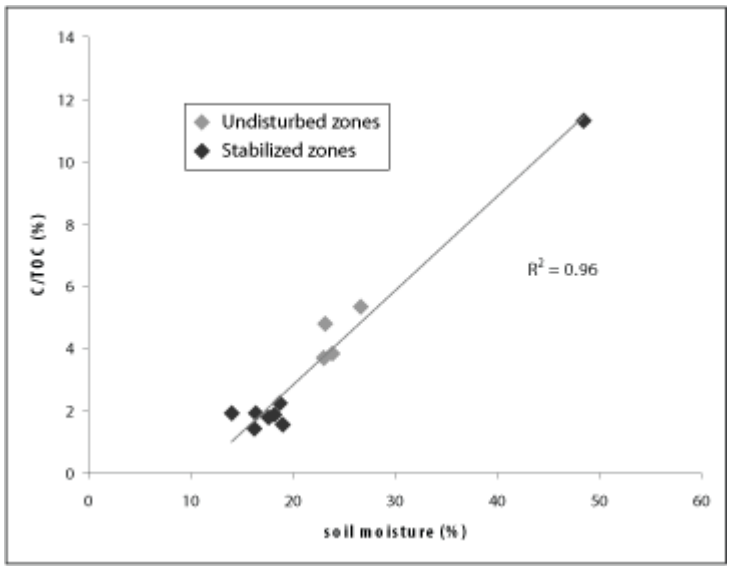

Figure 7 - Regression plot for dry-weight soil moisture content and Total Organic Carbon (TOC) content

5.6 Discussion

Retrogressive thaw slumps generally trigger following a storm (Aré et al., 2005) and expand inland as long as there is enough ice exposed to be melted by incoming heat fluxes. Once the surface is stabilized, succession toward a vegetation cover similar to the ones of the surrounding undisturbed areas is rapidly under way (Burn and Friele, 1989). However, changes in soil moisture conditions following disturbance can also induce changes in the environmental conditions, which in turn changes the species settling in the newly stabilized slump (Bartleman et al., 2001). Based on sedimentological and biogeochemical evidence, we argue that the environmental conditions in stabilized slump areas are fundamentally altered and that the species that will settle in those areas are different from the ones in undisturbed areas. Investigations are currently under way on Herschel Island to assess succession sequences in the coastal zone, but soil and vegetation survey by Smith (1988) have showed that stabilized areas were characterized by different vegetation species than the ones of the undisturbed ones.

The AMS radiocarbon record presented in this study shall be cautiously interpreted, since several of the samples collected for dating were misinterpreted as grass remains buried during the RTS activity that led to the creation of the stabilized surface. They nonetheless provide good indication that there has been a period of RTS activity on the coast of Herschel Island up until 270 BP, which is consistent with other traces of RTS activity in central Yukon (Lacelle et al., 2004). The lack of a continuous and detailed record of the late Holocene

paleoenvironmental record deters the possibility to correlate RTS activity to climatic variables, but it is possible to relate this past period of activity to the current period which is also a period of increased thermokarst and RTS activity in the area (Wolfe et al., 2001; Lantuit and Pollard, 2008). The current level of activity is probably due to the occurrence of strong and discrete coastal erosion events that occurred prior to the 1950s. From the analyses conducted by Lantuit and Pollard (2008), it appears that several of the slumps were already activated at this period. A series of storm events in the 1950s has probably helped to maintain ideal conditions for the initiation of failures in the coastal zone (as rotational failures in the coastal cliff or as skin flows in the backshore area) and triggered the initiation of these large slumps. The large shear strengths recorded in the floor of the slumps show that re-activation of stabilized slump floors was not a trivial phenomenon and that the shear stresses required to expose large chunks of massive ice in the coastal cliff previously buried could only have been possible through the renewed impact of strong storms and/or through strong precipitation events (see McRoberts and Morgenstern (1974) for engineering considerations on slope processes in periglacial regions).

Once the slump is initiated though, ablation is mostly depending from subaerial heat fluxes and the role of coastal erosion is subdued. At places like King Point, where the slump floor lies at elevations close to sea level, the role of coastal erosion is important in removing the product of the mudflow, but on Herschel Island, the headwall of "perched" slumps is virtually independent from the coast and the lobes "dive" into the sea at the cliff edge (figure 4), which facilitates the removal of sediment. The progression of the slump and its stabilization are therefore consequently very dependant on the summer heat budget and little on coastal erosion. The 300 BP date obtained for slump Slp A probably coincided with a slow-down in thermokarst activity, which typically for RTS is linked to the persistence of a layer of detached earth materials over the ice face throughout the thaw season. Massive ice nonetheless persisted in the slump but under layers of slumped material and mudflows. It disappeared in the immediate vicinity of the coast following expansion of the active layer depth downwards (Burn, 2000) in the active slump floor but remained in the upper part of the slope. Coastal erosion continued for several decades until it reached again the massive ice layer and exposed it during a storm re-initiating the RTS. In other words, we hypothesize the existence of a ~250 years cycle of RTS activity in the coastal zone on Herschel Island, provided massive ice is present homogeneously in the backshore zone. This cycle can be termed polycyclicity as long as it is made clear that there are two superposed types of polycyclicity: one spanning over centuries and one spanning over decades (that is, when

multiple RTS develop within the same slope during a thermokarst phase). The timespan at which these phases develop depends mainly on the coastal erosion rate (capacity to erode fast enough to expose the massive ice) and on the local morphology and cryostratigraphy. We can thus assert that current predictions of stronger coastal erosion rates in the Canadian Beaufort Sea (McGillivray *et al.*, 1993) could lead to a shortening of this cycle by exposing massive ice at less spaced time intervals. Coastal erosion rates will probably not catch up with headwall retreat rates since the current ratio between the two is approximately 1/10 but phases of RTS activity shall occur at higher frequency which will have considerable impact on nearshore zone bathymetry, longshore and cross-shore sediment dynamics and on the geochemical budget of the Beaufort Sea shelf.

5.7 Conclusion

This study determined that the slope, the sedimentology and the biogeochemistry of stabilized slump floors differ from the surrounding tundra, independently from their age or location. TOC contents are lower than the ones of undisturbed tundra and are associated with zones of low soil moisture contents. These differences in water supply (stabilized slump floors are drier) could subsequently results in potential changes in vegetation as observed elsewhere in the Yukon (Bartleman *et al*., 2001).

This study also emphasized that sediments from the surface of stabilized slump floors are characterized with slightly lower fine contents which highlights the role of mass-transport as opposed to mass-movement in the transfer of sediment downslope in a RTS. Re-deposition of melted sediments leads to consolidation and higher shear strengths in surficial materials but is not a deterrent to the development of new RTS, since most new RTS develop in these areas.

Finally, this study determined that RTS were particularly active up until 270 BP and are undergoing a similar period of activity nowadays. We hypothesize that RTS activity is cyclic and undergoes ~250 years interval cycle of activity in the Herschel Island area, but we emphasize controls by local morphology and cryostratigraphy in this process. Under scenarios of increasing coastal erosion rates, this cycle could be shortened and lead to higher frequencies of RTS activity in the coastal zone at the centennial scale.

Acknowledgements

The authors wish to express sincere appreciation to the Yukon Territorial Government, to the Yukon Parks (Herschel Island Qiqiktaruk Territorial Park), The Ivvavik National Park, the Yukon Department of Renewable Resources and to the Environmental Impact Screening

Committee (EISC), Inuvialuit Renewable Resource Committees for their support and encouragement of this project. Support from the Polar Continental Shelf Project (PCSP/ÉPCP publication number # 001-08) and the Aurora Research Institute (ARI) for the field component was greatly appreciated. The authors also wish to acknowledge financial support from the ArcticNet Network of Centres of Excellence. The field assistance of Jordan McLeod and Dennis Arey as well as the support from the Hunters and Trappers Committee from Aklavik, NWT were greatly appreciated. Ute Bastian and Tina Knobel, from the Alfred Wegener Institute for Polar and Marine Research provided considerable help for sample processing.

CHAPTER 6 – CONCLUSION

6.1 Results

This thesis explores several themes pertaining to Arctic coastal erosion and highlights the variety of processes acting upon coasts at the circum-Arctic, regional and local scales. The following conclusions are drawn from it:

1) . The use of monoscale linear datasets for the computation of sediment and organic carbon release from coastal erosion to the Arctic Ocean can result in differences in the amount of sediment released by 30% in some cases. This, in turn, can have considerable impact on the quantification of the Arctic Ocean carbon budget.
2) The computation of erosion using coastal area instead of length (i.e. buffers instead or shoreline lengths) can be easily implemented at the circum-Arctic scale. Using this method, variations in quantities of eroded sediment are on average 70% less affected by scale changes than with the former method.
3) Based on the long-term erosion dataset (1951-2006) for the Bykovsky Peninsula presented in chapter 4 (which is the first of its kind) a mean annual retreat rate of 0.59 m/yr is calculated, with total erosion (retreat distance) ranging from –434 m to +92 m (negative changes are erosional).
4) Erosion on the Bykovsky Peninsula is strongly controlled by local geomorphic factors (topography, cryostratigraphy, bathymetry, and hydrology).
5) There was no correlation between wind events (storms) recorded near the Peninsula and observed rates of erosion.
6) Rates of erosion have not been increasing on the Bykovsky Peninsula despite the dramatic decrease in sea ice cover and retreat rate trends are subdued by the strong decadal variability in storminess.
7) On ice-rich permafrost coasts, the stabilization of retrogressive thaw slumps leads to the establishment of steep surfaces, which differ from undisturbed tundra areas in terms of their sedimentology, biogeochemistry, geotechnical properties and topography.

8) Retrogressive thaw slump activity was particularly high on surfaces up until 300 BP which is consistent with the historical pattern of thermokarst activity in parts of the Yukon Territory in the southern Beaufort Sea.

6.2 Outlook

The evolution of arctic coastlines is driven mainly by meteorological and hydrodynamical factors that develop at the regional and circum-arctic scale. Concurrently, coastal currents and bathymetry influence the action of incident hydrodynamical forcing at the local scale. Coastal erosion is controlled locally by geomorphological and cryostratigraphical characteristics which can vary on the order of a few metres. This continuum of processes acting upon the coast at a wide range of spatial and temporal scales (Figure 1) is inherently difficult to understand if not investigated systematically.

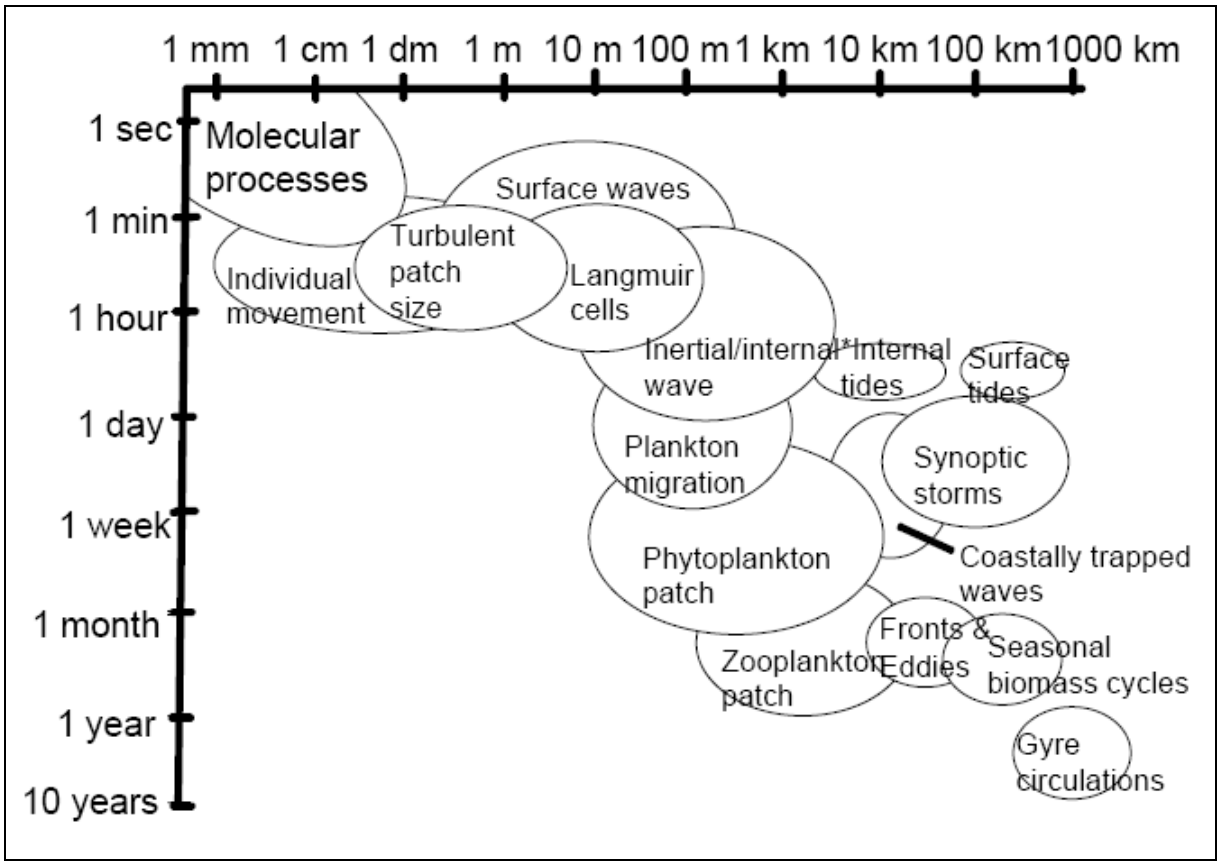

Figure 1 - A schematic representation of spatial and temporal scales of coastal and marine systems. After Gordon et al. (1996)

In the Arctic, year-long multi-scale investigations are rare and difficult to undertake since they require logistical capabilities far beyond the current operational means of the science community. Coastal erosion studies, which have traditionally been undertaken by a small group of researchers, are an example of a discipline lacking the spatial and temporal

coverage necessary to provide boundary parameters to the modelling community (see chapter 2). This thesis attempts to investigate changes of the Arctic coastline at multiple spatial scales, using the circum-Arctic (Manuscript #1) and local settings (Manuscripts #2 and #3) as spatial frameworks. It also attempts to reconcile past and present trends, and with possible future changes, using past records (Manuscripts #2 and #3) and studying the position of current shorelines and/or other present landforms (Manuscripts #1 and #2) to lay the basis for prognosis efforts (Manuscripts #1 and #3).

Most processes can be addressed separately and assigned to a specific spatial and temporal dimension, but this thesis argues that a realistic study of coastal processes is possible only if the coast is seen on a continuum of temporal and spatial scales. Indeed, this work attempts to use local coastline datasets to draw conclusions at the global scale (Manuscript #1). It also uses local wind and erosion datasets to illustrate the limitations of previous studies attempting to encompass both the offshore zone and the backshore (ice-rich coastal plains) of the coastal zone (manuscript #2). Similarly, Manuscript #3 used the present behaviour of retrogressive thaw slumps (one of the most dynamic and spectacular forms of thermokarst that occur in high concentrations along coastlines) to hypothesize the occurrence of an important thermokarst phase in the past. It also builds on this understanding of coastal thermokarst processes to predict the future behaviour of ice-rich permafrost coasts. As Tocqueville (1840) said, “when the past no longer illuminates the future, the spirit walks in darkness”.

The complexity of coastal systems in the Arctic is also due to the polar (high latitude) dimension of the geomorphic processes acting upon the coast. Sea ice and permafrost influence both the strength and the duration of hydrodynamical forcing and contribute to a specific “arctic coastal profile”, which is characterized by specific subaerial landforms and a shoreface profile modified by the presence of permafrost and sea ice. This thesis shows that this situation influences the morphodynamic development of the subaqueous profile at the coast as well as the sediment and geochemical budgets of the nearshore zone during the Holocene. It led to pulses of sediment release linked to retrogressive thaw slump activity (Manuscript #3) on the Yukon Coastal Plain or to the rapid erosion of the ice complex on the Laptev Sea Shelf (Manusrcript #2).

This relationship could potentially lead to dramatic changes in the pattern of coastal dynamics, following an expected lengthening of the open-water season. This thesis has shown that erosion on the shores of the Bykovsky Peninsula has so far remained stable, but that the disappearance of sea ice during the stormy month of October could lead to stronger storms

and greater erosion. On Herschel Island and at King Point, an increase of erosion could result in more frequent re-activation of retrogressive thaw slumps leading to the input of considerable amount of sediments into the nearshore zone.

The major difficulty in connecting these local observations to global predictions generally lies in the statistical approach to upscaling. Arctic coastal erosion has so far been studied at the circum-Arctic scale using linear datasets which aggregate coastal erosion rates in segments and conceptualize the coastline as a line. This thesis has shown that this assumption, which is widespread in coastal science, must be reconsidered to correctly represent volumetric erosion in the coastal zone.

Future investigations in the Arctic coastal zone should focus on the integration of spatial and temporal scales to correctly understand interconnections between the processes acting upon the coasts. A large effort to understand the nature of the physical processes involving mechanical and thermal transfers at the land-water interface is needed. Concurrently, monitoring efforts and data collection at the local scale will have to be pursued in greater numbers. The results of these investigations will feed into prognosis efforts at the global scale, for which the Arctic is one of the most sensitive regions. Finally, arctic coastal science will become a major focus in the future, because the coast crystallizes most of the contact between man and nature.

REFERENCES

Adams, M. 1807. Some account of a journey to the frozen sea, and of the discovery of the remains of a mammoth. Philosophical Magazine, 29, 141–143.

Ali, T. A. 2003. New methods for positional quality assessment and change analysis of shoreline features. Unpublished PhD Thesis, Ohio State University.

Anders, F. J. and Byrnes, M. R. 1991. Accuracy of shoreline change rates as determined from maps and aerial photographs. Shore and Beach (January 1991), 17-26.

Andrle, R. 1996. The west coast of Britain: statistical self-similarity vs. characteristic scales in the landscape. Earth Surface Processes and Landforms, 21, 955-962.

Anisimov, O.A., Vaughan, D.G., Callaghan, T.V., Furgal, C., Marchant, H., Prowse, T.D., Vilhjálmsson, H. and Walsh, J.E. 2007. Polar regions (Arctic and Antarctic). Climate Change 2007: Impacts, Adaptation and Vulnerability. Contribution of Working Group II to the Fourth Assessment Report of the Intergovernmental Panel on Climate Change, Parry, M.L., Canziani, O.F., Palutikof, J.P., van der Linden, P.J. and Hanson, C.E. Eds., Cambridge University Press, Cambridge, 653-685.

Aré, F. E. 1964. The influence of the thermophysical properties of frozen sediments on the erosion of the shores of the arctic seas. In: Teplovyye protsessy v merlykh gornykh porodakh (Thermal processes in frozen rocks). Moscow, Nauka, 111-116.

Aré, F. E. 1988. Thermal abrasion of sea coast. Polar Geography and Geology 12. VH. Winston& Sons, 157 pp.

Aré, F. E., Grigoriev, M. N., Hubberten, H.-W. and Rachold, V. 2005.Using thermoterrace dimensions to calculate the coastal erosion rate, Geo-marine letters 25, 121-126.

Atkinson, D. E. 2005. Observed storminess patterns and trends in the circum-Arctic coastal regime. Geo-Marine Letters, 25(2-3): 98-109.

Baer, K. E. von. 1843. Materials for the Study of the ‘Eternal Ground-Ice’ in Siberia.(Materialen zur Kenntniss des unverganglichen. Boden—Eises in Sibirien), unpublished manuscript,. St Petersburg, Russia, 1843

Bartleman, A.-P., Miyanishi, K., Burn, C. R. and Côté, M. M. 2001. Development of vegetation communities in a retrogressive thaw slump near Mayo, Yukon Territory: A 10-year assessment. Arctic 54, 149-156.

Bartley, J. D., Buddemeier, R. W., and Bennett, D. A. 2001. Coastline complexity: a

parameter for functional classification of coastal environments. Journal of Sea Research, 46, 87-97.

Bauch, H. A., Mueller-Lupp, T., Taldenkova, E., Spielhagen, R. F., Kassens, H., Grootes, P. M., Thiede, J. Heinemeier J. and Petryashov, V. V. 2001. Chronology of the Holocene transgression at the North Siberian margin. Global and Planetary Change, 31, 125–139.

Bouchard, M. 1974. Géologie des dépôts meubles de l'île Herschel, Territoire du Yukon. M.Sc. Thesis, Université de Montréal: Montréal, Quebec; 70 pp.

Brown, J. and Solomon, S. M. 1999. Arctic Coastal Dynamics. Geological Survey of Canada Open File 3929. Natural Resources, Ottawa, Canada.

Bruun, P. 1962. Sea level rise as a cause of shoreline erosion. Journal of Waterways and Harbours 1: 116-180.

Bruun, P. 1988. The Bruun rule of erosion by sea-level rise: A discussion on large-scale two- and three-dimensional usages. Journal of Coastal Research, 4(4), 627-648.

Bunge, A. A. 1895. Description of a journey to the mouth of the Lena River in 1881-1884. Proceedings of the Russian Station at the mouth of the Lena in 1882. St. Petersburg, Geograficheskoye obshchestvo, 96 pp.

Burn, C. R. 2000. The thermal regime of a retrogressive thaw slump near Mayo, Yukon Territory. Canadian Journal of Earth Sciences 37, 967-981.

Burn, C. R. and Friele, P. A. 1989. Geomorphology, vegetation succession, soil characteristics and permafrost in retrogressive thaw slumps near Mayo, Yukon Territory. Arctic 42, 31–40.

Burn, C. R. and Lewkowicz, A. G. 1990. Retrogressive thaw slumps. The Canadian Geographer 34 (3), 273-276.

Burn, C. R. and Smith, M. W. 1990. Development of thermokarst lakes during the Holocene at sites near Mayo, Yukon Territory. Permafrost and Periglacial Processes, 1, 161-176.

Couture N. and Spiridonov, V. 2006. Coastal changes. WWF Arctic Bulletin. 1.06:15-16.

Cowell, P.J., Stive, M.J.F., Niedoroda, A.W., De Vriend, D.J., Swift, D.J.P., Kaminsky, G.M., and Capobianco, M., 2003. The Coastal-Tract (Part 1): A conceptual approach to aggregated modelling of low-order coastal change. Journal of Coastal Research, 19, 812-827.

Crowell, M., Leatherman, S. P., and Buckley, M. K. 1993. Shoreline change rate analysis: Long term versus short term data. Shore and Beach (April 1993), 13-20.

Cwynar, L. C. 1982. A late-Quaternary history from Hanging Lake, northern Yukon. Ecological Monographs, 52, 1-24.

Dallimore, S. R., Wolfe, S. and Solomon, S. M. 1996. Influence of Ground Ice and Permafrost on Coastal Evolution, Richards Island, Beaufort Sea Coast, NWT. Canadian Journal of Earth Sciences 33: 664-675.

De Krom, V. 1990. Retrogressive thaw slumps and active layer slides on Herschel Island, Yukon. M.Sc. Thesis, McGill University: Montréal, Québec; 157 pp.

Denman, K. L. 1993. The ocean carbon cycle and climate change: an analysis of interconnected scales. In S. A. Levin and T. M. Powell and J. H. Steele (Eds.), Patch dynamics, 213-223. Berlin: Spinger Verlag.

Dolan, R., Hayden, B. P., May, P., and May, S. 1980. The reliability of shoreline change measurements from aerial photographs. Shore and Beach, October, 22-29.

Dolan, R., Fenster, M. S. and Holme, S. J. 1991. Temporal analysis of shoreline recession and accretion. Journal of Coastal Research, 7 (3), 723–744.

Dolan, R., Fenster, M. S., and Holme, S. J. 1992. Spatial analysis of shoreline recession and accretion. Journal of Coastal Research, 8(2), 263-285.

Dyke, L. D. 1991. Temperature changes and thaw of permafrost adjacent to Richards Island, Mackenzie Delta, N.W.T. Canadian Journal of Earth Sciences. 28: 1834-1842.

Eicken, H., Dmitrenko, I., Tyshko, K., Darovskikh, A., Dierking, W., Blahak, U., Groves, J., and Kassens, H. 2005 Zonation of the Laptev Sea landfast ice cover and its importance in a frozen estuary. Global and Planetary Change, 48 (1-3), 55-83.

Eid, B. M. and Cardone, V. J. 1992. Beaufort Sea extreme waves study (with French summary). Canada, Environmental Studies Research Funds. Report 114.

Forbes, D. L. and Taylor, R. B. 1994. Ice in the shore zone and the geomorphology of cold coasts. Progress in Physical Geography 18: 59-96.

Francis-Chythlook, O.P. 2004. Coastal processes in Elson Lagoon, Barrow, Alaska, Unpublished M.S. Thesis, Anchorage, Alaska, University of Alaska Anchorage, 130pp.

Franklin, Capt. J. 1828. Narrative of a second expedition to the shores of the polar seas, in the years 1825, 1826, 1827. London: J. Murray.

Fritz, M. 2008. Late Quaternary paleoenvironmental records from a glacially and permafrost affected island in the Canadian Arctic (Herschel Island, Yukon Coastal Plain). Unpublished Diploma thesis. University of Greifswald.

Gillie, R. D. 1988. Beaufort Sea artificial island data, Ityok Island, 1986. Environmental Studies Research Funds, Report 090. 119 pp.

Goodchild, M. F. 1980. Fractals and the accuracy of geographical measures. Mathematical Geology, 12(2), 85-98.

Gordon, Jr., D. C., Boudreau, P. R., Mann, K. H., Ong, J.-E. , Silvert, W. L., Smith, S. V., Wattayakorn, G., Wulff F. and Yanagi, T. 1996. LOICZ Biogeochemical Modelling Guidelines. LOICZ Reports & Studies No 5, 1-96.

Grigoriev, M. N. 1996, Permafrost in the Yakutian Coastal Zone. Nauka, Moscow, 180 pp., in Russian.

Grigoriev, N. F. 1962. The role of cryogenic factors in the formation of the sea coasts of Yakutia. In: Mnogoletnewmerzlyye porody I soputstvuyushcgiye im yavlenia na territorii Yakutskoy ASSR (Permafrost and associated phenomena in the Yakut ASSR), Moscow, Izdatel'stvo AN SSSR, 1962, 67-78.

Grosse, G., Schirrmeister, L., Kunitzky, V. V., and Hubberten, H. W. 2005. The use of CORONA images in remote sensing of periglacial geomorphology: an illustration from the NE Siberian coast. Permafrost and Periglacial Processes, 16, 163-172.

Grosse, G., Schirrmeister, L., Siegert, C., Kunitsky, V. V., Slagoda, E. A., Andreev, A. A. and Dereviagyn, A. Y. 2007. Geological and geomorphological evolution of a sedimentary periglacial landscape in Northeast Siberia during the Late Quaternary, Geomorphology, 86(1/2), 25-51.

Håkanson, L. 1978. The length of closed geomorphic lines. Mathematical Geology, 10(2): 141-167.

Håkanson, L. 1981. The length of open geomorphic lines. Zeitschrift für Geomorphologie, 25(4): 369-382.

Harper, J. R. 1990. Morphology of the Canadian Beaufort Sea Coast. Marine Geology 91: 75-91.

Harper, J. R. and Penland, P. S. 1982. Beaufort Sea sediment dynamics. Technical Report for Geological Survey of Canada. Woodward-Clyde Consultants: Victoria, British Columbia; 198 pp.

Hegginbottom, J. A. 1984. Continued headwall retreat of a retrogressive thaw flow slide, eastern Melville Island, Northwest Territories. In Current Research, part B. Geological Survey of Canada, Paper 84-1B, 363-365.

Heyes, S. A. and Jacobs, P. 2008. Turbulent times in the North In: Pollard, W.H., Couture, N., Lantuit, H. and Rachold, V. (eds.) Arctic Coasts - Circum-Polar Processes and Dynamics. (forthcoming 2008). McGill-Queens University Press. Accepted.

Héquette, A. and Barnes, P. W. 1990. Coastal retreat and shoreface profile variations in the Canadian Beaufort Sea. Marine Geology 91: 113-132.

Héquette, A., Desrosiers, M., Hill, P. R. and Forbes, D. L. 2001. The influence of coastal

morphology on shoreface sediment transport under storm-combined flows, Canadian Beaufort Sea. Journal of Coastal Research. 17: 507-516.

Hill, P. R. 1990. Coastal geology of the King Point area, Yukon Territory, Canada. Marine Geology, 91, 93-111.

Holland, M. M., Bitz, C. M. and Tremblay, B. 2006. Future abrupt reductions in the summer Arctic sea ice, Geophysical Research Letters, 33: L23503, doi:10.1029/2006GL028024.

Hoque, Md. A. and Pollard, W. H. 2008. Modeling block failures of vertical cliffs in the Arctic Coast. In: Pollard, W.H., Couture, N., Lantuit, H. and Rachold, V. (eds.) Arctic Coasts - Circum-Polar Processes and Dynamics. (forthcoming 2008). McGill-Queens University Press. Accepted.

Hudak, D. R. and Young, J. M. C. 2002. Storm Climatology of the Southern Beaufort Sea. Atmosphere-Ocean*, 40*, 145-158.

IASC Arctic Coastal Dynamics (ACD), 2001. Science and implementation plan. International Arctic Science Committee, Oslo

Jenner, K. A. and Hill, P. R. 1998. Recent, arctic deltaic sedimentation: Olivier Islands, Mackenzie Delta, North-west Territories, Canada. Sedimentology, 45: 987-1004.

Johnson K, Solomon SM, Berry D and Graham P. 2003. Erosion progression and adaptation strategy in a northern coastal community. Proceedings - 8th International Conference on Permafrost, Zurich, Switzerland, July 20-25, 2003. Edited by . Phillips, S.M. Springman and L.U. Arenson; International Permafrost Association 8:489-494.

Jorgenson, M. T. and Brown, J. 2005. Classification of the Alaskan Beaufort Sea Coast and estimation of carbon and sediment inputs from coastal erosion. Geo-Marine Letters, 25(2-3): 69-80.

Khmiznikov, P. K. 1934. Erosion of the shores of the Laptev Sea, in: Severnyy morskoy put' (The Northern Sea Route), St. Petersburg: Izdatel'stvo GUSMP, in Russian. 122-134.

Klyuyev, Ye. V. 1966. Manifestations of thermokarst on the bed of the Laptev Sea. Problemy Arktiki I Antarktiki, 23: 26-32, in Russian

Klyuyev, Ye. V. 1970. Thermal abrasion of near shore zone of polar seas. News of All-Russian Geographic Society, 102: 129-135, in Russian.

Kobayashi, N., Vidrine, J. C., Nairn, R. B. and Solomon, S. M. 1999. Erosion of frozen cliffs due to storm surge on Beaufort sea coast. Journal of coastal research 15: 332-344.

Lacelle, D., Bjornson, J., Lauriol, B., Clark, I.D. and Troutet, Y. 2004. Segregated-intrusive ice of subglacial meltwater origin in retrogressive thaw flow headwalls, Richardson Mountains, NWT, Canada. Quaternary Science Reviews, 23, 681-696.

Lang, A., Moya, J., Corominas, J., Schrott, L. and Dikau, R. 1999. Classic and new dating methods for assessing the temporal occurrence of mass movements. Geomorphology, 30, 33-52.

Lantuit, H. and Pollard, W. H. 2005, Temporal stereophotogrammetric analysis of retrogressive thaw slumps on Herschel Island, Yukon Territory. Natural Hazards and Earth System Science, 5: 413-423.

Lantuit, H. and Pollard, W. H. 2008. Fifty years of coastal erosion and retrogressive thaw slump activity on Herschel Island, southern Beaufort Sea, Yukon Territory, Canada. Geomorphology, doi:10.1016/j.geomorph.2006.07.040.

Lantuit H, Couture N, Pollard WH, Haltigin T, De Pascale G, Budkewitsch P, 2005. Short-term evolution of coastal polycyclic retrogressive thaw slumps on Herschel Island, Yukon Territory. Berichte zur Polar- und Meeresforschung (Reports on Polar and Marine Research), 506, 72-75.

Lantuit, H., Steenhuisen, F., Graves-Gaylord, A., Ødegård, R., Atkinson, D., Rachold, V. 2008, in press. The Arctic Coastal Dynamics geospatial framework in Pollard, W. H., Couture, N., Lantuit, H. and Rachold, V. 2007. Arctic Coastal Dynamics

Leffingwell, E. de K., 1919. The Canning river region, Northern Alaska, United States. Geological Survey Professional Paper, 109.

Leibman, M. O. 1995. Preliminary results of cryogenic landslides study on Yamal Peninsula, Russia. Permafrost and Periglacial Processes 6, 259-264. DOI: 10.1002/ppp.3430060307

Leont'yev, I. O. 2003. Modeling erosion of sedimentary coasts in the western Russian Arctic. Coastal Engineering. 47(4), 413-429

Lewkowicz, A. G. 1987a. Nature and Importance of thermokarst processes, Sand Hills, Banks Island, Canada. Geografiska Annaler 69A, 1077-85.

Lewkowicz, A. G. 1987b. Headwall retreat of ground-ice failures, Banks Island, Northwest Territories. Canadian Journal of Earth Sciences 24, 1077-1085.

Lewkowicz, A. G. 1990. Morphology, frequency and magnitude of active layer detachment slides, Fosheim Peninsula, Ellesmere island, N.W.T. Proceedings of the Fifth Canadian Permafrost Conference. Quebec City, Université Laval; 111-118.

Lewkowicz, A. G. 1991. Climatic Change and the Permafrost Landscape. In Woo MK and Gregor DJ. 1991. Arctic environment: Past, Present and Future, proceedings of a symposium, Nov 14-15, 1991, Dpt. Of Geography, McMaster University, Hamilton; 91-104.

Li, R. 2001. A Comparative Study on Shoreline Mapping Techniques. PACON 2001 Conference, San Francisco, CA, July 9-11, 2001.

Li, R., Liu, J.-K., and Felus, Y. 2001. Spatial modeling and analysis for shoreline change detection and coastal erosion monitoring. Marine Geodesy, 24, 1-12

Mackay, J. R. 1959. Glacier ice-thrust features of the Yukon coast. Geographical Bulletin 13, 5-21.

Mackay, J. R. 1960. Notes on small boat harbours of the Yukon Coast. Geography Bulletin 15: 19-30.

Mackay, J. R. 1963. Notes on the shoreline recession along the coast of the Yukon Territory. arctic 16: 195-197.

Mackay, J. R. 1986. Fifty years of coastal retreat west of Tuktoyaktuk, District of Mackenzie in Current Research, Part A, Geological Survey of Canada, Paper 86-1A: 727-735.

Mandelbrot, B. 1967. How long is the coast of Britain? Statistical self-similarity and fractional dimension. Science, 155, 636-638.

Mars, J. and Houseknecht, D. 2007. Quantitative remote sensing study indicates doubling of coastal erosion rate in past 50 yr along a segment of the Arctic coast of Alaska. Geology, 35 (7), 583–586.

Matushenko, N. 2000. What can we offer? – Russia is optimistic about the future of the NSR, in The 21st Century -Turning Point for the Northern Sea Route? Proceedings of the Northern Sea Route User Conference, 18–20 November 1999, Oslo, Norway, vol. 307, edited by C. L. Ragner, pp. 51-53, Springer, Berlin.

Maxwell, B. 1997. Responding to global climate change in Canada's arctic. Vol. II of the Canada Country Study: Climate impacts and adaptation. Environnement Canada. Downsview, Ontario. 82pp.

McDonald BC and Lewis CP. 1973. Geomorphologic and Sedimentologic Processes of Rivers and Coast, Yukon Coastal Plain. Environmental-Social Committee, Northern Pipelines, Canada; Rept. No. 73-39, 245 pp

McGillivray DG, Agnew TA, McKay GA, Pilkington GR. and Hill MC. 1993. Impacts of climatic change on the Beaufort sea-ice regime: Implications for the arctic petroleum industry. Climate Change Digest CCD 93-01, Environnement Canada: Downsview, Ontario; 36pp.

McRoberts, E. C and Morgenstern, N. R. 1974. The stability of. thawing slopes. Canadian Geotechnical Journal, 11, 447–469.

Monteiro, L. S., Moore, T. and Hill, C. 2005. What is the accuracy of DGPS? The Journal of

Navigation, 58, 207-225.

Ogorodov, S. A. 2003. The Role of Sea Ice in the Coastal Zone Dynamics of the Arctic Seas. Water Resources, 30(5): 509-518. Translated from Vodnye Resursy 30 (5), 555-564.

Ogorodov, S. A. 2005. Human impacts on coastal stability in the Pechora Sea. Geo-Marine Letters, 25(2-3): 190-195.

Opsahl, S., Benner, R. and Amon, R. M. W. 1999. Major flux of terrigenous dissolved organic matter through the Arctic Ocean. Limnology and Oceanography 44: 2017-2023.

Ostroumov, V., Rachold, V., Vasiliev, A. and Sorokovikov, V. 2005. An application of a Markov-chain model of shore erosion for describing the dynamics of sediment flux. Geo-Marine Letters, 25(2-3): 196-203.

Pavlova, E. Y. and Dorozhkina, M. V. 2002. The Holocene alluvial delta relief complex and hydrological regime of the Lena River delta. Polarforschung, 70, 89-100.

Peel, M. C., Finlayson, B. L. and McMahon, T. A. 2007. Updated world map of the Köppen-Geiger climate classification. Hydrology and Earth System Sciences, 4, 439-473.

Pollard, W. H. 1990. The nature and origin of ground ice in the Herschel Island area, Yukon Territory. In: Proceedings, Fifth Canadian Permafrost Conference, Québec, Canada. 23-30.

Pollard, W. H. 1991. Observations on massive ground ice on Fosheim Peninsula, Ellesmere Island, Northwest Territories; Current Research, Part E, Geological Survey of Canada, Paper 91-1E, 223 - 231.

Pollard, W. H. and Dallimore, S. R. 1988. Petrographic characteristics of massive ground ice, Yukon coastal plain, Canada. In Permafrost, Proceedings of the 5th International Conference, Trondheim, Norway, August 1988. Tapir, Trondheim, 1, 224-229.

Proshutinsky, A., Pavlov, V., and Bourke, R. H. 2001. Sea level rise in the Arctic Ocean. Geophysical Research Letters, 28(11): 2237-2240.

Rachold, V., Grigoriev, M. N., Are, F. E., Solomon, S., Reimnitz, E., Kassens, H. and Antonow, M. 2000. Coastal erosion vs. riverine sediment discharge in the Arctic shelf seas. International Journal of Earth Sciences, 89: 450-460.

Rachold, V., Brown, J. and Solomon, S. (eds.) 2002: Arctic Coastal Dynamics - Report of an International Workshop, Potsdam (Germany) 26-30 November 2001. Rep. Polar Research 413, 27 extended abstracts, 103 pp.

Rachold, V., Eicken, H., Gordeev, V. V., Grigoriev, M. N., Hubberten, H-W., Lisitzin, A. P., Shevchenko, V. P. and Schirrmeister, L. 2003 Modern terrigenous organic carbon input

to the arctic Ocean., In: Stein, R. and Macdonald, R.W. (Eds.) Organic Carbon Cycle in the arctic Ocean: Present and Past. Springer Verlag, Berlin, 33-55.

Rachold, V., Bolshiyanov, D. Y., Grigoriev, M. N., Hubberten, H. -W., Junker, R., Kunitsky, V. V., Merker, F., Overduin, P. P. and Schneider, W. 2007. Near-shore Arctic Subsea Permafrost in Transition, Eos Transactions of the American Geophysical Union, 88(13): 149-156.

Rampton, V. N, 1982. Quaternary geology of the Yukon coastal plain. Geological Survey of Canada, Bulletin, 317.

Reimer P. J., Baillie, M. G. L., Bard, E., Bayliss, A., Beck, J. W., Bertrand, C. J. H., Blackwell, P. G., Buck, E. E., Burr, G. S., Cutler, K. B., Damon, P. E., Edwards, R. L., Fairbanks, R. G., Friedrich, M., Guilderson, T. P., Hogg, A. G., Hughen, K. A., Kromer, B., McCormac, G., Manning, S., Ramsey, C. B., Reimer, R. W., Remmele, S., Southon, J. R., Stuiver, M., Talamo, S., Taylor, F. W. , van der Plicht, J. and Weyhenmeyer, C. E. 2004. IntCal04 – Terrestrial radiocarbon age calibration, 0–26 cal kyr BP. Radiocarbon, 46, 1029–1058.

Reimnitz, E. and Barnes, P. W. 1987. Sea-ice influence on arctic coastal retreat. Proceedings, Coastal Sediments 87 (New Orleans). New-York, American Society of Civil Engineers, 1578-91.

Reimnitz, E., Grave, S. M. and Barnes, P. W. 1988. Beaufort Sea Coastal Erosion, Shoreline Evolution, and the Erosional Shelf Profile. U.S. Geological Survey. Miscellaneous Investigation series.

Rekant, P., Cherkashev, G., Vanstein, B., ans Krinitsky, P. 2005. Submarine permafrost in the nearshore zone of the southwestern Kara Sea. Geo-Marine Letters, 25(2-3): 183-189

Richardson, L., 1961. The problem of contiguity: An appendix of statistics of deadly quarrels. General Systems Yearbook, 6, 139-187.

Robinson, S.D., 2000. Thaw slump derived thermokarst near Hot Weather Creek, Ellesmere Island, Nunavut. Environmental Response to Climate Change in the Canadian High Arctic (M. Garneau and B.T. Alt, editors). Geological Survey of Canada Bulletin 529, Ottawa, p. 335-345.

Romanovskii, N. N., Hubberten, H. -W., Gavrilov, A. V., Tumskoy, V. E., Tipenko, G. S., Grigoriev M. N. and Siegert, C. 2000. Thermokarst and land-ocean interactions, Laptev Sea region, Russia. Permafrost and Periglacial Processes, 11, 137-152.

Ruz, M.-H., Héquette, A. and Hill, P. R. 1992. A model of coastal evolution in a transgressed thermokarst topography, Canadian Beaufort Sea. Marine Geology, 106: 251-278.

Savelieva N. I., Semiletov, I. P. Vasilevskaya, L. N. and Pugach, S. P. 2000. A climate shift in seasonal values of meteorological and hydrological parameters for Northeastern Asia. Progress in Oceanography, 47, 279–297.

Serreze, M. C., Box, J. E., Barr, R. G. and Walsh, J. E. 1993. Characteristics of Arctic Synoptic Activity, 1952–1989. Meteorology and Atmospheric Physics, 51, 147–164.

Serreze, M. C., Walshg, J. E., Chapin, F. S., Osterkamp, T., Dyurgerov, M., Romanovsky, V., Oechel, W. C., Morison, J., Zhang, T., Barry. R. G. 2000. Observational evidence of recent change in the northern high-latitude environment. Climatic Change. 46: 159-207.

Schirrmeister, L., Siegert, C., Kuznetsova, T. , Kuzmina, S., Andreev, A. A., Kienast, F., Meyer, H. and Bobrov, A. A. 2002. Paleoenvironmental and paleoclimatic records from permafrost deposits in the Arctic region of Northern Siberia, Quaternary International, 89, 97-118.

Siegert, C., Schirrmeister, L. and Babiy, O. 2002. The sedimentological, mineralogical and geochemical composition of late Pleistocene deposits from the ice complex on the Bykovsky peninsula, northern Siberia, Polarforschung, 70, 3-11.

Smith, C. A. S, Kennedy, C. E, Hargrave, A. E. and McKenna, K. M. 1989. Soil and vegetation of Herschel Island, Yukon Territory. Yukon Soil Survey Report No. 1. Land Resource Research Centre, Agriculture Canada, Ottawa.

Smith, S. and Burgess, M. M. 2000. Ground temperature database for northern Canada. Geological Survey of Canada Open File Report 3954, 57 pp.

Smith, S.V., 2005. Length of the global coastal zone. in: Crossland, C.J., Kremer, H.H., Lindeboom, H.J., Marshall Crossland, J.I., and Le Tissier, M.D.A., (Eds.). Coastal Fluxes in the Anthropocene. Springer, Berlin Heidelberg, New York, p. 3.

Solomon, S. M. 2005. Spatial and temporal variability of shoreline change in the Beaufort-Mackenzie region, northwest territories, Canada. Geo-Marine Letters, 25(2-3), 127-137.

Solomon, S. M, Forbes, D. L. and Kierstead, B. 1994. Coastal Impacts of Climate Change: Beaufort Sea Erosion Study. Canadian Climate Centre, Report 94-2 Environment Canada: Downsview, Ontario, Canada; 34 pp

Solomon, S. M. and Covill, R. 1995. Impacts of the September 1993 storm on the Beaufort Sea. Proceedings, 1995 Canadian Coastal Conference, 2, 779-795.

Soluri, E. A. and Woodson, V. A. 1990. World Vector Shoreline. International Hydrographic Review, LXVII(1), 27-35.

Srivastava, A., Niu, X., Di, K., and Li, R. 2005. Shoreline modelling and erosion prediction. Paper presented at the ASPRS 2005 Annual Conference, Baltimore, Maryland, March

7-11, 2005.

Stein, R. and Macdonald, R. W. (Eds.). 2003. The Organic Carbon Cycle in the Arctic Ocean, Springer-Verlag, Berlin, 363 pp.

Stive, M. J. F., Aarninkhof, S. G. J., Hamm, L., Hanson, H., Larson, M., Wijnberg, K. M., Nicholls, R. J., and Capobianco, M. 2002. Variability of shore and shoreline evolution. Coastal Engineering, 47, 211-235.

Stroeve, J., Holland, M. M., Meier, W., Scambos, T. and Serreze, M. 2007. Arctic sea ice decline: Faster than forecast, Geophys. Res. Lett., 34, L09501, doi:10.1029/2007GL029703.

Thieler, E. R. and Danforth, W. W. 1994. Historical shoreline mapping (I): Improving techniques and reducing positioning errors. Journal of Coastal Research, 10(3): 549-563.

de Tocqueville, A. 1840. De la démocratie en Amérique. Furet, Garnier-Flammarion, Paris, 1981, vol. II, 399 pp.

Toll', E. V. 1897. Fossil glaciers on the New Siberian Islands, their relationship to the mammoth carcasses and to the glacial period. Zapiski Russkogo Geograficheskogo obshchestva. 32(1), 139pp.

U.S. Army Corps of Engineers 2002. Coastal Engineering Manual. Engineer Manual 1110-2-1100, U.S. Army Corps of Engineers, Washington, D.C. (in 6 volumes).

van Everdingen, Robert, ed. 1998 revised May 2005. Multi-language glossary of permafrost and related ground-ice terms. Boulder, CO: National Snow and Ice Data Center/World Data Center for Glaciology.

Vasiliev, A. 2003. Permafrost controls of coastal dynamics at the Marre-Sale key site, Western Yamal. In: Proceedings of the 8th International Conference on Permafrost. Zurich ,Switzerland, 21-25 July 2003, 1173-1178.

Vasiliev, A., M. Kanevskiy, G. Cherkashov, G., and B. Vanshtein (2005), Coastal dynamics at the Barents and Kara Sea key sites. Geo Marine Letters, 25(2-3), 110-120.

Walker, H. J. 1982. Arctic, coastal morphology. In Schwartz, M. (ed.), The Encyclopedia of Beaches and Coastal Environments. New York: Van Nostrand Reinhold Co., 57-61.

Walker, H. J. 2005. Arctic, Coastal Geomorphology. In: Schwartz, M L. (ed). Encyclopedia of Coastal Science, Springer, Dordrecht, 49-55.

Whalen, D., Solomon, S., Manson, G. and Forbes, D. 2006. Past, Present and Future Coastal Flooding in the Western Canadian Arctic. Oral presentation. Coastal Zone Canada 2006 Conference. Tuktoyaktuk, NT, Canada, 14-18 August 2006.

Wolfe, S. A.; Kotler, E. and Dallimore, S. R.: Surficial characteristics and the distribution of thaw landforms (1970 to 1999), Shingle Point to Kay Point, Yukon Territory., Geological Survey of Canada, Open File 4088, 2001.

Zenkovich, V. P. 1985. Arctic USSR. In Bird, E.C.F., and Schwartz, M. L. (eds.), The World's Coastline. New York, Van Nostrand Reinhold Co., 863-869.

ANNEX A – MANUSCRIPT #4

Sensitivity of Coastal Erosion to Ground Ice Contents: An Arctic-Wide Study Based on the ACD Classification of Arctic Coasts

Hugues Lantuit
Alfred Wegener Institute for Polar and Marine Research, Potsdam, Germany
Pier Paul Overduin
Alfred Wegener Institute for Polar and Marine Research, Potsdam, Germany
Nicole Couture
Dept. of Geography, McGill University, Montréal, Canada
Rune Strand Ødegård
Gjøvik University College, Gjøvik, Norway

Abstract

Changing sea ice conditions and thawing permafrost in the Arctic could lead to dramatic changes in coastal erosion dynamics. To address this issue, The Arctic Coastal Dynamics (ACD) project brought together experts from all circum-Arctic countries around a common project: The ACD classification of Arctic coasts. This paper uses close to 600 segments from the beta version of the ACD classification to investigate statistical relations between coastal erosion rates on Arctic coasts and ground ice content. Ground ice contents and retreat rates are only weakly correlated statistically ($r = 0.48$), but the multifactor nature of coastal erosion in the Arctic shows us that ground ice is a major factor affecting erosion processes. The current study integrates several geographical settings and time scales and is therefore integrative enough to be used as a benchmark for future empirical models

Keywords: Arctic, coastal erosion, GIS, ground ice.

Introduction

Arctic coasts are among the most vulnerable environments to climate change. Changing sea ice conditions and thawing permafrost could lead to dramatic changes in coastal erosion dynamics. To address this issue, ACD was initiated to provide a comprehensive review of coastal erosion processes at the Arctic scale. This paper uses data from the beta version of the ACD classification to investigate statistical relations between coastal erosion rates on Arctic coasts and ground ice content. Close to 600 segments were used to systematically compare and plot ground ice content and coastal erosion rates. The specific aims of this paper are to document the statistical relation between ground ice and coastal erosion rates and to compare those relations with previously published studies. The statistical relationship extracted from this study will be used as a benchmark for empirical models of coastal erosion.

Background

Arctic Coastal erosion

Coastal erosion in the Arctic is different from its counterpart in temperate regions due to the short open-water season (3-4 months) and to the presence of permafrost, and thus of ground ice, in coastal sediment.

Coastal retreat rates are also highly variable both spatially and temporally (Lantuit and Pollard, 2007; Rachold et al., 2000; Solomon, 2005). Spatial variability is mainly due to changes in the lithology, cryology and geomorphology of coastal cliffs, including ground ice content.

Ground ice is a unique feature of polar coastal systems. It is present in the subaerial part of the shore profile, but also underneath the water column, as submarine ground ice (Mackay, 1972; Rachold et al., 2007). Its presence affects both the response of the shore to thermal-hydrodynamical forcing and the sediment budget of the coast (Are, 1988; Dallimore et al., 1996). The presence of ground ice leads to a process termed "thermal abrasion" (Are,1988) which encompasses the combined action of waves and thawing of the permafrost. It has been shown to facilitate erosion (Héquette and Barnes, 1990; Kobayashi et al., 1999), through the presence of ice in coastal cliffs, or through the occurrence of large thermokarst features in the coastal zone (Lantuit and Pollard, 2005; Lantuit and Pollard, 2007; Wolfe et al., 2001). Dallimore et al. (1996) suggested that thaw settlement of ice-rich sediments in the nearshore zone could induce a change in the shoreface profile, hence enhancing wave efficiency during storms.

However, not all Arctic coastlines are characterized by subsea ice-rich permafrost and other explanations must be sought. Héquette and Barnes (1990) attributed those to the occurrence of ice scours and sediment entrainment by sea ice in the offshore zone, which as shown by Forbes and Taylor (1994) can alter significantly the coastal sediment budget. They based their hypothesis on the weak correlation between retreat rates and several factors including ground ice, wave height and grain size (Figure 1). This paper attempts at providing an expanded characterization (Arctic-wide) of the statistical relation between ground ice contents and re-evaluating the relation proposed by Héquette and Barnes (1990) for the southern Beaufort Sea by using the ACD classification of Arctic coasts.

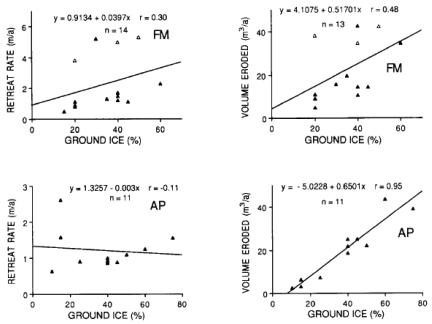

Figure 1 Coastal retreat and erosion as a function of visible ground ice in the bluffs. FM -- field measurement sites; AP -- aerial photograph sites; open triangles indicate minimum values of retreat rate (after Héquette & Barnes, 1990)

The ACD classification of Arctic coasts

The ACD Classification was conceived as a broad enough framework to encompass existing classification schemes while capturing fundamental information for the assessment of climate change impacts and coastal processes. The implementation of the classification was done by so-called "regional experts", who, based on digital and paper products and personal knowledge provided information which was subsequently gathered into a circum-Arctic coastal database. The classification was primarily geomorphological in nature and considered: (1) the shape or form of the subaerial part of the coastal tract, (2) the marine processes acting upon the coast, (3) the shape or the form of the subaqueous part of the coastal tract and (4) the lithofacies of the materials constituting the coastal zone

The beta version of the classification is made of 1331 segments each characterized by a series of geomorphological quantitative and qualitative variables. The classification is stored as an ISO 19115-compliant personal geodatabase and is therefore mappable in off-the-shelf Geographical Information Systems (GIS) (e.g. Figure 2).

Methods

The first step of the processing consisted in reducing the dataset to a set of usable segments: Of the 1331 segments available in the beta version of the ACD classification of Arctic coasts, only segments for which ground ice content, coastal erosion rate, and backshore elevation (i.e. cliff height) were conjointly available were retained. The resulting dataset was reduced to 561 segments.

Subsequently, we consolidated the dataset by removing segments for which the presence of permanent sea ice cover in the summer hampered the development of erosion. The objective was to remove segments for which ground ice contents can be medium to high, yet unaffected by erosion due to sea ice presence in the summer. We used the NSIDC 1979-2000 median sea ice edge position and simply excluded segments located within the permanent sea ice zone in the dataset. We chose not to take into account the marked decreases observed in recent years in order to remain consistent with the times at which coastal erosion rates were mostly determined in the ACD classification. Using this criterion to consolidate the datasets we brought down the number of segments for analysis to 545.

We then ran two sets of analysis using retreat rates in m/yr and eroded volumes in m^3/yr (for a 1m stretch of coastline). Eroded volumes were calculated by combining backshore elevations and retreat rates and constraining the calculation to a 1mkm? stretch of coastline.

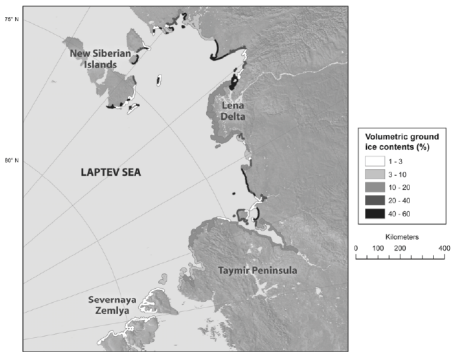

Figure 2 An example of the ACD classification capabilities: Volumetric ground ice contents of shore sediments in the Laptev Sea region (after Lantuit et al., 2008)

Results and discussion

Simple regression analyses

The analysis of the retreat rates versus the percentages of visible ground-ice revealed a relatively weak relationship with a correlation coefficient r = 0.48 (R^2 = 0.23)(Figure 3). The correlation between volumes eroded and ground ice was weaker (r = 0.41, R^2 = 0.17)(Figure 4).

Both relations were statistically significant at α=0.01. Though weak, the correlation coefficient relating ground ice contents to retreat rates is considerably greater than the coefficients published by Héquette and Barnes (1990)(Figure 1). In contrast, the correlation coefficient relating ground ice contents to eroded volumes is lower than the one observed by Héquette and Barnes (1990).

One can logically conclude that coastal erosion in the Arctic is not uniquely related to the presence of ground ice, but that the presence of ground ice significantly influences the process. The data available in the classification doesn't include hydrodynamic forcing and a multi-regression analysis is not currently possible. It should nevertheless be conducted in the future to better assess the statistical weight of ground ice in the thermal abrasion process.

Discussion

The lack of a correct indicator for ground ice in the nearshore zone is a strong deterrent in attempting to establish such relationships. The complex nature of ground ice, including its temperature and cryostructure, make it difficult to correctly statistically relate ground ice to other variables using volumetric ice contents. One would gain from incorporating heat transfer and temperature properties for instance. For the lack of a better dataset, the relationship established using the ACD classification of Arctic coasts is probably the most detailed attempt at establishing such a relation.

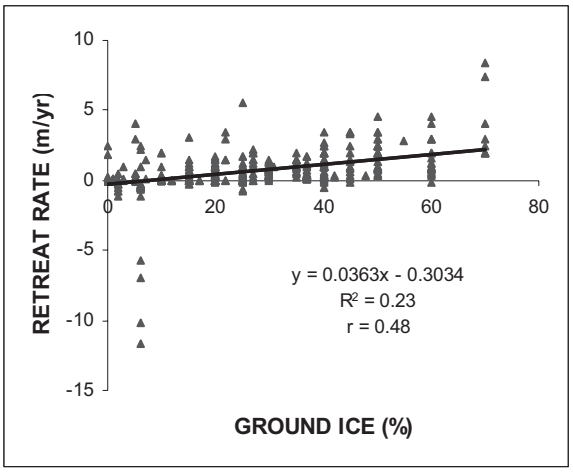

Figure 3 Retreat rate as a function of volumetric ground ice contents

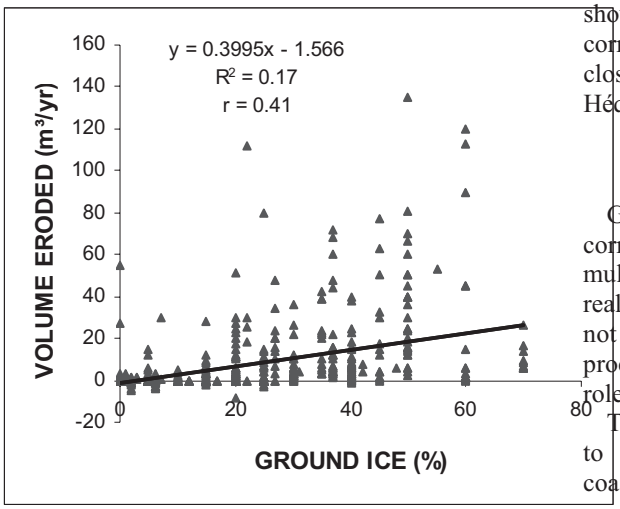

Figure 4 Volume eroded as a function of volumetric ground ice contents

These contradictory results between this paper and Héquette and Barnes (1990) can be explained by the multifaceted interaction of ground ice with coastal processes. Ground ice presence in the nearshore zone influences the course of erosion by modifying the shoreface profile (see above) when it thaws. It also provides the sediments at sea level with a transient strength which lasts until beach sediments are removed during storms and ice-rich sediments are exposed. Most importantly it induces the presence of large thermokarst processes in the subaerial part of the nearshore zone.

Thermokarst processes in the nearshore zone, such as retrogressive thaw slumps, are cyclic and their activity is intimately linked to the removal of sediment by storms. Following periods of large activity, the amount of sediment released by direct melting of ground ice by short-wave radiation influx above water accumulates at the foot of these landforms and progressively impedes the development of new slumps. This lasts until large storms occur and remove the sediment lobes, providing room for a new cycle of activity (Wolfe et al., 2001, Lantuit and Pollard, 2007). The timescales at which these processes occur are comprised between 10^1 and 10^2 years (Lantuit and Pollard, 2007) and are necessarily larger than the timespans used to calculate erosion rates or eroded volumes. Furthermore, because the cycle is strongly associated with storm activity, it is necessarily local.

This paper hypothesizes that the statistical relations extracted from the ACD classification of Arctic coasts, by their wide geographic distribution integrate this cyclic dimension better than the data from the Beaufort Sea only and should therefore be used in future applications. The two correlation coefficients obtained in this study are much closer to one another than the ones obtained by Héquette and Barnes (1990).

Conclusion

Ground ice contents and retreat rates are only weakly correlated statistically. However, due to the presence of multiple factors acting upon the coast in the Arctic realm, one can not exclude that ground ice is a major, if not the most important, factor affecting erosion processes. Further studies will be needed to assess the role of each factor in a single integrated framework.

The relation presented in this paper should contribute to parameterization of future empirical models of coastal erosion as the most extensive effort to relate ground ice to retreat rates.

Acknowledgments

The authors wish to thank F. Steenhuisen, from the Arctic Centre, Groningen, The Netherlands and the members of the ACD group for their contribution to the beta version of the ACD classification of Arctic coasts.

References

Aré, F. E. 1988. Thermal abrasion of sea coast. Polar Geography and Geology 12. VH. Winston& Sons, 157 pp.

Dallimore, S.R., Wolfe, S.A. & Solomon, S.M. 1996. Influence of ground ice and permafrost on coastal evolution, Richards Island, Beaufort Sea coast, N.W.T. *Canadian Journal of Earth Sciences,* 33: 664-675.

Forbes, D.L. & Taylor, R.B. 1994. Ice in the shore zone and the geomorphology of cold coasts. *Progress in Physical Geography*, 18: 59-89.

Héquette, A. & Barnes, P.W. 1990. Coastal retreat and shoreface profile variations in the Canadian Beaufort Sea. *Marine Geology*, 91: 113-132.

Kobayashi, N., Vidrine, J. C., Nairn, R. B. & Solomon, S. M. 1999. Erosion of frozen cliffs due to storm surge on Beaufort sea coast. *Journal of coastal research* ,15: 332-344.

Lantuit, H. & Pollard, W.H. 2005. Temporal stereophotogrammetric analysis of retrogressive thaw slumps on Herschel Island, Yukon Territory. *Natural. Hazards and Earth System. Sciences*, 5: 413-423.

Lantuit, H. & Pollard, W.H. 2007. Fifty years of coastal erosion and retrogressive thaw slump activity on Herschel Island, southern Beaufort Sea, Yukon Territory, Canada. *Geomorphology* doi:10.1016/j.geomorph.2006.07.040.

Lantuit, H., Steenhuisen, F., Graves-Gaylord, A., Ødegård, R. & Atkinson, D. accepted. 2008. The Arctic Coastal Dynamics geospatial framework. In: Pollard, W.H., Couture, N., Lantuit, H. and Rachold, V. (eds.) *Arctic*

Coasts - Circum-Polar Processes and Dynamics. McGill-Queens University Press, Montréal, Canada.

Mackay, J.R., 1972. Offshore permafrost and ground ice, southern Beaufort Sea, Canada. *Canadian Journal of Earth Sciences*, 9: 1550-1561.

Rachold, V., Grigoriev, M.N., Are, F.E., Solomon, S. Reimnitz, E., Kassens, H. & Antonow, M. 2000. Coastal erosion vs. riverine sediment discharge in the Arctic shelf seas. *International Journal of Earth Sciences*,89: 450-460.

Rachold, V., Bolshiyanov, D.Y., Grigoriev, M.N., Hubberten, H.-W., Junker, R., Kunitsky, V.V., Merker, F., Overduin, P.P. & Schneider, W. 2007. Near-shore Arctic Subsea Permafrost in Transition, *EOS Transaction of the American Geophysical Union*, 88(13): 149-156.

Solomon, S.M. 2005. Spatial and temporal variability of shoreline change in the Beaufort-Mackenzie region, northwest territories, Canada. *Geo-Marine Letters*, 25(2-3): 127-137.

Wolfe, S.A., Kotler, E. and Dallimore, S.R., 2001. Surficial characteristics and the distribution of thaw landforms (1970 to 1999), Shingle Point to Kay Point, Yukon Territory. Open File 4115, Geological Survey of Canada.